TRANSPORTATION RESEARCH RECORD

521

Formerly issued as Highway Research Record

Asphalt Concrete Pavement Design and Evaluation

6 reports prepared for the 53rd Annual Meeting of the Highway Research Board

TRB

TRANSPORTATION RESEARCH BOARD

NATIONAL RESEARCH COUNCIL

Washington, D. C., 1974

Transportation Research Record 521
Price $3.60
Edited for TRB by Joan B. Silberman

subject areas
25 pavement design
26 pavement performance
31 bituminous materials and mixes
63 mechanics (earth mass)

These papers report research work of the authors that was done at institutions named by the authors. The papers were offered to the Transportation Research Board of the National Research Council for publication and are published here in the interest of the dissemination of information from research, one of the major functions of the Transportation Research Board.

Before publication, each paper was reviewed by members of the TRB committee named as its sponsor and accepted as objective, useful, and suitable for publication by the National Research Council. The members of the review committee were chosen for recognized scholarly competence and with due consideration for the balance of disciplines appropriate to the subject concerned.

Responsibility for the publication of these reports rests with the sponsoring committee. However, the opinions and conclusions expressed in the reports are those of the individual authors and not necessarily those of the sponsoring committee, the Transportation Research Board, or the National Research Council.

Each report is reviewed and processed according to the procedures established and monitored by the Report Review Committee of the National Academy of Sciences. Distribution of the report is approved by the President of the Academy upon satisfactory completion of the review process.

The National Research Council is the principal operating agency of the National Academy of Sciences and the National Academy of Engineering, serving government and other organizations. The Transportation Research Board evolved from the 54-year-old Highway Research Board. The TRB incorporates all former HRB activities but also performs additional functions under a broader scope involving all modes of transportation and the interactions of transportation with society.

LIBRARY OF CONGRESS CATALOGING IN PUBLICATION DATA

National Research Council. Highway Research Board.
Asphalt concrete pavement design and evaluation.

(Transportation research record; 521)

1. Pavements, Asphalt concrete—Design and construction—Addresses, essays, lectures. 2. Pavements, Asphalt concrete—Testing—Addresses, essays, lectures. I. National Research Council. Transportation Research Board. II. Title. III. Series.
TE7.H5 no. 521 [TE270] 380.5'08s [625.8'5]
ISBN 0-309-02366-1 75-6797

CONTENTS

FOREWORD

This RECORD contains six research papers that address several topics related to the design and evaluation of pavement systems. They should be of interest to researchers and practicing engineers alike.

Chou, Hutchinson, and Ulery present a design method for flexible airfield pavements. The basis of the method was the correlation between performance data of full-scale test pavements and the computed stresses and strains within the pavements due to traffic loads. Limiting design criteria were developed relating critical stresses or strains to number of coverages. Through an illustrative example, they show the application of the method for new and overlay design.

The paper by Jung and Phang also describes an analysis in which computed responses are related to performance. They found that calculated subgrade deflection under a 9,000-lb (40 kN) wheel load was the best indicator of performance for Ontario pavement systems. Deflections were calculated by using both a computer solution to elastic-layered systems and a simplified procedure proposed by Odemark.

In the paper by Shahin and McCullough a model for predicting temperature cracking was developed. Inputs to the model include material properties and environmental variables. The output is temperature cracking per unit area as a function of age and time. Analysis of test roads in Canada was used to validate the model.

The paper by Shook and Lambrechts reports on the development of relationships between a panel rating of performance and measured deflection and base thickness for the San Diego test road. The results were used to develop equivalency factors for the various base materials used at San Diego.

Kamel analyzed sections at the Brampton Test Road by using computer programs for relating pavement response to performance. The results indicate good correlations between the calculated responses (stress, strain, deflection) and serviceability and age histories, surface rutting, and measured deflection. The paper also gives base layer equivalencies for the Brampton materials and presents an application of the results to pavement design and management systems of Ontario.

Systematic data collection procedures are recognized by Walker and Hudson as an important part of the pavement design. The authors are concerned with the development of suitable descriptors for characterizing pavement riding quality. The authors describe the use of digital filtering techniques on road profile data collected by the surface dynamics road profilometer as a tool to find a set of descriptors.

—R. G. Hicks

DESIGN METHOD FOR FLEXIBLE AIRFIELD PAVEMENTS

Y. T. Chou, R. L. Hutchinson, and H. H. Ulery, Jr.,
U.S. Army Engineer Waterways Experiment Station, Vicksburg, Mississippi

A design method for flexible airfield pavements is discussed. The method is based on correlations of performance data of numerous full-scale accelerated traffic test pavements and computed critical stresses and strains of test pavements. The test pavements consisted of conventional flexible pavements and full-depth asphaltic concrete pavements. The loadings include single and multiple wheels. The stresses and strains in the pavement structures were computed by the finite-element technique incorporated with nonlinear stress-strain relations of pavement materials. Limiting criteria considered include radial tensile strains at the bottom of asphaltic concrete, maximum radial tensile strains and minimum ratio of radial tensile stress to vertical stress in the unbound granular layers, and vertical strains at the subgrade surface. The second criterion was developed only for single-wheel loads. The principle of superposition was used in the computations for multiple-wheel loads. The salient features of the design method are discussed, and limiting criteria are applied to the design of pavements and evaluation of pavement performance under mixed traffic and with overlays.

•COMMONLY USED methods for the design of pavements in engineering practice are the theoretical analysis approach and the experimental field approach. Much effort has been expended on both approaches, and in general there is poor correlation between them. Many theoretical methods, such as elastic layered systems and the finite-element method of analysis, are designed to compute the stress, strain, and displacement in the pavement structure but are not capable of evaluating the performance, i.e., cracking, distortion, etc., that is of primary interest to pavement design engineers. On the other hand, although an experimental, full-scale, field-test section approach produces reliable performance data, such test sections are both expensive and time-consuming and provide only minimum amounts of basic test data. In many cases, extrapolations must be used to estimate pavement behavior for cases not covered in field tests; consequently, criteria based on limited amounts of test data are generally conservative. Therefore, there is a definite need to bridge the gap between theory and performance. When such relationships, based on a broad spectrum of test conditions, can be established, design and evaluation of a pavement structure for a new aircraft can be accomplished by direct computations without full-scale tests being conducted for each new need. This method of combining theory and field performance is sound.

For years, the U.S. Army Corps of Engineers (CE) has gained its expertise in pavement design through the use of full-scale accelerated traffic tests. The observed pavement performance is expressed in terms of coverages to failure. Failure criteria are based on the cracking and rutting of pavements. Test results provide reliable and valuable information on the response of real pavements to actual traffic loads. From this information, failure criteria were established; however, it is the full-scale field test that is subject to criticism. The criticisms are generally technically unassailable because each test section represents but one test condition and extrapolation of the results into untested regions is dangerous. However, an improved pavement design methodology can and should be developed by taking full advantage of the valuable

Publication of this paper sponsored by Committee on Flexible Pavement Design.

information from full-scale traffic test results. [This can be done by correlating the field performance and the computed critical parameters (stresses and strains) of each test section, and then establishing limiting values of critical stresses and strains at different coverage levels (performance).]

With the limiting values, prediction of the performance of a pavement structure designed at a particular coverage level for a new aircraft that has never been tested becomes possible. Therefore, the design of new pavements that will be subjected to new aircraft can be done by computers without full-scale tests being conducted. This is theoretically justified because this methodology is based on results of numerous test pavements that were of different thicknesses, materials, and subgrade strengths and that were subjected to loads of different magnitudes and gear configurations. This method of combining theory and field performance not only has eliminated the disadvantages of full-scale testing but has fully exploited the data bank of full-scale testing results that are available at the U.S. Army Engineer Waterways Experiment Station.

Test pavements analyzed consisted of conventional flexible pavements and full-depth asphaltic concrete pavements. The loadings include single and multiple wheels. The stresses and strains in the pavement structures were computed by the finite-element technique incorporated with nonlinear stress-strain relations of pavement materials. The limiting criteria include radial tensile strains at the bottom of the asphaltic concrete, maximum radial tensile strains and minimum ratio of radial tensile stress to vertical stress in the unbound granular base course layers, and vertical strains at the subgrade surface. The second criterion was developed only for single-wheel loads. The principle of superposition was used in computing multiple-wheel load assemblies.

Although the results of the full-scale accelerated traffic tests used were limited only to aircraft loadings, it is believed that the criteria, after appropriate modifications, can be used for designing pavements subjected to highway loadings.

THEORETICAL COMPUTATIONS

Finite-Element Analysis

The nonlinear finite-element program (FEPAVE) used was obtained from the University of California at Berkeley. The program is suitable only for the analysis of axisymmetric solids (a single load with a circular loaded area). The surface load was applied stepwise so that the nonlinear stress-strain behavior and the modulus-stress dependency of the material could be included in the analysis. Ten and twelve load increments were used.

Material Characterizations

Because pavement materials are subjected to repetitive applications of traffic loads and because the stress intensities in the pavements are generally small and well below failure strengths of the materials, it was felt that the resilient modulus could best characterize pavement material behavior under traffic loads as compared to other types of material characterizations. Therefore, better correlations between performance and computed values could be expected. A discussion of the various stress-strain relations for different pavement materials included in this study follows.

Asphaltic Concrete—Because of the thermo-viscoelastic nature of asphaltic materials, the most important factors influencing the stress-strain relationships of asphaltic materials are temperature and rate of loading. The resilient moduli of asphaltic materials should be evaluated in the laboratory at different temperatures and at different rates of loading. However, such data for the actual asphaltic mixtures used by CE were not available during the preparation of this report; therefore, resilient moduli of asphaltic mixtures developed by the Asphalt Institute were used (1). It is believed that the patterns of resilient moduli of asphaltic mixtures used by CE would be similar to those developed by the Asphalt Institute (1). For each test pavement, a mean temperature versus depth relation for the whole traffic period was determined and was used in the computations. Poisson's ratio of 0.4 was used for all asphaltic mixtures in this study.

Untreated Granular Materials—The characterizations of untreated granular materials were based on research conducted at the University of California (2). The resilient modulus, M_R, increases with the sum of principal stress, Θ, according to

$$M_R = k_1 \Theta k_2 \quad (1)$$

where k_1 and k_2 characterize the resilient property of the granular material. Because laboratory results characterizing the resilient properties of granular materials used by CE were not available, representative values from other sources were chosen (2). For well-compacted base-course materials, k_1 and k_2 were 8,300 and 0.71 respectively, and for sand and gravel subbase materials, k_1 and k_2 were 2,900 and 0.47 respectively. The method for selecting the values of these constants will be described later.

The Poisson's ratio of granular material is also known to be stress-dependent. Because of lack of experimental results, a constant Poisson's ratio of 0.48 was used for both base and subbase materials. It was believed that, because granular materials under a thin asphaltic concrete surface course in a pavement structure tend to expand under the heavy aircraft load, a large Poisson's ratio would represent field conditions better than a small one.

Subgrade Soils—Extensive studies of the behavior of fine-grained materials in laboratory repeated-load tests have been made at the University of California (3). It was found that the resilient modulus did not depend on the confining pressure but was sensitive to deviator stress. At low-stress levels, the resilient modulus decreases rapidly with increasing values of the deviator stress, and as the deviator stress further increases, there is only a slight increase in resilient modulus. Because information on resilient modulus for subgrade soils used by CE was not available, this empirical equation (4) was used in the analysis:

$$E \text{ (psi)} = 1{,}500 \text{ CBR} \quad (2)$$

Poisson's ratio of 0.4 was used in the computations.

CORRELATION OF THEORY AND PERFORMANCE

This section applies the concept and computational procedures described to the analysis of performance data of full-scale accelerated traffic tests. Tables 1 and 2 give test data from many selected test sections for single- and multiple-wheel loads; the data cover a broad spectrum of loads, gear configurations, pavements, subgrade soils, and coverage levels. The failure criteria, from which the coverage levels were determined, were based on a subjective rating of pavement performance and primarily on rutting and cracking of the pavements. One coverage is defined to be sufficient passes of load tires in adjacent tire paths to cover a given width of surface area one time. The moving test loads were normally distributed across the surface of the traffic lane.

FEPAVE assumes that the pavement structure is an elastic medium with nonlinear stress-strain characteristics. The computed stress, strain, and displacement are, therefore, the response of the pavement to load before initial failure occurs or, preferably, during the early stage of traffic. Evaluation of the performance of full-scale test sections under traffic, however, is based on the integral pavement behavior up to the point of functional failure. Therefore, finite element programs can be used to predict pavement behavior during the early stage of traffic but cannot be used to predict failure coverage of the pavement. In fact, there is not a single computer program available to date that is capable of predicting functional failure of pavement in a simple and straightforward manner. Therefore, effort was confined to correlating computed values and actual observed coverages to failure of the test pavements from which the parameters controlling the pavement performance could be identified. This was based on the hypothesis that correlations must exist between performance of the pavement and stresses and strains actually developed in the pavement under load. Because the stresses and strains have to be theoretically computed, the success of the

correlation depends entirely on how good the stress-strain relations of pavement materials put into the computer program are. It was apparent that the more closely the input represented material properties, the better would be the correlations.

The rationale for determining the granular material constants k_1 and k_2 in Eq. 1 follows.

For all of the test pavements analyzed (Tables 1 and 2), there were generally three basic types of pavement structures:

1. Full-depth asphaltic concrete pavements resting on 4-CBR buckshot clay subgrade soil.
2. Conventional flexible pavements consisting of a 3-in.-thick (7.6 cm) asphaltic concrete layer, a 6-in.-thick (15.2 cm) base course, various thicknesses of subbase layer, and subgrade soils with various CBRs. (In most cases, the thickness of the subbase layer was much greater than the base course; therefore, the subbase layer practically controlled the performance of the pavement.)
3. Pavements with a 3-in.-thick (7.6 cm) asphaltic concrete layer, a thick, crushed-stone base course, and subgrade soils with various CBRs.

If improper stress-strain relations of pavement materials were used in the computations for these three different types of pavements, it is obvious that good correlations between computed values and observed performance of test pavements could not be obtained and, more than likely, three different correlations would result. On the other hand, if correct stress-strain relations were used, a single good correlation should be obtained. Values of k_1 and k_2 were carefully determined based on this logic.

Because all of the full-depth asphaltic concrete pavements were constructed over 4-CBR subgrade soil, good correlations between computed values and performance were first established. Computations for the conventional flexible pavements and pavements with thick, crushed-stone base courses were then made. In Eq. 1, k_1 and k_2 were initially assumed to be 2,900 and 0.47 for subbase materials and 3,933 and 0.61 for base-course materials (2). Correlations for conventional flexible pavements agreed well with those of full-depth asphaltic concrete pavements, but correlations for thick, base-course pavements did not; these values were much too large. These relationships indicated that the constants k_1 and k_2 chosen for subbase materials were reasonable but that the constants selected for the base-course materials were too small. Higher values of k_1 and k_2 were tried to obtain good correlations, and the final values selected and used were 8,300 for k_1 and 0.71 for k_2.

Single-Wheel Test Data

Table 1 gives test data from 25 selected test pavements. The base-course material was well-compacted crushed stone, and the subbase material was gravelly sand. The traffic on the pavement for test point 14 was actually applied at two ambient temperature conditions: (a) 60 to 70 F (15.6 to 21 C) and (b) 90 to 115 F (32 to 45.5 C). The observed performances of the pavements were identical, indicating that the 3-in.-thick (7.6 cm) temperature-dependent asphaltic concrete surface layer had little effect on the performance of the pavement. The results for the cooler traffic period were used in this analysis.

Figure 1 shows the relations between vertical strain at the subgrade surface and performance. Figure 2 shows similar relations for radial tensile strain at the bottom of asphaltic concrete layers. Uncertainties exist in the computed values for pavements with subgrades having CBRs greater than 10; these are pavement test points 4, 5, 6, 7, and 8 shown in Figures 1 and 2 by open circles. These pavements were excluded from the final analysis but will be discussed separately.

In Figure 1, the best-fit line was drawn through the points for all pavements with greater than 100 coverages to failure. It seems that another straight line could have been drawn through the pavements with coverages less than 100. From the distribution of pavement points in Figure 2, it was concluded that, for pavements with coverages less than 100, the subgrade condition was not critical before initial failure had occurred; the critical factor was the radial tensile strain at the bottom of the asphaltic

Table 1. Single-wheel data.

Test Point	Reference	Wheel Load (kips)	Tire Contact Area (in.^{2})	Thickness (in.)			Subgrade CBR[a]	Coverages at Failure
				Surface	Base	Subbase		
1	5	200	1,500	7	13	19	6	150
2	5	200	1,500	7	15	21.5	9	1,700
3	5	200	1,500	6	13	30	8	1,300
4	5	200	1,500	6	12	0	16/6 (41.5 in.)	10
5	5	200	1,500	6.5	14	0	18/6 (45.5 in.)	60
6	5	200	1,500	6.5	14.5	25	15.5/6 (39.5 in.)	360
7	5	200	1,500	7	14	9	17.5/6 (34 in.)	1,500
8	6	30	150	3	6	6	14	216
9	7	15	250	2	8	0	8	3,760
10	7	15	250	2	8	0	9	3,760
11	8	50	285	3	6	6	3.7	6
12	8	30	285	3	6	6	3.7	120
13	6	30	150	1.5	10.5	0	7	178
14	6	30	150	2	10	0	6	203
15	9	10	91	0	5	0	6	40
16	7	50	667	3	23	0	5	3,000
17	7	20	334	3	14.5	0	5	5,000
18	7	15	250	2	0	10	5	582
19	7	25	416	2	4	12	5	385
20	10	75	270	15	0	0	4	6
21	10	75	270	15	0	0	4	8
22	8	50	285	3	6	15	4	200
23	10	75	270	9	0	15	4	12
24	10	75	270	24	0	0	4	90
25	11	75	270	3	21	0	4	50

Note: 1 kip = 4.448 222 kN. 1 in.^{2} = 6.451 600 cm^2.

[a]Single entries indicate a CBR that is representative of the entire depth of test; double entries indicate a change of CBR at depth (e.g., for test point 4, the upper 41.5 in. of subgrade had a CBR of 16 and below that depth, a CBR of 6 was representative).

Table 2. Multiple-wheel data.

Test Point	Reference	Aircraft Type	Assembly Load (kips)	Tire Contact Area (in.^{2})	Thickness (in.)			Subgrade CBR	Coverages at Failure
					Surface	Base	Subbase		
1	8	Boeing 747	240	290	3	6	24	3.8	40
2	8	Boeing 747	240	290	3	6	24	4	40
3	8	Boeing 747	240	290	3	6	32	4	280
4	8	C-5A	360	285	3	6	6	3.7	8
5	8	C-5A	360	285	3	6	24	3.8	1,500
6	8	C-5A	360	285	3	6	24	4	1,500
7	10	C-5A	360	285	3	12[a]	0	4	98
8	10	C-5A	360	285	15	0	0	4	425
9	8	C-5A	360	285	3	6	15	4	104
10	10	C-5A	360	285	9	0	15	4	734
11	10	C-5A	360	285	9	15[a]	0	4	2,198
12	11	C-5A	360	285	3	21	0	4	5,000
13	11	Boeing 747	200	285	3	21	0	4	890

Note: 1 kip = 4.448 222 kN. 1 in.^{2} = 6.451 600 cm^2.

[a]Asphalt-stabilized.

Figure 1. Relationship between vertical strain at subgrade surface and performance of pavement under single-wheel loads.

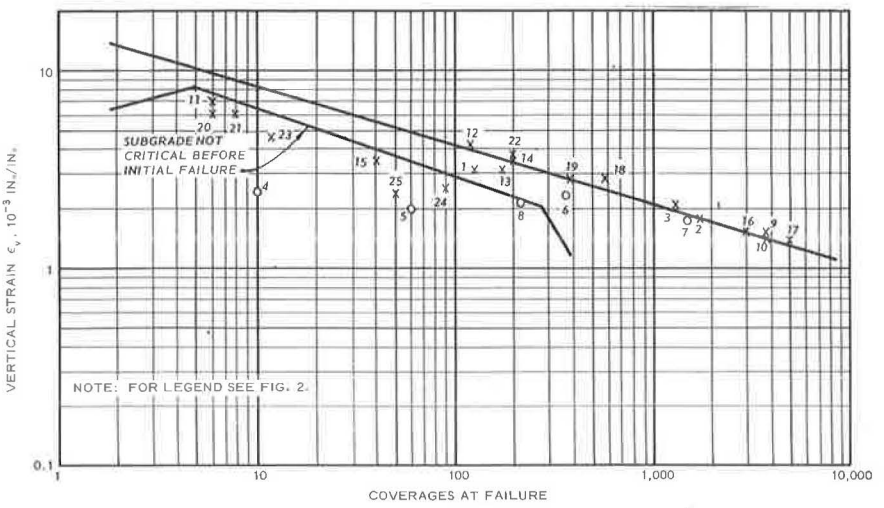

Figure 2. Relationship between radial tensile strain at bottom of asphaltic concrete and performance of pavement under single-wheel loads.

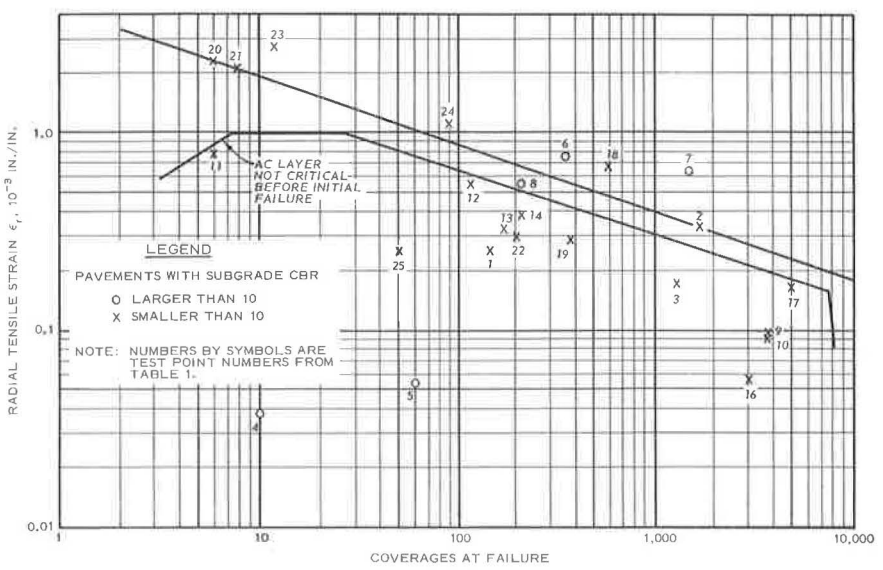

Figure 3. Relationship between maximum radial strain in granular materials and performance of pavement under single-wheel loads.

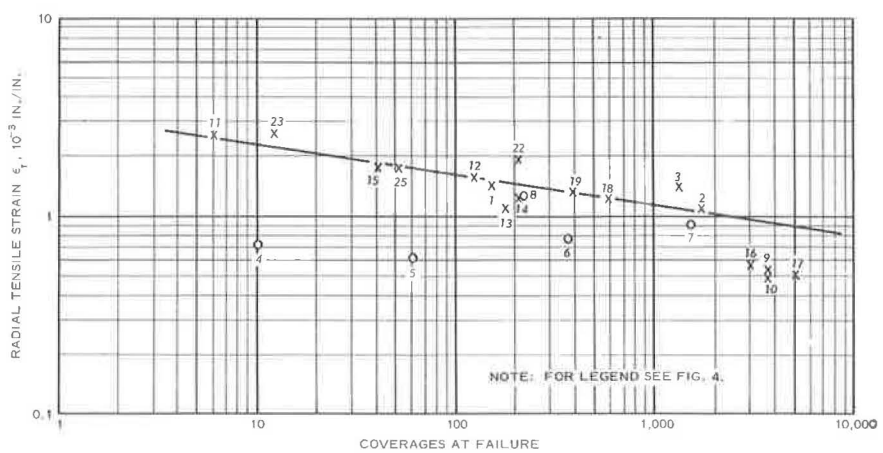

concrete layer. The straight line in Figure 2 was drawn accordingly and passed through test point 2. Sufficient failure test data were not available at high coverage levels; therefore, the validity of the criteria established at high coverages needs to be further verified by additional field performance data. The radial tensile strains for pavement points below the line were not considered to be critical before initial failure.

FEPAVE computes the pavement's elastic stresses and strains, which give an indication of the response of the pavement structure to load before initial failure occurs but do not provide information on the failure modes of the pavements. Figures 1 and 2, for example, do not show that pavements represented by points 20 and 21 were failed in the asphaltic concrete layers and that neither was failed in the subgrade soils. Rather, during the initial stage of the traffic, asphaltic concrete layers under the 75-kip (336 kN) load, 278-psi (1920 kPa) contact pressure were more critical than the subgrade. As load repetition increased, small cracks could have developed in the asphaltic concrete layers and therefore could have reduced its stiffness. As a result, the vertical strains at the subgrade surface would have increased and caused the subgrade soil to fail, which in turn would have increased the cracks in the asphaltic concrete. Eventually, the pavements would fail both in the asphaltic concrete and in the subgrade soil, as was actually observed in the test sections. One can see that the computed values provide information on the most critical factors contributing to the pavement failures rather than indicate the failure modes of the pavement under load.

For pavements with thin asphaltic concrete surface layers, i.e., 2 or 3 in. (5.1 or 7.6 cm) thick, it is believed that such thin layers would not contribute to pavement failure as much as other pavement components. Therefore, design considerations should not be solely based on the thin layer of asphaltic concrete even though the computations indicate that this thin layer is critical under the load (Fig. 2, point 18).

The results of analysis of pavements with base courses of unbound granular materials are shown in Figures 3 and 4; full-depth asphaltic concrete pavements were excluded. Figure 3 shows the results of maximum radial tensile strains. The computer output indicated that locations of the maximum strains were generally near the load axis but varied in depth. The straight line was drawn based on the following reasoning. Because the failure coverages of the pavements (shown by points 2, 18, 19, 1, and 12) could be predicted by the correlation of subgrade vertical strains (Fig. 1), it was reasonable to assume that the failure coverages of these pavements should be at least equal to or greater than those predicted by the criteria of shear failure in the unbound granular materials. The straight line was therefore drawn through these pavement data points. Note that the straight line also went through data points 15 and 11. The pavement shown by point 15 had no asphaltic concrete surface but consisted of a 5-in.-thick (12.7 cm) crushed-stone base placed on 6-CBR subgrade soil. Figure 1 shows that the failure of this pavement did not initiate from the subgrade soil and that, because this pavement had no other component layer but the granular material, the failure of this pavement had to initiate from the unbound granular material under the 10,000-lb (4530 kg) load and 110-psi (760 kPa) contact pressure. Pavement 11 had thin structural layers [3-in.-thick (7.6 cm) asphaltic concrete over a 6-in. base and 6-in. (15.2 cm) subbase] and was subjected to a relatively heavy load [50,000 lb (22 600 kg)] at a high tire-contact pressure [175 psi (1210 kPa)]. Figures 1 and 2 show that the initiation of failure of test pavement 11 was not from the asphaltic concrete layer but was probably from the subgrade soil. Figure 3 shows that failure of this pavement was initiated from the granular materials because of the excessive shear stress.

Pavement data points 7, 9, 10, 13, and 14 (Fig. 3) plotted below the straight line indicate that failure of these pavements was not initiated from the unbound granular materials. In fact, these pavement points all plotted along the vertical strain criterion in Figure 1.

Because of the possibility of shear failure of unbound bases induced by tensile stresses, Brown and Pell (12) suggested that the design criteria for unbound materials should be a horizontal tensile stress that should not exceed 0.5 times the vertical stress plus the horizontal overburden pressure. For all the pavements analyzed, it was found from the computer output that shear failure of unbound bases did not occur. Figure 4 shows the plot of the ratios of radial tensile stress to vertical stress in the unbound

Figure 4. Relationship between vertical strain at subgrade surface and performance of pavement under single-wheel loads.

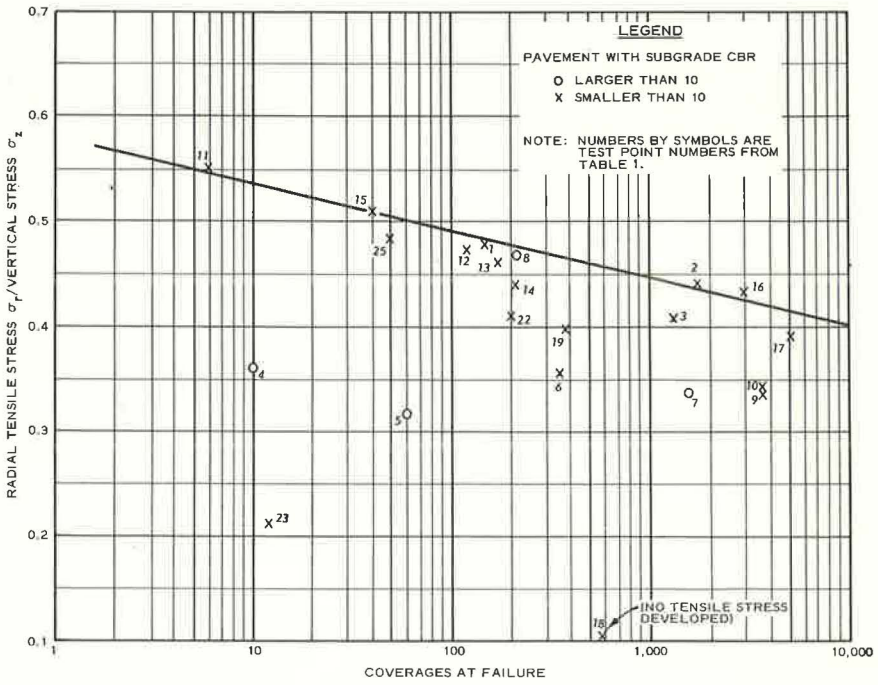

Figure 5. Relationship between vertical strain at subgrade surface and performance of pavement under multiple-wheel loads.

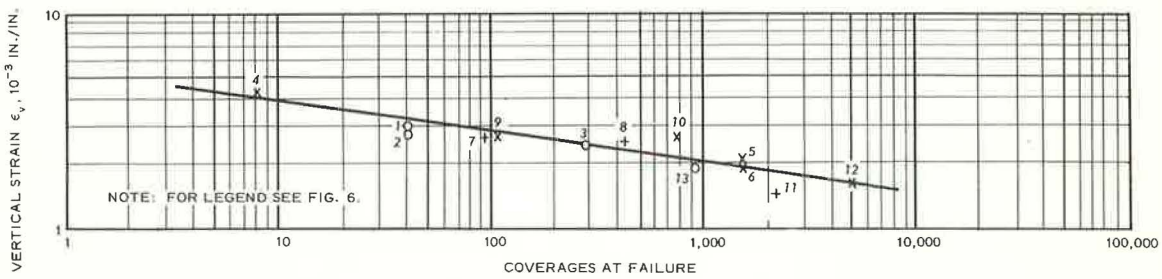

Figure 6. Relationship between radial tensile strain at bottom of asphaltic concrete and performance of pavement under multiple-wheel loads.

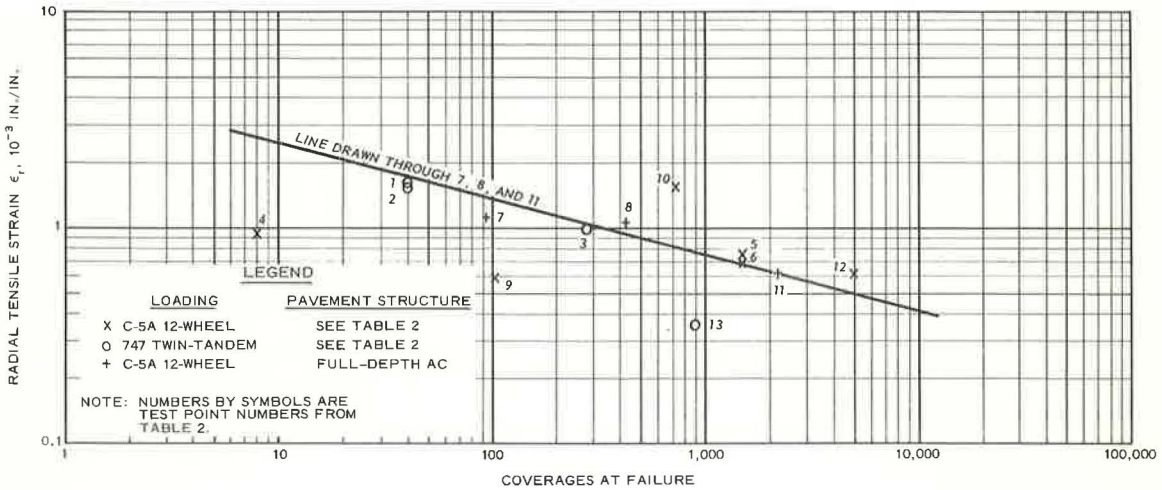

granular materials versus failure coverages of test pavements. The ratios were the maximum values selected within the unbound bases. In most cases, this ratio and the maximum tensile strain do not occur at the same element. The straight line, which was very compatible with the line in Figure 3, was drawn through the upper boundary of the plotted points. Similarly, the points located below the line were the pavements in which the shear failures of unbound granular layers were not critical. The results shown in Figures 3 and 4 are both for unbound granular materials, but they use different parameters. The relations were good except for test points 16, 19, and 22.

The information shown in Figures 1 to 4 could be used to optimize the design of a pavement. For instance, the pavement shown as test point 2 had an optimum design, because the subgrade, the unbound base, and the asphaltic concrete were all equally critical under the 200-kip (890 kN) wheel load.

There were uncertainties in the computed results for test pavements 4 to 8. These pavements had subgrade soils with high CBRs ranging from 14 to 18. The test points are represented by open circles in Figures 1 to 4 and were not considered in drawing the straight lines in the figures. The computed values for pavements 4 (CBR = 16) and 5 (CBR = 18) were much too low in Figures 1 to 4; this indicates that the moduli computed by the relation E = 1,500 CBR were too high. However, the computed results for pavements 6 (CBR = 15.5), 7 (CBR = 17.5), and 8 (CBR = 14) seem to fit the line fairly well and indicate the relation E = 1,500 CBR was not bad. The situation is puzzling. Nevertheless, the moduli determined from the relation E = 1,500 do not seem to be adequate for high-CBR subgrade soils.

Multiple-Wheel Test Data

Table 2 gives test data for 13 selected test pavements under multiple-wheel, heavy gear loads. The pavements were trafficked by full prototype loadings of a 12-wheel assembly (one main gear of a C-5A) and a twin-tandem assembly (one twin-tandem component of a Boeing 747).

FEPAVE is not capable of handling multiple-wheel loads. In fact, such a nonlinear program is not available currently. Thus, the superposition principle was used to obtain solutions for multiple-wheel loads. This was done by first constructing the stress basins under the single-wheel load and then superposing the ordinates for different wheels. A computer program was prepared to compute the stresses and strains at any location under the multiple-wheel loads. The limitations on the use of the principle of superposition and the validity of the superposition principle are discussed elsewhere (13, 14). Stresses and strains were computed along the load axis of one wheel of the assembly, maxima were not searched for. For the C-5A gear assembly, the wheel was chosen to be either one of the inner wheels in the second row of the 12-wheel assembly. When computations are made for thick pavements, the values computed are smaller than the real maxima. This could be one of the factors contributing to the scattering of results in Figures 5 and 6.

Figure 5 shows the relation between vertical strains on the subgrade surface and failure coverages; a straight line could be drawn through pavement points at all coverage levels. The correlations indicate that pavement performance subject to multiple-wheel loads could be predicted by computed values of vertical strain on a subgrade surface. However, the correlation (Fig. 5) should not be interpreted because all of these pavements were failed in the subgrade soil.

Figure 6 shows the relation between radial tensile strain at the bottom of asphaltic concrete layers and performance of the test pavements under multiple-wheel loads. For pavements with 3-in.-thick (7.6 cm) asphaltic concrete surface layers, the radial tensile strain (at the bottom of the concrete) under a single-wheel load was the same as the strain under one wheel of the multiple-wheel load. This is because the asphaltic concrete was thin and the wheels were spaced so far apart. For the full-depth asphaltic concrete pavements, at the bottom of the thick pavement, the radial tensile strain under one wheel had added strains that were contributed by the other wheels. Therefore, it was believed that radial tensile strain in pavements with thin asphaltic concrete layers should not be considered as the controlling factor in predicting pavement performance.

The line in Figure 6 was drawn through the full-depth pavements, test points 7, 8, and 11; pavements 1 to 6, 12, and 13, which were flexible pavements with 3-in.-thick (7.6 cm) asphaltic concrete surfaces, were not considered. Computed radial tensile strains in pavements 1, 2, 4, and 13 were small as compared with those of the full-depth asphaltic concrete pavements because of the nature of the thin asphaltic concrete layer. For pavements 3, 5, 6, and 12, however, they fell rather close to the straight line, but the closeness was considered to be only coincidental. In fact, the computed radial strains at the bottom of the 3-in.-thick (7.6 cm) asphaltic concrete layer in pavements 1 to 6 were nearly the same. The reason for test point 10 being located so far above the line is not known. One possible explanation is that the temperature input into the computer program was incorrect for the 9-in.-thick (22.8 cm) asphaltic concrete layer.

The results shown in Figures 5 and 6 are limited to subgrade soils with a strength of 4 CBR. The question arises whether the criteria established would be applicable to subgrade soils of different strengths. Because of the criteria for single-wheel loads (Figs. 1 to 4), in which the results for pavements on low-CBR subgrades were mixed well with those for pavements with higher CBR subgrades, one can justifiably conclude that the correlations in Figures 5 and 6 for multiple-wheel loads can be used for pavements other than those on 4-CBR subgrade soils.

Criterion for shear failure in unbound granular materials was not established for pavements subjected to multiple-wheel loads because of the difficulty in searching for maximum radial tensile strain (Fig. 3) and the maximum stress ratio (Fig. 4) in the unbound layers when the principle of superposition is used.

Special Remarks

Although the nonlinear finite-element method possesses many deficiencies in computing stresses and strains in pavement structures under traffic loads, it still yields reasonably good results. Apparently, this method is a good and powerful tool to find correlations between theory and observed performance. This is manifested by the good correlations shown in Figures 1 to 6.

Tensile strains (fatigue cracking) in an asphaltic concrete layer are more critical in cold weather. Most test pavements analyzed in this study were trafficked in relatively warm weather. Some full-depth asphaltic concrete pavements should be tested in cold weather and information obtained would undoubtedly enhance the proposed criteria.

It should be emphasized that the purpose of this study was not to predict the stresses and strains in the pavement structures; the purpose was to use the computed values to predict pavement performance. Attempts were made to compute the stresses and strains in pavement structures as close as possible to those actually measured. Because the computed values are computer-generated reproducible numbers the performance of a new pavement subject to a new aircraft can be predicted from the established correlations through computations. When better stress-strain relations of pavement materials are formulated and when more information on traffic tests are collected, the established correlations can be refined and the design procedures can be improved and updated. Therefore, the nonlinear finite-element method is not only the best method to fulfill the goal of this study, but it holds promise for the future.

Because of space limitations, many important features of the proposed design method cannot be presented in detail (13).

APPLICATION OF ANALYSIS

The results shown in Figures 1 to 6 represent correlations between theory and performance. The computed values are reproducible quantities generated by the computer and are based on the nonlinear theory of elasticity; the repetitions at failure are observed performance from full-scale accelerated traffic test sections. Test data covered a broad spectrum of test sections, wheel loads and configurations, subgrade soil strengths, and coverage levels (Table 2). Confidence is justified in using the limiting criteria for the design of pavements for new aircraft. We believe that cor-

relations developed can be used for designing and evaluating pavements subjected to mixed traffic and overlays of existing flexible airfield pavements.

Design of New Pavements

Although the CBR equation has been used satisfactorily by CE in the design of flexible airfield pavements for many years, there are certain pavement characteristics that are not adequately accounted for by the CBR equation because of the lack of supporting information. Designs for pavements in this category tend to be conservative. Pavements designed by the CBR equation have adequate thickness over the subgrade and over each layer of the structure to prevent shear failure. There is, however, no benefit given for use of materials stronger than the required minimum. For instance, when subbase material is replaced by material qualified as base course, the total thickness of the pavement structure is not reduced and the designed coverage level is not increased. The lack of consideration of these aspects in the CBR equation is not because of lack of knowledge but is mainly because of the lack of sufficient experimental data to support these considerations, and the CBR equation was based on test results of conventional flexible pavements and is, therefore, not adequate for designing pavements with full-depth asphaltic concrete or pavements with unconventional materials. However, with the proposed method in this study, i.e., computing the critical stresses and strains for the particular pavement section, some of the drawbacks inherent in the CBR equation can be overcome.

The design method has the capability of analyzing more sophisticated future pavements made of new pavement materials. The characterization of the new materials as determined in the laboratory is required for this. From the criteria in Figures 1 to 6 and FEPAVE, the thickness of each component layer of the pavement can be optimized so that the failure of the pavement initiates in surface, base, and subgrade layers at the same coverage level.

For multiple-wheel gear loads, the results in Figures 5 and 6 have their special merit because the influence of gear configuration on a particular pavement can be evaluated. For instance, the performance of pavements under the loading of the C-5A assembly has been evaluated experimentally in recently completed full-scale traffic tests (7). The performance of pavements under the loading of other multiple-wheel assemblies with different gear configurations can be evaluated readily by the method in this paper, and there is no need to conduct another full-scale traffic test that would be costly and time-consuming. It is also known (8) that the advantage of increasing the number of wheels in a gear assembly, such as the 12-wheel, main-gear C-5A assemblies, is that the load can be spread out into a larger area and, consequently, the deflections and shearing strains in the pavement are more reduced than those under an equivalent single-wheel load. The question often arises whether it is more economical to increase the number of wheels in a gear assembly or to increase the thickness of the airfield pavement to accommodate the demands imposed by ever-increasing heavy aircraft loads. The method in this paper provides a powerful tool for determining an optimum design for such a situation.

Evaluation of Pavements for Mixed Traffic and Overlays

The correlations in Figures 1 to 6 can be used to evaluate the performance of pavements subjected to mixed traffic and overlays of existing flexible pavements; the procedures for such an evaluation follow.

Mixed Traffic—When a certain percentage of the service life of an airfield pavement has been used by a given aircraft load, the remaining life of this pavement for another type of aircraft loading can be evaluated by using the proposed criteria as follows:

1. Required. For a pavement that was designed for 5,000 coverages for a 30-kip (133 kN) single-wheel load that has been trafficked for 2,000 coverages, determine the remaining service life of this pavement under a 50-kip (222 kN) single-wheel load.
2. Solution. A computation is first made for this pavement under a 50-kip (222 kN)

load and the anticipated coverages at failure are determined—for illustration, assume that the result is 1,000 coverages. Because 40 percent of the design service life of the pavement has already been used by the 30-kip (13 N) load, the pavement would sustain 600 more coverages of the 50-kip (22 N) load.

Overlays—For the pavement described in the previous example, 3 in. (7.6 cm) of asphaltic concrete may be required for resurfacing the old pavement to satisfy durability requirements when the load is increased from 30 (133 kN) to 50 kips (222 kN). The remaining service life of the pavement with the overlay can be evaluated accordingly. Computation is first made for the new pavement, i.e., the original pavement plus the overlay, and the anticipated coverages at failure are then determined. Assuming that 1,500 coverages are indicated instead of the original 1,000, the pavement with overlay would then be expected to sustain 900 additional coverages under the 30 (133 kN) to 50 kips (222 kN) load.

The method of evaluating existing pavements described is still tentative. Its validity needs further verification by field performance comparisons and from controlled tests.

CONCLUSIONS

Good correlations have been established between the observed performance of numerous accelerated traffic test pavements, under both single- and multiple-wheel gear loads, and the stresses and strains computed for these pavements by the nonlinear finite-element method. The limiting criteria are vertical strain on the subgrade surfaces, shear failure in unbound bases, and radial tensile strain in the asphaltic concrete layers.

Good correlations were obtained for pavements with subgrade soils of low and medium CBRs when the relation E = 1,500 CBR was used in the analysis, but such correlations were not obtained for pavements with subgrade soils with high CBRs.

The criteria developed are applicable to designing new pavements for new aircrafts and to evaluating pavement performance under mixed traffic and with overlays. With the limiting criteria, the thickness of each component layer of the pavement can be optimized, i.e., failure would initiate in the surface, base, and subgrade layers at the same coverage level.

REFERENCES

1. Kingham, R. I., and Kallas, B. F. Laboratory Fatigue and Its Relationship to Pavement Performance. Proc., Third Internat. Conf. on the Structural Design of Asphalt Pavements, 1972, Figs. 6 and 7.
2. Hicks, R. G. Factors Influencing the Resilient Properties of Granular Materials. Univ. of California, PhD dissertation, 1970.
3. Seed, H. R., Chen, C. K., and Lee, C. E. Resilience Characteristics of Subgrade Soils and Their Relation to Fatigue Failures in Asphalt Pavements. Proc., First Internat. Conf. on the Structural Design of Asphalt Pavements, 1962.
4. Heukelom, W., and Foster, C. R. Dynamic Testing of Pavements. Journal of Soil Mechanics and Foundations Div., ASCE, 1960.
5. Accelerated Traffic Test at Stockton Airfield, Stockton, California (Stockton Test No. 2). O. J. Porter and Company, Consulting Engineer, for U.S. Army Corps of Engineers, Sacramento District, May 1948.
6. Investigation of Effects of Traffic With High-Pressure Tires on Asphalt Pavements. U.S. Army Engineer Waterways Experiment Station, Corps of Engineers, Vicksburg, Miss., Tech. 3-312, May 1950.
7. Flexible Pavement Behavior Studies. U.S. Army Engineer Waterways Experiment Station, Corps of Engineers, Vicksburg, Miss., Interim Rept. 2, May 1947.
8. Ahlvin, R. G., et al. Multiple-Wheel Heavy Gear Load Pavements Tests. U.S. Army Engineer Waterways Experiment Station, Corps of Engineers, Vicksburg, Miss, Tech. Rept. S-71-17, Vol. 1-4, Nov. 1971.
9. A Limited Study of Effects of Traffic With High-Pressure Tires on Asphalt Pavements. U.S. Army Engineer Waterways Experiment Station, Corps of Engineers, Vicksburg, Miss., Tech. Rept. 3-587, Jan. 1962.
10. Burns, C. D., Ledbetter, R. H., and Grau, R. W. Study of Behavior of Bituminous-

Stabilized Pavement Layers. U.S. Army Engineer Waterways Experiment Station, Corps of Engineers, Vicksburg, Miss., misc. paper S-73-4, March 1973.
11. Grau, R. W. Evaluation of Structure Layers in Flexible Pavement. U.S. Army Engineer Waterways Experiment Station, Corps of Engineers, Vicksburg, Miss., misc. paper S-73-26, May 1973.
12. Brown, S. F., and Pell, P. S. A Fundamental Structural Design Procedure for Flexible Pavements. Proc., Third Internat. Conf. on the Structural Design of Asphalt Pavements, 1972.
13. Chou, Y. T. A Method for Predicting Performance of Flexible Airfield Pavements. U.S. Army Engineer Waterways Experiment Station, Corps of Engineers, Vicksburg, Miss., in preparation.
14. Ahlvin, R. G., Chou, Y. T., and Hutchinson, R. L. The Principle of Superposition in Pavement Analysis. Highway Research Record 466, 1973, pp. 153-160.

ELASTIC LAYER ANALYSIS RELATED TO PERFORMANCE IN FLEXIBLE PAVEMENT DESIGN

Friedrich W. Jung and William A. Phang,
Ministry of Transportation and Communications, Ontario

From experience in Ontario with flexible pavements and from results of the AASHO Road Test, it was found that the calculated subgrade deflection under a standard wheel load is the best indicator of performance of the pavement as a whole when it is compared with other stress, strain, and deformation values calculated by elastic layer theory. In the calculations, layer equivalencies obtained from experience and variations in subgrades were expressed in terms of elastic moduli. Subgrade deflections can be calculated more simply by using Odemark's concept of equivalent layer thickness. Expressions for load equivalency factors were derived from AASHO Road Test data by using this simplified deflection calculation. Finally, a functional relationship between subgrade deflection, number of standard load applications, and present serviceability index was established. The findings constitute major parts of a design subsystem to be used within a management system for flexible pavements.

•THROUGH a process of continual pavement evaluation, pavement design engineers in Ontario were able to compile a table of successful thickness designs (1). The table recognizes differences in thickness caused by the traffic, road class, and type of subgrade. Elastic layer analysis was used to examine the table to find a more rational method of flexible pavement design. It was hoped that a possible clue to the success of the conventional designs listed in the table might be found.

The method of investigation was to assign values of elastic moduli to each pavement layer and subgrade class and to calculate stresses, strains, and deflections in each layer for a standard wheel load. The elastic moduli assigned to each pavement layer and to each class of subsoil were selected after a study of available literature. The calculated stresses, strains, and deflections were examined for a constant value of these parameters within each traffic or highway class. A constant value within the same road class over the six major subgrade types identified within Ontario could indicate a common distress mechanism and would provide a practical criterion for design.

In this process of calculation, in which the Chevron computer program was used, many different sets of moduli were assigned to the pavement layers and subgrades. Through this procedure, it was discovered that only the vertical deflection on top of the subgrade emerged as the response value, which could be made to remain constant within each traffic or road class. Several sets of assumed moduli were successful in this respect. Subgrade deflections were also calculated by a simplified method that uses the principle of equivalent layer thickness as proposed by Odemark (3).

The course of investigation was then directed to the best documented experiment available.

AASHO ROAD TEST

Two sets of moduli, which had been applied successfully to the Ontario designs,

Publication of this paper sponsored by Committee on Flexible Pavement Design.

were assigned to the layers of the main factorial designs of the AASHO Road Test (5, 6), and the subgrade deflections were calculated for both the applied single-axle load in each loop and the standard 18-kip (80 kN) axle load. A statistical analysis of these calculated deflections not only resulted in a formula for load equivalency factors but culminated in finding a relationship between the loss of performance or serviceability and the number of equivalent standard load applications for given values of subgrade deflection.

By using sets of elastic moduli for calculating subgrade deflections, we demonstrated that this deflection is linked to standards of performance or serviceability. The design subsystem of this research is shown in Figure 1. An equation was derived for determining the necessary total equivalent granular thickness so that the design method could be completed.

EXPLORING SUCCESSFUL ONTARIO DESIGNS

Ontario's successful designs, which have survived an average of about 11.5 years, are given in Tables 1 and 2. The lines in the table pertain to traffic or road classes indicated by approximate average daily traffic values. The columns of the table pertain to the types of subgrade soils as they are classified in Ontario.

For each of the calculations, basically two sets of moduli were assumed and subsequently varied and modified into different sets with which calculations were continued. These two sets were the subgrade moduli E_n, which constitute a decreasing sequence from hard subgrades (granular) to soft subgrades (soft clay) and the layer moduli E_1, E_2, and E_3 for asphaltic hot mix, granular base, and sand subbase. Cases 1, 2, 3, and 4 of these calculations were finally assembled, which may be thought of as being based on true or realistic relations between the assumed moduli. The moduli E_1, E_2, and E_3 of these four cases are related to the layer equivalencies, valid in Ontario, as follows:

$$\text{hot mix : base : subbase} = 1 : 2 : 3 = \frac{1}{\sqrt[3]{E_1}} : \frac{1}{\sqrt[3]{E_2}} : \frac{1}{\sqrt[3]{E_3}} \qquad (1)$$

The relationship between the set of layer moduli and the set of subgrade moduli is different in all four cases, and this indicates insensitivity about this relationship.

For a wheel load of 9,000 lb (40 kN) and a pressure area radius of 6.4 in. (16.3 cm), all stresses, strains, and deflections at the layer interfaces were calculated. The most important of these are shown in Figure 2 and their values for cases 3 and 4 are given in Tables 3 and 4. In all four cases assembled, only the deflections on top of the subgrade were approximately equal for each of the five traffic or road classes. This indicates that this deflection could be a powerful design criterion.

SUBGRADE DEFLECTION AS DESIGN CRITERION

The calculations on the successful Ontario designs revealed that the most promising design parameter for flexible pavements was the vertical deflection on top of the subgrade. This hypothesis is in line with previous research findings (2) in which the vertical compressive strain on the subgrade was declared the dominating design parameter. These findings were based on the AASHO Road Test, which was carried out on the same subsoil. For constant subgrade modulus the two criteria are indeed equivalent, but the strain criterion obviously breaks down if a wide range of subgrades is considered. The same is true for the corresponding stress.

Tensile stress or strain in the asphaltic layer must be considered, although it is probably a secondary design criterion. For instance, the thickness of the asphaltic layers, as a portion of the total equivalent thickness, could possibly be determined by the magnitude of tensile strain under repeated loads (fatigue) and under varying temperature conditions, whereas the total thickness is still determined by the subgrade deflection.

If only subgrade deflections are needed, then it is more economical to calculate them by the method suggested by Odemark (3, 4). The deviations of the following design equations based on subgrade deflections can be studied in more detail in the

Figure 1. Pavement design subsystem.

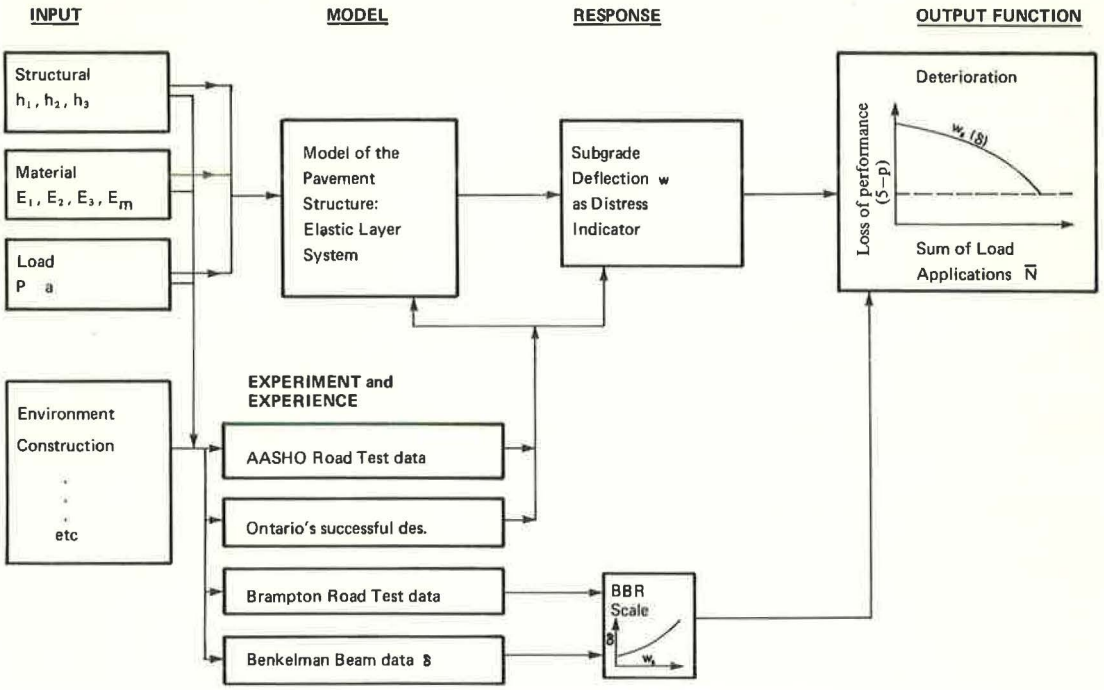

Table 1. Moduli of successful Ontario designs.

		Subgrade Material, psi					
		Grain Type of Materials Suitable as Granular Borrow	Sandy Silt and Clay, Loam Till			Clay	
Case	Modulus		Silt <40, Very Fine Sand and Silt <45	Silt 40 to 50, Very Fine Sand and Silt 45 to 60	Silt >50, Very Fine Sand and Silt >60	Hard Lacustrine	Soft Varved and Leda
1	E_1	400,000	400,000	400,000	400,000	400,000	400,000
	E_2	50,000	50,000	50,000	50,000	50,000	50,000
	E_3	—	15,000	15,000	15,000	15,000	15,000
	E_s[2]	15,000	8,500	7,000	5,700	7,500	3,800
2	E_1	320,000	320,000	320,000	320,000	320,000	320 000
	E_2	40,000	40,000	40,000	40,000	40,000	40,000
	E_3	—	12,000	12,000	12,000	12,000	12,000
	E_s	15,000	8,400	6,900	5,700	7,600	3,900
3	E_1	400,000	400,000	400,000	400,000	400,000	400,000
	E_2	50,000	50,000	50,000	50,000	50,000	50,000
	E_3	—	15,000	15,000	15,000	15,000	15,000
	E_s	11,000	6,000	5,000	4,000	5,300	2,700
4	E_1	600,000	600,000	600,000	600,000	600,000	600,000
	E_2	75,000	75,000	75,000	75,000	75,000	75,000
	E_3	—	22,000	22,000	22,000	22,000	22,000
	E_s	11,000	6,000	5,000	4,000	5,300	2,700

Note: 1 psi = 6.8948 kPa.

Table 2. Average subgrade deflections of successful Ontario designs.

Class and Road	Thickness	Subgrade Material Thickness, in.						Average Deflection Values, in.[b]			
		Grain Type of Materials Suitable as Granular Borrow	Sandy Silt and Clay Loam Till			Clay					
			Silt <40, Very Fine Sand and Silt <45	Silt 40 to 50, Very Fine Sand and Silt 45 to 60	Silt >50, Very Fine Sand and Silt >60	Hard Lacustrine	Soft Varved and Leda				
King's highways Multilane	h_1	5.5	5.5	5.5	5.5	5.5	5.5	0.0128	0.0136	0.0163	0.0144
	h_2	7.5, 6.5[a]	6	6	6	6	6				
	h_3	—	15	21, 20[a]	27	18	42	0.0119	0.0129	0.0152	0.0133
Two lanes, AADT	h_1	4.5	4.5	4.5	4.5	4.5	4.5	0.0136	0.0145	0.0172	0.0151
	h_2	7.5	6	6	6	6	6				
>2,000	h_3	—	15	21, 20[a]	27	18	42	0.0128	0.0138	0.0162	0.0142
Two lanes, AADT	h_1	3.5	3.5	3.5	3.5	3.5	3.5	0.0167	0.0178	0.0212	0.0186
	h_2	6	6	6	6	6	6				
<2,000	h_3	—	12, 11[a]	15	21	12	30	0.0159	0.0170	0.0206	0.0177
Secondary roads, AADT >1,000	h_1	1.5	1.5	1.5	1.5	1.5	1.5	0.0202	0.0217	0.0259	0.0227
	h_2	6, 6.5[a]	6	6	6	6	6				
	h_3	—	9	12	21, 18[a]	12	30, 27[a]	0.0200	0.0200	0.0260	0.0230
Township roads, AADT >200	h_1	1.5	1.5	1.5	1.5	1.5	1.5	0.0268	0.0286	0.0347	0.0297
	h_2	4	6	6	6	6	6				
	h_3	—	4	6	9	6	18	0.0260	0.0280	0.0338	0.0298

Note: 1 in. = 2.54 cm.

[a]Modified thicknesses only used for cases 3 and 4. [b]Upper values for each entry set are for Chevron; the bottom for Odemark.

Table 3. Calculated criteria for case 3.

Class of Road	Type of Criterion or Distress Indicator	Subgrade Material						
		Grain Type of Materials Suitable as Granular Borrow[a]	Sandy Silt and Clay Loam Till			Clay		Average Deflection Values (in.)
			Silt <40, Very Fine Sand and Silt <45[b]	Silt 40 to 50, Very Fine Sand and Silt >45[c]	Silt >50, Very Fine Sand and Silt >60[d]	Hard[e]	Soft[f]	
King's highways Multilane	Subgrade deflection, Chevron, in.	0.0157	0.0159	0.0163	0.0168	0.0162	0.0171	0.0163
	Subgrade deflection, Odemark, in.	0.0152	0.0151	0.0158	0.0153	0.0153	0.0155	0.0152
	Total deflection, Chevron, in.	0.0186	0.0236	0.0249	0.0265	0.0246	0.0284	0.0244
	Total deflection, Odemark, in.	0.0168	0.0191	0.0194	0.0198	0.0194	0.0199	0.0191
Two lanes, >2,000 AADT	Subgrade deflection, Chevron, in.	0.0167	0.0170	0.0177	0.0176	0.0172	0.0179	0.0172
	Subgrade deflection, Odemark, in.	0.0161	0.0162	0.0172	0.0162	0.0164	0.0162	0.0162
	Total deflection, Chevron, in.	0.0203	0.0262	0.0274	0.0289	0.0271	0.0308	0.0268
	Total deflection, Odemark, in.	0.0182	0.0211	0.0213	0.0214	0.0213	0.0214	0.0208
Two lanes, <2,000 AADT	Subgrade deflection, Chevron, in.	0.0207	0.0208	0.0206	0.0207	0.0216	0.0228	0.0212
	Subgrade deflection, Odemark, in.	0.0200	0.0199	0.0199	0.0198	0.0210	0.0211	0.0203
	Total deflection, Chevron, in.	0.0245	0.0306	0.0319	0.0334	0.0321	0.0370	0.0316
	Total deflection, Odemark, in.	0.0223	0.0251	0.0255	0.0256	0.0261	0.0267	0.0252
Secondary road, paved >1,000 AADT	Subgrade deflection, Chevron, in.	0.0262	0.0263	0.0264	0.0250	0.0254	0.0263	0.0259
	Subgrade deflection, Odemark, in.	0.0263	0.0266	0.0267	0.0253	0.0257	0.0257	0.0260
	Total deflection, Chevron, in.	0.0316	0.0402	0.0418	0.0426	0.0408	0.0460	0.0405
	Total deflection, Odemark, in.	0.0305	0.0354	0.0360	0.0353	0.0352	0.0357	0.0346
Township road, paved >200 AADT	Subgrade deflection, Chevron, in.	0.0334	0.0357	0.0340	0.0344	0.0327	0.0326	0.0347
	Subgrade deflection, Odemark, in.	0.0334	0.0337	0.0346	0.0351	0.0332	0.0332	0.0338
	Total deflection, Chevron, in.	0.0376	0.0487	0.0463	0.0488	0.0449	0.0505	0.0461
	Total deflection, Odemark, in.	0.0362	0.0400	0.0415	0.0427	0.0403	0.0416	0.0404
King's highways Multilane	Vertical subgrade stress, psi	-6.88	-2.09	-1.51	-1.03	-1.70	-0.532	—
	Vertical subgrade strain, in.	-0.000505	-0.000314	-0.000269	-0.000223	-0.000287	-0.000167	—
	Radial asphalt stress, psi	142.0	142.0	140.0	139.0	141.0	137.0	—
	Radial asphalt strain, in.	0.000204	0.000204	0.000202	0.000200	0.000203	0.000198	—
Two lanes, >2,000 AADT	Vertical subgrade strain, psi	-7.82	-2.44	-1.72	-1.14	-1.96	-5.69	—
	Vertical subgrade strain, in.	-0.000583	-0.000370	-0.000311	-0.000251	-0.000334	-0.000179	—
	Radial asphalt stress, psi	153.0	159.0	157.0	156.0	158.0	154.0	—
	Radial asphalt strain, in.	0.000227	0.000233	0.000231	0.000230	0.000232	0.000227	—
Two lanes, <2,000 AADT	Vertical subgrade stress, psi	-11.7	-3.72	-2.55	-1.64	-3.14	-8.98	—
	Vertical subgrade strain, in.	-0.000849	-0.000535	-0.000467	-0.000369	-0.000543	-0.000285	—
	Radial asphalt stress, psi	179.0	173.0	171.0	169.0	172.0	167.0	—
	Radial asphalt strain, in.	0.000269	0.000262	0.000260	0.000258	0.000262	0.000256	—
Secondary road, paved >1,000 AADT	Vertical subgrade stress, psi	-18.9	-6.03	-4.30	-2.51	-4.45	-1.22	—
	Vertical subgrade strain, in.	-0.000138	-0.000925	-0.000793	-0.000574	-0.000776	-0.000395	—
	Radial asphalt stress, psi	82.0	74.9	73.1	73.6	74.0	74.4	—
	Radial asphalt strain, in.	0.000186	0.000176	0.000174	0.000175	0.000175	0.000176	—
Township road, paved >200 AADT	Vertical subgrade stress, psi	-28.3	-10.6	-6.99	-4.73	-7.24	-1.95	—
	Vertical subgrade strain, in.	-0.001870	-0.001570	-0.001270	-0.001080	-0.001240	-0.000645	—
	Radial asphalt stress, psi	135.0	117.0	72.3	68.7	73.2	69.4	—
	Radial asphalt strain, in.	0.000264	0.000223	0.000172	0.000168	0.000174	0.000170	—

Note: Modulus of (a) hot mix asphalt E_1 = 400,000; (b) the base E_2 = 50,000; and (c) the subbase E_3 = 15,000. 1 in. = 2.54 cm. 1 psi = 6.8948 kPa.

[a]E_m = 11,000. [b]E_m = 6,000. [c]E_m = 5,000. [d]E_m = 4,000. [e]E_m = 5,300. [f]E_m = 2,700.

Figure 2. Diagram of multilayer structure.

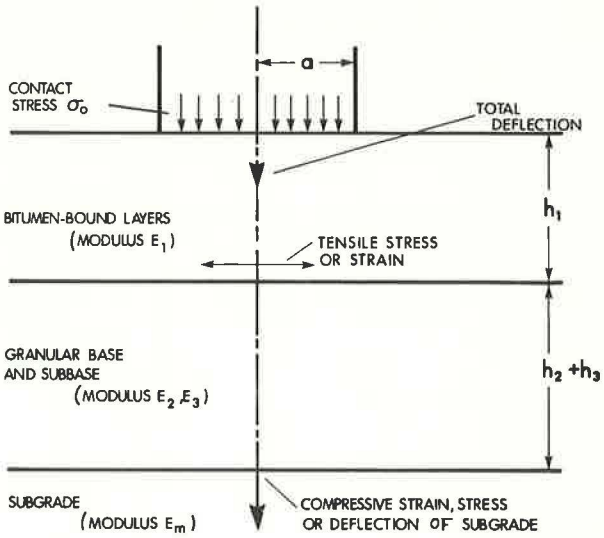

Table 4. Calculated criteria for case 4.

Class of Road	Type of Criterion or Distress Indicator	Subgrade Material: Grain Type of Materials Suitable as Granular Borrow[a]	Sandy Silt and Clay Loam Till: Silt <40, Very Fine Sand and Silt <45[b]	Sandy Silt and Clay Loam Till: Silt 40 to 50, Very Fine Sand and Silt >45[c]	Sandy Silt and Clay Loam Till: Silt >50, Very Fine Sand and Silt >60[d]	Clay: Hard[e]	Clay: Soft[f]	Average Deflection Values (in.)
King's highways								
Multilane	Subgrade deflection, Chevron, in.	0.0138	0.0141	0.0145	0.0150	0.0144	0.0146	0.0144
	Subgrade deflection, Odemark, in.	0.0134	0.0132	0.0133	0.0134	0.0134	0.0136	0.0134
	Total deflection, Chevron, in.	0.0159	0.0195	0.0205	0.0217	0.0202	0.0225	0.0200
	Total deflection, Odemark, in.	0.0143	0.0154	0.0157	0.0159	0.0157	0.0161	0.0155
Two lanes, >2,000 AADT	Subgrade deflection, Chevron, in.	0.0146	0.0150	0.0153	0.0157	0.0153	0.0152	0.0151
	Subgrade deflection, Odemark, in.	0.0142	0.0143	0.0143	0.0142	0.0144	0.0142	0.0143
	Total deflection, Chevron, in.	0.0172	0.0214	0.0223	0.0235	0.0221	0.0243	0.0218
	Total deflection, Odemark, in.	0.0153	0.0170	0.0171	0.0172	0.0171	0.0172	0.0168
Two lanes, <2,000 AADT	Subgrade deflection, Chevron, in.	0.0182	0.0181	0.0181	0.0184	0.0189	0.0201	0.0186
	Subgrade deflection, Odemark, in.	0.0177	0.0175	0.0175	0.0174	0.0184	0.0185	0.0178
	Total deflection, Chevron, in.	0.0210	0.0250	0.0260	0.0271	0.0262	0.0299	0.0259
	Total deflection, Odemark, in.	0.0190	0.0204	0.0206	0.0206	0.0213	0.0217	0.0206
Secondary road, paved >1,000 AADT	Subgrade deflection, Chevron, in.	0.0231	0.0230	0.0230	0.0220	0.0221	0.0233	0.0227
	Subgrade deflection, Odemark, in.	0.0235	0.0235	0.0235	0.0223	0.0226	0.0226	0.0230
	Total deflection, Chevron, in.	0.0270	0.0327	0.0337	0.0341	0.0328	0.0368	0.0328
	Total deflection, Odemark, in.	0.0261	0.0286	0.0289	0.0280	0.0281	0.0283	0.0280
Township road, paved >200 AADT	Subgrade deflection, Chevron, in.	0.0249	0.0314	0.0297	0.0299	0.0286	0.0288	0.0297
	Subgrade deflection, Odemark, in.	0.0302	0.0298	0.0305	0.0309	0.0293	0.0290	0.0299
	Total deflection, Chevron, in.	0.0332	0.0408	0.0384	0.0400	0.0372	0.0411	0.0384
	Total deflection, Odemark, in.	0.0320	0.0335	0.0345	0.0353	0.0334	0.0339	0.0338
King's highways								
Multilane	Vertical subgrade stress, psi	-5.43	-1.64	-1.20	-0.824	-1.34	-0.426	—
	Vertical subgrade strain, in.	-0.000388	-0.000242	-0.000207	-0.00172	-0.000220	-0.000130	—
	Radial asphalt stress, psi	151.0	144.0	142.0	140.0	143.0	137.0	—
	Radial asphalt strain, in.	0.000142	0.000137	0.000136	0.000134	0.000136	0.000132	—
Two lanes, >2,000 AADT	Vertical subgrade stress, psi	-6.17	-1.91	-1.36	-0.910	-1.54	-0.455	—
	Vertical subgrade strain, in.	-0.000447	-0.000286	-0.000238	-0.000193	-0.000257	-0.000139	—
	Radial asphalt stress, psi	161.0	161.0	158.0	156.0	159.0	153.0	—
	Radial asphalt strain, in.	0.000157	0.000157	0.000155	0.000153	0.000156	0.000151	—
Two lanes, <2,000	Vertical subgrade stress, psi	-9.29	-2.92	-1.99	-1.29	-2.54	-0.715	—
	Vertical subgrade strain, in.	-0.00656	-0.000412	-0.000358	-0.000280	-0.000419	-0.000217	—
	Radial asphalt stress, psi	190.0	175.0	172.0	169.0	174.0	167.0	—
	Radial asphalt strain, in.	0.000188	0.000176	0.000174	0.000172	0.000176	0.000170	—
Secondary road, paved >1,000 AADT	Vertical subgrade stress, psi	-15.10	-4.75	-3.36	-1.95	-3.49	-0.966	—
	Vertical subgrade strain, in.	-0.001070	-0.000722	-0.000611	-0.000435	-0.000600	-0.00298	—
	Radial asphalt stress, psi	80.6	69.1	67.9	69.6	68.7	71.1	—
	Radial asphalt strain, in.	0.000122	0.000112	0.000112	0.000113	0.000112	0.000114	—
Township road, paved >200 AADT	Vertical subgrade stress, psi	-23.30	-8.44	-5.48	-3.67	-5.68	-1.51	—
	Vertical subgrade strain, in.	-0.000490	-0.001240	-0.000984	-0.000822	-0.000965	-0.000480	—
	Radial asphalt stress, psi	150.0	114.0	66.2	62.9	67.2	65.5	—
	Radial asphalt strain, in.	0.000173	0.000146	0.000110	0.000107	0.000110	0.000110	—

Note: Modulus of (a) the hot-mix asphalt E_1 = 600,000; (b) the base E_2 = 75,000; and (c) the subbase E_3 = 22,000. 1 in. = 2.54 cm. 1 psi = 6.8948 kPa.

[a] E_m = 11,000. [b] E_m = 6,000. [c] E_m = 5,000. [d] E_m = 4,000. [e] E_m = 5,300. [f] E_m = 2,700.

Appendix. The variable measurements may be either U.S. customary or metric units.

$$w = \frac{P}{2E_m z} \times \frac{1}{\sqrt{1 + \frac{a}{z}}} \tag{2}$$

where

$$z = 0.9 \times \sum_{i=1}^{m-1} h_i \sqrt[3]{\frac{E_i}{E_m}} \tag{3}$$

and where

w = subgrade deflection in inches;
m = number of layers including subgrade;
h_i = thickness of layer i in inches;
E_i = modulus of layer i in psi;
E_m = subgrade modulus in psi;
a = radius of loaded area in inches; and
P = wheel load in lb.

The deflections w calculated in Eqs. 1 and 2 differ slightly from the subgrade deflections calculated with the Chevron program (Tables 2, 3, and 4). The correlation coefficient r between the two calculated deflections, however, was found to be close enough to unity (r = 0.993 to 0.997) so that the much simpler method of calculation by Eqs. 2 and 3 is justified. The correlation between the two deflections of case 3 is shown in Figure 3.

SUBGRADE DEFLECTIONS OF AASHO ROAD TEST SECTIONS

Subgrade deflections w have been calculated for all designs given in Tables 1 and 2 and, for the moduli of cases 1 through 4, these deflections were approximately equal for each highway traffic class. In these calculations the applied load was constant, but the subgrade material E_m was one of the main variables.

In contrast to this, the main factorial design sections of the AASHO Road Test were built on a uniform subgrade material (soft clay), but were exposed to a variety of axle loads (5). By using Eqs. 2 and 3, subgrade deflections w were calculated for these AASHO Road Test designs. The wheel loads P of the single-axle weights in each loop were assumed to be uniformly distributed over a circle of radius a according to recorded tire pressures (6).

Based on a scale (7, fig. 28) and a soil support value of S = 3, the modulus of the subgrade was assumed to be E_m = 3,000 psi (20.7 MPa). The moduli of the pavement layers were assumed to be the same as in the calculations on the Ontario designs (Tables 3 and 4).

The number of weighted, i.e., seasonably adjusted, load applications N for a terminal present serviceability index (PSI) p = 2.5 and the corresponding values of $N_{1.5}$ for p = 1.5 are given elsewhere (5, table 8; 5, table 6 respectively). Correlation regression analyses were performed on all four sets of data ($N_{2.5}$ and $N_{1.5}$, cases 3 and 4) for loops 3, 4, 5, and 6 separately, and the results are given in Tables 4 and 5.

If separate plots for each loop in each case are made and if each regression equation in the tables is drawn and modified, the regression analyses could be harmonized into the following expression based on a constant rounded average value of six for the slopes (exponent of w).

$$N = \frac{1}{w^6 \times 10^{K-0.09P}} \tag{4}$$

Figure 3. Correlation of subgrade deflections.

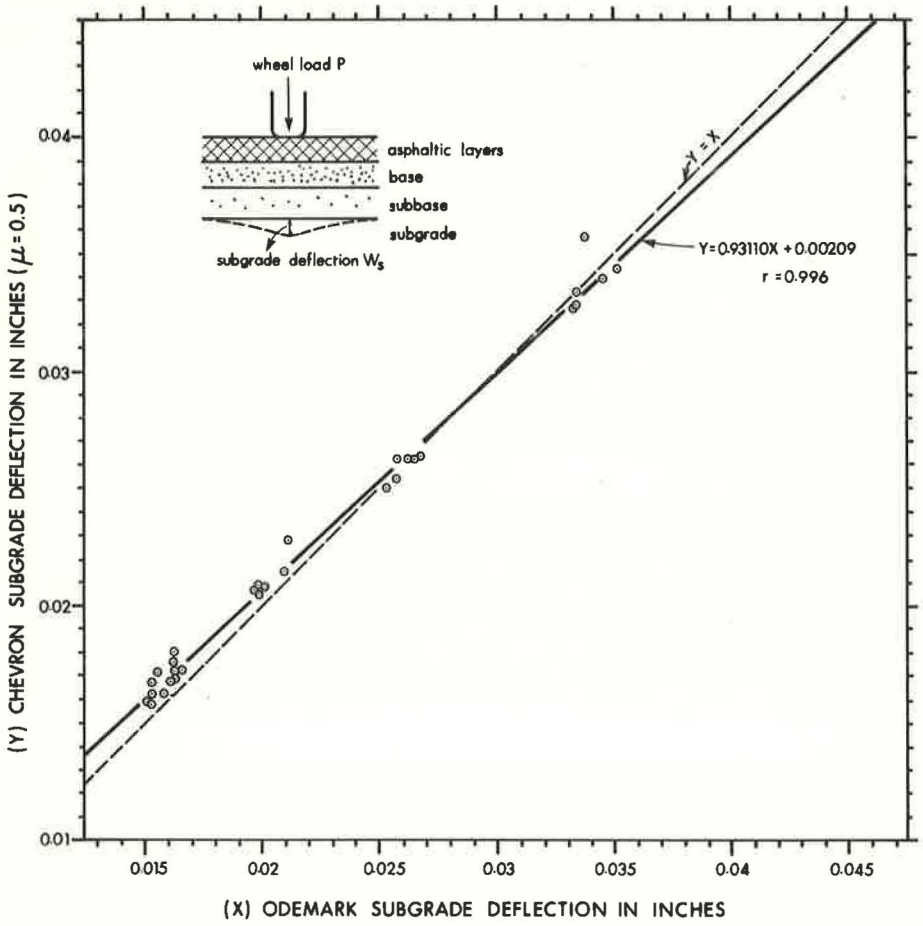

Table 5. Correlation regression equations for AASHO Road Test results (p = 2.5).

Loop Number	Axle Load (kips)	Equations for Case 3	Equations for Case 4	Sample Size
3	12	log N = -4.567 log w - 1.529	log N = -4.520 log w - 1.715	27
4	18	log N = -5.843 log w - 2.892	log N = -5.795 log w - 3.151	28
5	22.4	log N = -5.745 log w - 2.729	log N = -5.672 log w - 2.959	27
6	30	log N = -6.156 log w - 2.857	log N = -6.118 log w - 3.152	27
Suggested predicting equation[a] for $\overline{N} = e^{N}$		log $\overline{N}$ = -6 log w_s - 3.22	log $\overline{N}$ = -6 log w_s - 3.56	109

Note: Measurement of w and w_s is in inches. 1 in. = 2.54 cm. 1 kip = 4.448 222 N.

[a]Standard error of prediction of log $\overline{N}$ = 0.26; standard error in slope = 0.19. Standard error in Y-intercept = 0.58; correlation coefficient = -0.95.

where the following are values for the constant K

Values	Case 3	Case 4
For p = 2.5	4.03	4.37
For p = 1.5	3.94	4.28
Difference, $K_{2.5} - K_{1.5}$	0.09	0.09

and the wheel load P is to be measured in 1,000-lb (4.45 kN) units.

LOAD EQUIVALENCY FACTOR

Equation 4 was established for a wide range of wheel loads P. The number of load applications N and the subgrade deflections w pertain to wheel load P. Equation 4 is also valid for the standard wheel load P_s, which is 9,000 lb (40 kN) ($P_s = 9$) or for any other value within the range of the loads being investigated. If a load of $P_s = 9$ is applied on any design section, the calculated subgrade deflection will be w_s, and, with these two values, Eq. 4 will predict the number of equivalent standard axle load applications N_s. From these considerations, the load equivalency factor $e = N_s/N$ can be derived and was found to be

$$e = \left(\frac{w}{w_s}\right)^6 \times 10^{-0.09\,(P - P_s)} \qquad (5)$$

The following equation is presented for large values of z and for a constant radius of tire pressure area $a = a_s$ = constant (which is the same for P and P_s):

$$e = \left(\frac{P}{P_s}\right)^6 \times 10^{-0.09\,(P - P_s)} \qquad (6)$$

(If P and P_s are metric, then the -0.09 coefficient changes accordingly.) Equation 6 has been plotted in Figure 4 for $P_s = 9$ [9,000 lb (40 kN)] together with equivalency factors derived by Shook and Chastain (8, 9). If Eq. 6 is true, it follows that the destructive effects of heavy axle loads $P > \bar{P}_s$ have usually been overestimated.

PREDICTION OF EQUIVALENT STANDARD AXLE LOAD APPLICATIONS

The weighted axle load applications $N_{2.5}$ and $N_{1.5}$ (5, tables 6 and 8) were converted into numbers of equivalent standard 18-kip loads ($\bar{N}_{2.5} = e \times N_{2.5}$ and $\bar{N}_{1.5} = e \times N_{1.5}$) by using equivalency factors e calculated by Eq. 5.

$\bar{N}_{2.5}$ and $\bar{N}_{1.5}$ were then correlated with all the calculated deflections of loops 3, 4, 5, and 6 for cases 3 and 4. The results of these correlation regression analyses, each based on over 100 pairs of values $w_s - \bar{N}$, are as follows:

1. For case 3, p = 2.5: $\log \bar{N}_{2.5} = -5.93 \log w_s - 3.12$;
2. For case 3, p = 1.5: $\log \bar{N}_{1.5} = -5.94 \log w_s - 3.06$;
3. For case 4, p = 2.5: $\log \bar{N}_{2.5} = -5.90 \log w_s - 3.41$; and
4. For case 4, p = 1.5: $\log \bar{N}_{1.5} = -5.92 \log w_s - 3.35$.

In all four cases correlation coefficients $r \approx -0.95$, errors of prediction ≈ 0.26, 95 percent confidence limits of the slopes are approximately 5.5 to 6.3, and average standard error of the slope ≈ 0.19. The errors of prediction (≈ 0.26) compare favorably with the root-mean-square residual of the AASHO Road Test data, which is 0.31.

These correlation regression equations were then harmonized as before based on a constant slope of 6. The same equations were obtained as from Eq. 4 for P = 9 kips (40 kN). They are given in log form on the bottom of Tables 5 and 6. Plots of the points and the regression lines for cases 3 and 4 and for p = 2.5 are shown in Figures 5 and 6.

Thus, the subgrade deflection principle or model has been successfully applied to the AASHO Road Test data even with gross assumptions for the elastic moduli and layer

Figure 4. Load equivalency factor versus wheel load.

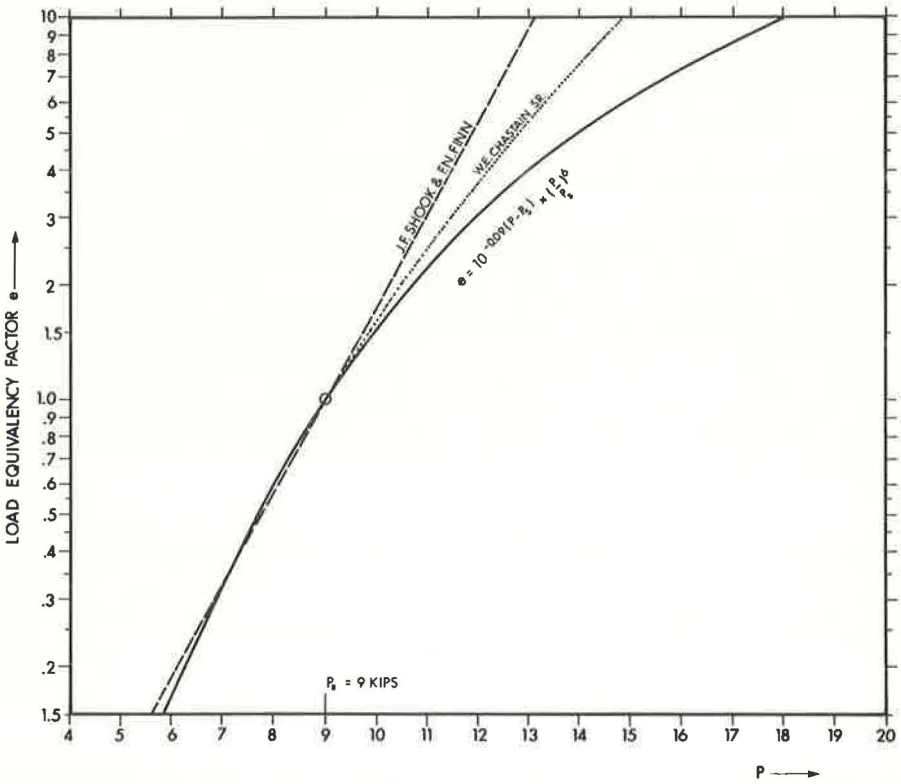

Table 6. Correlation regression equations for AASHO Road Test results (p = 1.5).

Loop Number	Axle Load (kips)	Equations for Case 3	Equations for Case 4	Sample Size
3	12	log N = -4.358 log w - 1.174	log N = -4.214 log w - 1.212	25
4	18	log N = -5.838 log w - 2.805	log N = -5.785 log w - 3.056	25
5	22.4	log N = -5.766 log w - 2.647	log N = -5.652 log w - 2.823	25
6	30	log N = -5.891 log w - 2.414	log N = -5.849 log w - 2.689	22
Suggested predicting equation[a] for $\overline{N}$ = e N		$\log \overline{N}_{18} = -6 \log w_s - 3.13$	$\log \overline{N} = -6 \log w_s - 3.47$	97

Note: Measurement of w and w_s is in inches. 1 in. = 2.54 cm. 1 kip = 4.448 222 N.

[a]Standard error of prediction of log $\overline{N}$ = 0.26; standard error in slope = 0.20. Standard error in Y-intercept = 0.59; correlation coefficient = -0.95.

Figure 5. Verification of predicting Eq. 4 for case 3.

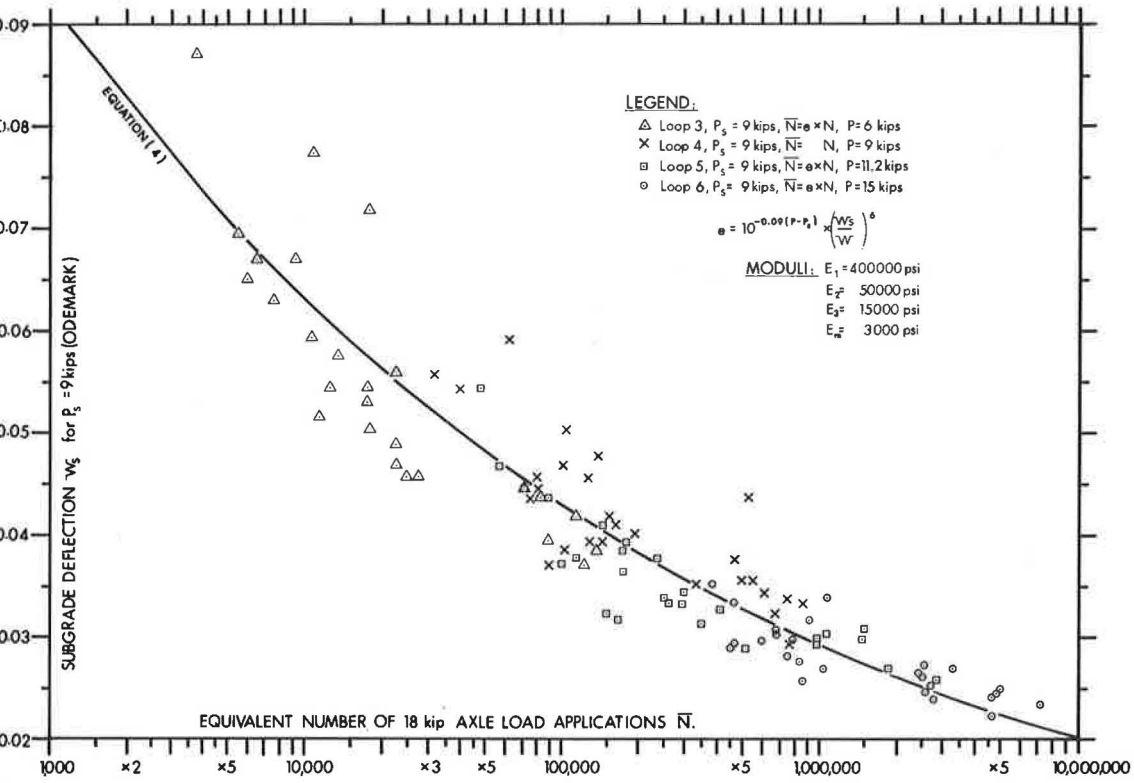

Figure 6. Verification of predicting Eq. 4 for case 4.

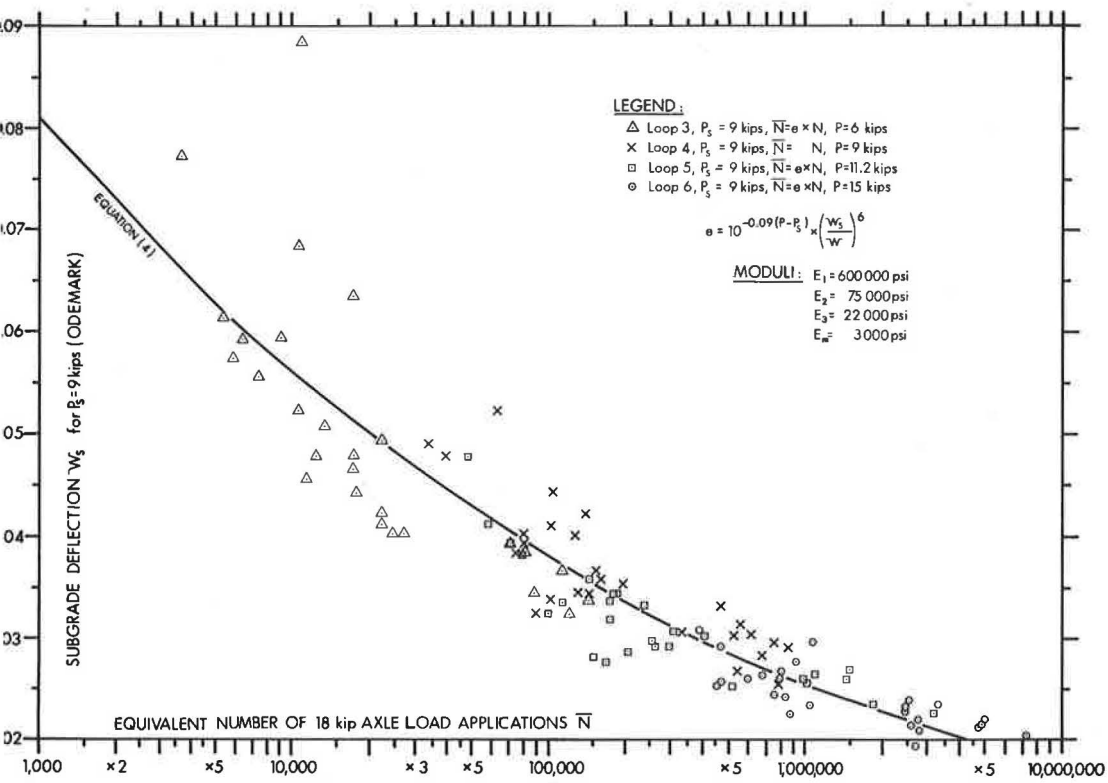

equivalencies. Equations 4, 5, and 6 and the regression equations were derived concurrently for both cases 3 and 4 with concordant results. This shows that the subgrade deflection model is not sensitive about the relation between subgrade and pavement layer moduli. From here on, investigations are restricted to case 3 as an example only.

LOSS OF SERVICEABILITY

The number of equivalent 18-kip axle load applications $\bar{N}$ for the two terminal levels of serviceability p = 2.5 and 1.5 (PSI) can be calculated by Eq. 4 by setting P = 9 kips (40 kN). This substitution leads to two expressions that have been combined into one performance equation relating $\bar{N}$ to the subgrade deflection w_s and to the loss in performance. With Eq. 4, and by using the K-values of case 3, by setting P_s = 9 kips (18-kip axle) [40 kN (80 kN)], and by assuming an initial value of p_0 = 4.2 (5), one can derive the following equation by connecting the three points p_0 = 4.2, p_1 = 2.5, and p_2 = 1.5 by a cubic parabola:

$$p = 4.200 - (1.22275\ \psi + 4.4024\ \psi^3) \tag{7}$$

where

$$\psi = 1000 \times w_s^6 \times \bar{N} \quad \text{for } w_s \text{ in inches} \tag{8}$$

or

$$\psi = 3.7238\ w_s^6 \times \bar{N} \quad \text{for } w_s \text{ in cm} \tag{9}$$

and where

w_s = deflection on top of the subgrade as a design parameter for the standard wheel load P_s = 9 kips (40 kN),
p = PSI, and
$\bar{N}_p$ = number of equivalent 18-kip (80 kN) axle weight applications.

The last term of Eq. 7 can be interpreted as the loss in PSI because of traffic loading.

$$p_L = 1.2228\ \psi + 4.402\ \psi^3 \tag{10}$$

In this form, the predicting equation could eventually be used more universally, for instance for other initial values p_0 and in other environments by including another loss term to account for additional losses from environmental forces, a concept which at present is being applied to the results of the Brampton Road Test (10, 11, 12). Figure 7 shows the losses p_L as a function of $\bar{N}$ and w_s.

REQUIRED EQUIVALENT GRANULAR THICKNESS

Equation 2 can be solved explicitly for z, and the resulting equation, with Eq. 3, can be multiplied by

$$\sqrt[3]{E_m/E_{2g}} \tag{11}$$

where E_{2g} is the modulus for granular A base material. In this way, a design equation may be derived:

$$H_e = \frac{1}{0.9} \times \sqrt{\left(\frac{P_s}{2E_m w_s}\right)^2 - a^2} \times \sqrt[3]{\frac{E_m}{E_{2g}}} \tag{12}$$

where H_e is the required granular thickness for the particular design in terms of granular A material. This thickness requirement H_e is the sum of all layer thicknesses multiplied by layer equivalency coefficients.

$$H_e = c_1h_1 + c_2h_2 + c_3h_3 + \ldots \tag{13}$$

Figure 7. Loss of performance or serviceability because of traffic loading (mean values).

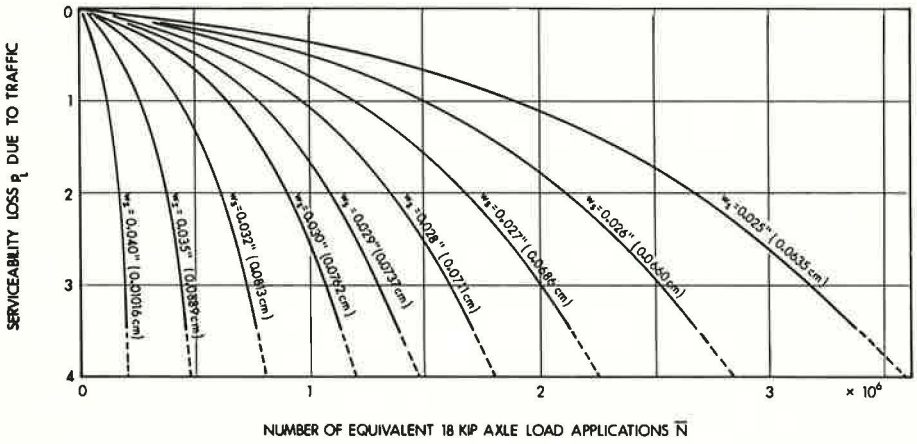

Figure 8. Design chart for flexible pavements in Ontario.

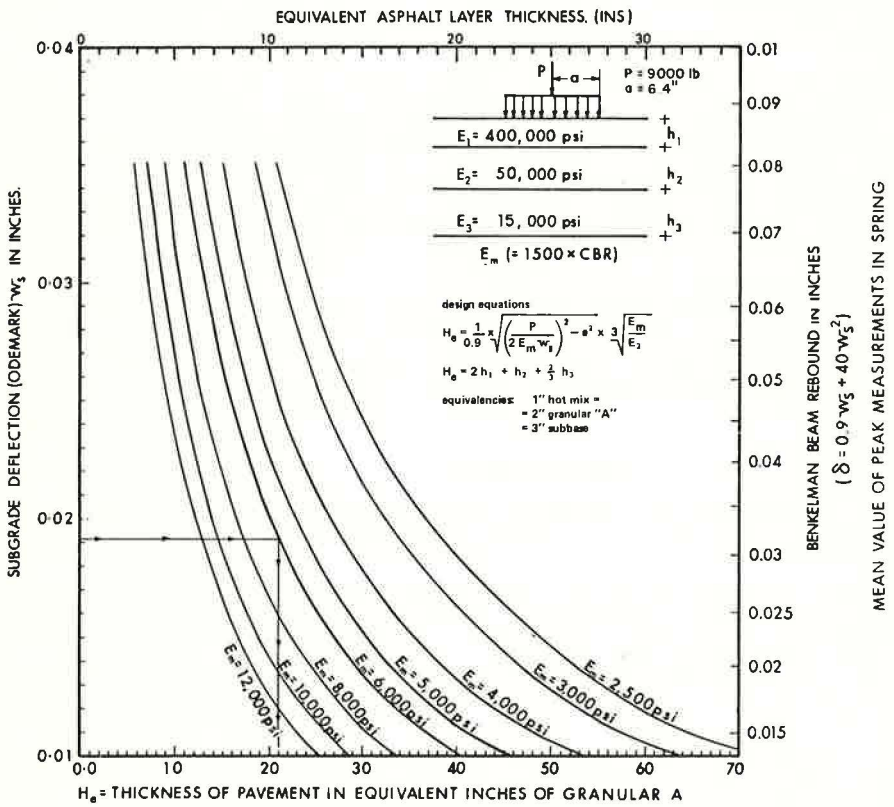

TYPICAL SUBGRADE MODULI IN ONTARIO

GRAN. TYPE MATERIALS SUITABLE AS GRAN. BORROW	SANDY SILT AND CLAY LOAM TILL			LACUSTRINE CLAYS	VARVED AND LEDA CLAYS
	SILT < 40 V.F. Sa and Si. < 45	SILT 40 - 50 V.F. Sa. and Si. 45-60	SILT > 50 V.F. Sa. and Si. > 60		
psi	psi	psi	psi	psi	psi
11,000	5,000 TO 7,000	4,000 TO 6,000	3,000 TO 5,000	3,500 TO 6,000	2,000 TO 4,500

These coefficients express the effect of each layer in resisting load P_s to generate a vertical deflection w_s on the subgrade, which is the design parameter. Therefore, they are (as in Eq. 3) related to the pavement layer moduli as follows:

$$c_1 = \sqrt[3]{\frac{E_1}{E_{2_g}}} \quad c_2 = \sqrt[3]{\frac{E_2}{E_{2_g}}} \quad c_3 = \sqrt[3]{\frac{E_3}{E_{3_g}}} \tag{14}$$

In this paper, coefficients were based on experience gained in Ontario, especially from the Brampton Road Test results (10): $c_1 = 2$, $c_2 = 1$, and $c_3 = \frac{2}{3}$. They determine the relation $E_1:E_2:E_3$ of the pavement layer moduli (Eq. 1) within the subgrade deflection concept (Eqs. 2 and 3). In other words, the pavement layer moduli were based on layer equivalencies determined from experience. This is justified if the performance is linked to the subgrade deflections w calculated by Eqs. 2 and 3. [The similarity of design Eqs. 12 and 13 with the Kansas formula (13, 14) is recognized.]

A design chart for determining the required total thickness in terms of H_s was drawn with Eq. 12 and is shown in Figure 8. The following example may show how to use the chart. The assigned Odemark subgrade deflection is $w_s = 0.019$ (to be taken from a suitable performance diagram similar to Fig. 7). The subgrade is a clay loam till with 30 percent silt and with very fine sand and silt of about 40 percent; therefore, select $E_s = 6{,}000$ psi (41.4 MPa) from the table in Figure 8. The required granular A thickness from the same figure is $H_s = 21$ in. (53 cm).

CONCLUSIONS

A practicable system of flexible pavement design, which is a subsystem of the whole pavement management system, can be based on simple concepts of linear elastic theory. An elastic layer system can serve as a structural design pavement model. The subgrade deflection for this model was found to be the most relevant distress indicator for the loss of performance of the pavement as a whole. The link between the response of this model, in terms of vertical deflections on the subgrade, and the output function, in terms of loss of performance, was established by considering past experience with successful Ontario designs and the AASHO Road Test.

The material characterizations and load applications of the input variables of this model, although not definitely established, were demonstrated and exemplified. Thus, experiences in Ontario were mainly used to establish realistic relations between layer and subgrade moduli, and AASHO Road Test data were used to exemplify the necessary range of loads.

REFERENCES

1. Phang, W. A., and Slocum, R. Pavement Decision Making and Management System. Ministry of Transportation and Communications, Ontario, Rept. RR174, Oct. 1971.
2. Dormon, G. M., and Edwards, J. M. Shell 1963 Design Charts for Flexible Pavements, An Outline of Their Development. Shell International Petroleum Co. Ltd., London, O.P.D. Rept. 232/64M, April 1964.
3. Odemark, N. Investigations as to the Elastic Properties and Soils and Design of Pavements According to the Theory of Elasticity. Statens Vaeginstitut, Stockholm, 1949.
4. Shook, J. F., and Finn, F. N. Thickness Design Relationships for Asphalt Pavements. Proc., International Conference on the Structural Design of Flexible Pavements, Univ. of Michigan, Ann Arbor, Aug. 1962, p. 52.
5. The AASHO Road Test, Report 5: Pavement Research. HRB Special Rept. 61 E, 1962.
6. The AASHO Road Test, Report 6: Special Studies. HRB Special Rept. 61 F, 1962.
7. Evaluation of AASHO Interim Guides for Design of Pavement Structures. NCHRP Rept. 128, 1972.
8. Schnitter, G., and Jentasch, R. J. Designing Flexible Road Pavements. Proc., International Conference on the Structural Design of Flexible Pavements, Univ. of Michigan, Ann Arbor, Aug. 1962, p. 537.

9. Secor, K. E., and Monismith, C. L. Viscoelastic Properties of Asphalt Cement. HRB Proc., Vol. 41, 1962, pp. 299-320.
10. Kamel, N. I., Morris, J., Haas, R. C. G., and Phang, W. A. Layer Analysis of the Brampton Test Road and Application to Pavement Design. Highway Research Record 466, 1973, pp. 113-126.
11. Phang, W. A. Four Years' Experience at the Brampton Test Road. Ministry of Transportation and Communications, Ontario, Research Rept. RR153, Oct. 1969.
12. Phang, W. A. The Effect of Seasonal Strength Variation on the Performance of Selected Base Materials. Ministry of Transportation and Communications, Ontario, Research Rept. IR39, April 1971.
13. De Barros, S. T. A Critical Review of Present Knowledge of the Problem of Rational Thickness of Design of Flexible Pavements. Highway Research Record 71, 1965, pp. 105-128.
14. Yoder, E. J. Principles of Pavement Design. John Wiley and Sons, New York, 1959.
15. Szechy, K. Der Grundbau, Vol. 1. Springer-Verlag, Vienna, 1963, p. 249.

APPENDIX

DESIGN FORMULA BASED ON SUBGRADE DEFLECTIONS

A design formula based on subgrade deflections can be derived by using various existing concepts such as the solution of an elastic stress analysis for the isotropic half space and the equivalent layer thickness suggested by Odemark (3, 8).

Newmark (15) gives a formula for the vertical deflection in the center of a wheel load that is equally distributed over a circular contact area at depth z of a uniform elastic half space.

$$w_s = (1 + \mu) \times \frac{\sigma_o a}{E} \times \left[\sin \alpha + (1 - 2\mu) \frac{1 - \cos \alpha}{\sin \alpha}\right] \qquad (15)$$

where

w_s = vertical deflection at the top of the subgrade;
μ = Poisson's ratio;
σ_o = tire pressure, uniformly distributed over a circular area;
a = radius of the loaded circular area;
α = angle as indicated in the figures; and
$\alpha = \arctan \frac{a}{z}$.

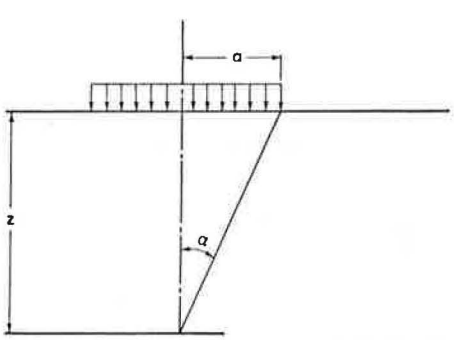

Equation 15 is rewritten so that an important simplification can be achieved:

$$w_s = K \times \frac{\sigma_o a}{E} \times \sin \alpha \tag{16}$$

where

$$K = (1 + \mu) \left[(1 - 2\mu) \times \frac{1 - \cos \alpha}{\sin^2 \alpha} \right] \tag{17}$$

For $\mu = 0.25$ to 0.50 and for $\alpha = 0$ to 40 degrees the coefficient varies only slightly from K = 1.5 to K = 1.6, and a constant value can be selected. In particular, the coefficient K increases slightly by decreasing Poisson's ratio ($\mu < 0.5$) and by increasing α. A fixed value of $K = 1.5708 = \frac{\pi}{2} > 1.5$ is suggested.

For a Poisson's ratio of $\mu = 0.5$, Eq. 15 is simply

$$w_s = 1.5 \times \frac{\sigma_o a}{E} \times \sin \alpha \tag{18}$$

This is a well-known equation (2, 3, 4). By referring to Eq. 16, the following substitution can be made

$$\sin \alpha = \frac{\tan \alpha}{\sqrt{1 + \tan^2 \alpha}}, \quad \tan \alpha = \frac{a}{z}, \quad \text{and} \quad P = \pi a^2 \sigma_o$$

$$w_s = \frac{K P}{\pi E z} \times \frac{1}{\sqrt{1 + \left(\frac{a}{z}\right)^2}} \tag{19}$$

Solving for z,

$$z = \sqrt{\left(\frac{K P}{\pi E w_s}\right)^2 - a^2} \tag{20}$$

where P = design wheel load = $\pi a^2 \sigma_o$, and $\frac{K}{\pi} = \frac{1}{2}$.

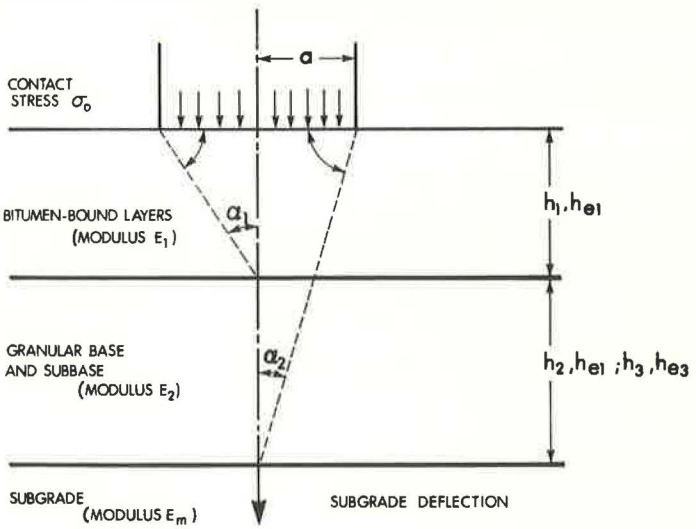

Figure 9. Diagram of elastic layered system.

According to Odemark (3), an elastic layered system as shown in Figure 9 can be transformed into a uniform elastic half space by introducing an equivalent layer thickness h_{ei}.

$$h_{ei} = n h_i \times \sqrt[3]{\frac{E_i}{E_m}} \tag{21}$$

where

E_i = modulus of layer i,
E_m = modulus of subgrade = reference modulus,
h_i = thickness of layer i,
h_{ei} = equivalent thickness of layer i, and
n = reduction factor, for flexible pavements = 0.9.

For flexible pavements, Odemark (3) has suggested a value of n = 0.9. This was verified by numerous comparative calculations.

The depth z can be expressed by Eq. 21 as

$$z = \sum_{i=1}^{m-1} h_{ei} = n \sum_{i=1}^{m-1} h_i \sqrt[3]{\frac{E_i}{E_m}} \tag{22}$$

DAMAGE MODEL FOR PREDICTING TEMPERATURE CRACKING IN FLEXIBLE PAVEMENTS

Mohamed Y. Shahin and B. F. McCullough, University of Texas at Austin

A model for predicting temperature cracking has been developed. Temperature cracking as predicted by the model is the appropriate addition of low-temperature cracking, which occurs when the thermal tensile stress exceeds the asphalt concrete tensile strength; and thermal-fatigue cracking, which occurs when the thermal-fatigue distress due to daily temperature cycling exceeds the asphalt concrete fatigue resistance. During model development, stochastic variations in material properties were considered. The model has since been computerized. Inputs to the program are the basic material properties and conventional weather variables that can be easily obtained. The major output from the program is the temperature cracking in ft/1,000 ft^2 (m/1000 m^2) as a function of age from construction. Analysis of the Ontario test roads and the Ste. Anne Test Road has shown the model predictions to be reasonable. The model is in a modular form so that any change that may develop through the advancement of asphalt concrete technology can be added without major revision of the basic framework.

•TEMPERATURE cracking is one of the severe problems with flexible pavements in the United States and Canada. The problem is not only the bad effect on the highway user but also the distress that occurs in the pavement later. The consequence, which depends on the type of subgrade, could be loss of support or swelling, but above all there is a loss of ridability and an increase in the frequency and cost of maintenance. The most common method for selecting an asphalt concrete mixture to avoid temperature cracking involves determining the fracture temperature, the temperature at which the tensile stress exceeds the tensile strength. According to this method, the pavement will fail thermally as soon as its temperature drops to the fracture temperature. However, there have been many cases in which only a few thermal cracks form at first, which increase in number yearly until the road is considered to be failed. The purpose of this research is to develop a model for predicting temperature cracking in asphalt concrete during its service life by using materials laboratory data and available weather information. Temperature cracking as predicted is the addition of two forms of cracking:

1. Low-temperature cracking, which occurs when the thermal tensile stress exceeds the asphalt concrete tensile strength; and
2. Thermal-fatigue cracking, which occurs when the thermal-fatigue distress due to daily temperature cycling exceeds the asphalt concrete fatigue resistance.

In comparisons of the temperature cracking predicted by the model and that measured in the Ontario test roads (1) and the Ste. Anne Test Road (2, 3, 4), the model predictions have been reasonable. The model is a tool that will help the highway design engineer select the most appropriate asphalt concrete mixture that will result in no or very little temperature cracking. The model can also be used to distinguish among the different

Publication of this paper sponsored by Committee on Flexible Pavement Design.

asphalt suppliers and to select the best asphalt for avoiding temperature cracking; this will help reduce the maintenance cost.

DESIGN APPROACH

To make the right approach to any problem requires that the causes be known. After the causes are known, the next step is to develop models for analyzing the problem; then one can construct a simple and useful system.

A general system approach to pavement design involves

1. Inputs—material characteristics, load frequency and intensity, environmental conditions, variations associated with the inputs, etc.;
2. Submodels—techniques developed to analyze the problem under consideration, which can be based on theory, experience, axioms, etc.;
3. Outputs—stress, strain, strength, etc.;
4. Distress—cracks, roughness, rutting, etc.; and
5. Performance—evaluation of distress manifestations from the user's point of view.

The major part of the model is the development of the temperature cracking submodels. The four submodels that were developed, each of which has its own function and serves as an input to the next one, are

1. Submodel 1—simulation of pavement temperatures;
2. Submodel 2—estimation of asphalt concrete stiffness, prediction of in-service aging of asphalt, and estimation of thermal stresses;
3. Submodel 3—prediction of low-temperature cracking; and
4. Submodel 4—prediction of thermal-fatigue cracking.

Because of space limitations, however, only submodels 3 and 4 are discussed here; complete details of submodels 1 and 2 will be published in a future report.

PREDICTION OF LOW-TEMPERATURE CRACKING

It is believed that asphalt concrete properties vary over the entire road length and, therefore, a single fracture temperature is an unsatisfactory criterion. Instead, the variability of the mixture properties should be accounted for by an appropriate stochastic approach.

The factors that control low-temperature cracking are the stress σ and the strength T. So that the variability of asphalt concrete properties in a particular road may be accounted for, it is assumed that both the stress and the strength vary normally and randomly along that road. The probability of failure is then defined as the probability of the stress exceeding the strength at any point on the road:

$$P(\text{failure}) = P(F) = P(\sigma > T) \tag{1}$$

By introducing $X = \sigma - T$, Eq. 1 can be rewritten as

$$P(F) = P(\sigma - T > 0) = P(X > 0) \tag{2}$$

Figure 1 shows a conceptual diagram showing the probability of failure on the normal distribution of X.

Because the density functions $f(\sigma)$ and f(T) are assumed to be normally distributed, f(X) is normally distributed and

$$f(X) = \frac{1}{SD_X\sqrt{2\pi}} \exp\left[-\frac{1}{2}\left(\frac{X - \overline{X}}{SD_X}\right)^2\right] \tag{3}$$

where

Figure 1. Difference distribution (X = stress strength).

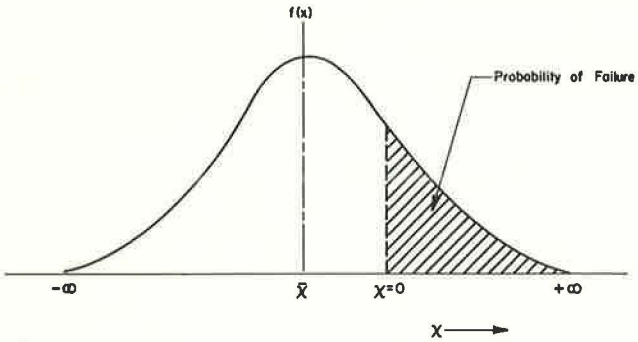

Figure 2. Effect of mean strength on low-temperature cracking.

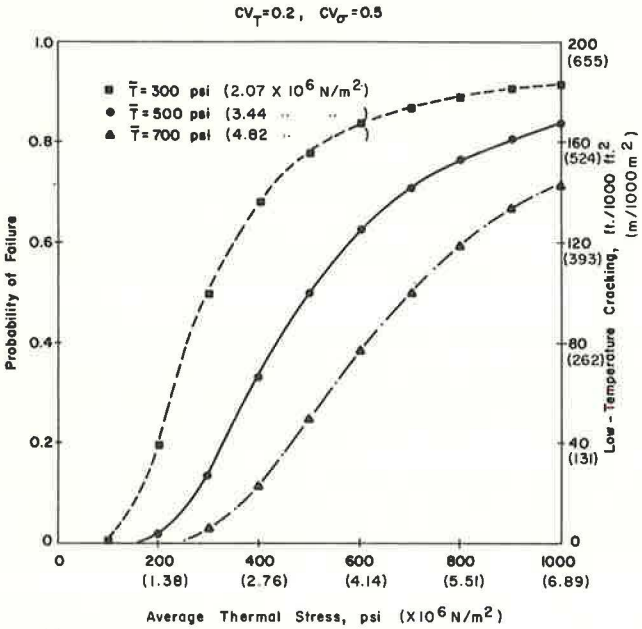

$\bar{T}$ = mean value of the tensile strength,

CV_T = coefficient of variation of the strength,

CV_σ = coefficient of variation of the stress.

$f(X)$ = the density function of X,
SD_X = standard deviation of X, and
$\overline{X}$ = mean value of X.

Therefore,

$$P(F) = P(X > 0) = \int_0^\infty f(X)dX \tag{4}$$

By substituting Eq. 3 into Eq. 4,

$$P(F) = \frac{1}{SD_X\sqrt{2\pi}} \int_0^\infty \exp\left[-\frac{1}{2}\left(\frac{X - \overline{X}}{SD_X}\right)^2\right] dX \tag{5}$$

Variable X was normalized so that the normal tables could be used:

$$Z_X = \frac{X - \overline{X}}{SD_X} \tag{6}$$

Accordingly, the limits of the integration in Eq. 5 will be

1. Where X = o,

$$Z_{X_{min}} = -\frac{\overline{X}}{SD_X}$$

2. Where X = ∞,

$$Z_{X_{max}} = \infty$$

3. $dX = SD_X dZ$.

Equation 5 can then be rewritten in terms of Z as

$$P(F) = \frac{1}{\sqrt{2\pi}} \int_{Z_{X_{min}}}^{Z_X=\infty} e^{-\frac{z^2}{2}} dZ \tag{7}$$

If the lower limit of the integration of Eq. 7 is known, then the normal tables can be used to determine the probability of failure P(F):

$$Z_{X_{min}} = \frac{-X}{SD_X} = -\frac{(\overline{\sigma} - \overline{T})}{\sqrt{SD_\sigma^2 + SD_T^2}} \tag{8}$$

where

$\overline{\sigma}$ = mean value of the stress,
$\overline{T}$ = mean value of the strength,
SD_σ = standard deviation of the stress, and
SD_T = standard deviation of the strength.

As an example, the following values were assumed:

$\overline{\sigma}$ = 100 psi (689.4 kPa),
SD_σ = 50 psi (344.7 kPa),
$\overline{T}$ = 200 psi (1378.9 kPa),
SD_T = 40 psi (275.7 kPa), and

$$Z_{\chi_{min}} = -\frac{(100 - 200)}{\sqrt{50^2 + 40^2}} \cong +1.56.$$

From the normal tables, P(F) ≅ 6.0 percent, which means that 6.0 percent of the area of a road will fail if the assumed values of stress and strength occur.

Because thermal cracks take the form of transverse cracks, they are usually reported as the average frequency per mile or, as reported in the AASHO Road Test, in lin ft/1,000 ft^2. The minimum spacing between transverse cracks ranges from 4 to 5 (1.2 to 1.5 m). Consequently, it can be assumed that, if the spacing between transverse cracks reaches 5 ft (1.5 m) and the pavement is no longer restrained, the area of influence of each transverse crack will be equal to its length times a width of 5 ft (1.5 m). Therefore, to transfer a predicted area of thermal cracking, the area can be divided by the width of influence, which is about 5 ft (1.5 m).

For example, if the probability of failure is 6.0 percent, 60 ft^2 will fail every 1,000 ft^2 (60 m^2/1000 m^2). In terms of linear cracking that will be 60/5 or 12 ft/1,000 ft^2 (60/1.5 or ~ 40 m/1000 m^2).

Equation 8 is mainly used in the low-temperature cracking submodel. The four variables in Eq. 8 were varied over a reasonable range so that the model's behavior could be studied. The results of this analysis are shown in Figures 2, 3, and 4 from which the following conclusions are drawn:

1. When the average tensile stress is equal to the average tensile strength, the probability of failure is 50 percent, regardless of the stress and strength coefficients of variation.
2. For both stress and strength, the higher the coefficient of variation is, the higher the low-temperature cracking will be, up to a probability of failure of 50 percent, after which the reverse is true.

PREDICTION OF THERMAL-FATIGUE CRACKING

Pavement behavior (stress, strain, etc.) under temperature cycling was analyzed so that the relation between temperature cycling and the fatigue concept could be studied. The analysis showed that temperature cycling simulates a constant strain rather than a constant stress-fatigue distress. The distress effect of each cycle depends on the maximum stiffness and strain during that day (cycle) (Fig. 5). The pavement is subjected to one cycle/day (360 cycles/year); each cycle has a different distress intensity from all others. Furthermore, hardening of asphalt is an important phenomenon that should be considered. As time passes, the asphalt gets harder and hence, on the average, the asphalt concrete stiffness increases year after year. It is believed that stiffness is the major factor distinguishing asphalt concrete mixes, with reference to their ability to withstand repeated temperature cycling. Figure 6 shows a conceptual relation between strain level and the number of cycle applications until failure for different stiffnesses. The general relation may be written as

$$\overline{N}_{ij} = A_j \left(\frac{1}{\epsilon_i}\right)^{B_j}$$

where

i = the strain level,
j = the stiffness level,
$\overline{N}_{ij}$ = the average number of cycle applications until failure under strain level i and stiffness level j,

Figure 3. Effect of coefficient of variation of strength on low-temperature cracking.

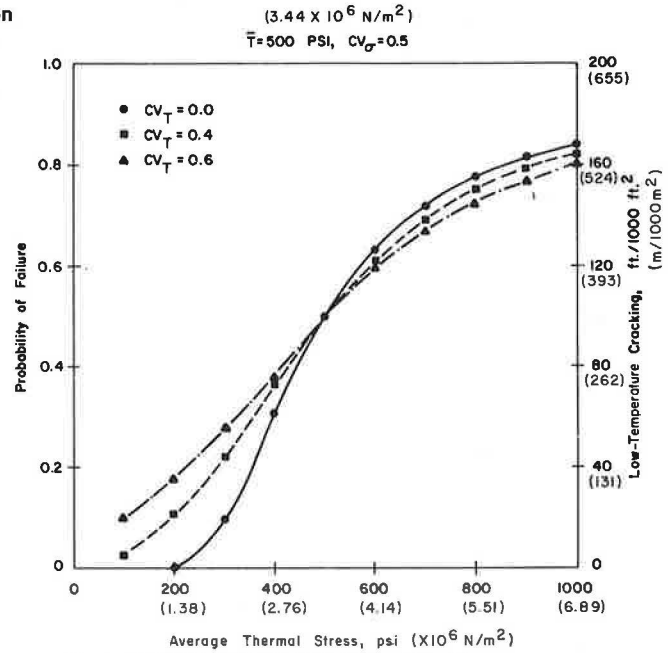

CV_T = coefficient of variation of the strength,

$\bar{T}$ = mean value of the tensile strength,

CV_σ = coefficient of variation of the stress.

Figure 4. Effect of coefficient of variation of stress on low-temperature cracking.

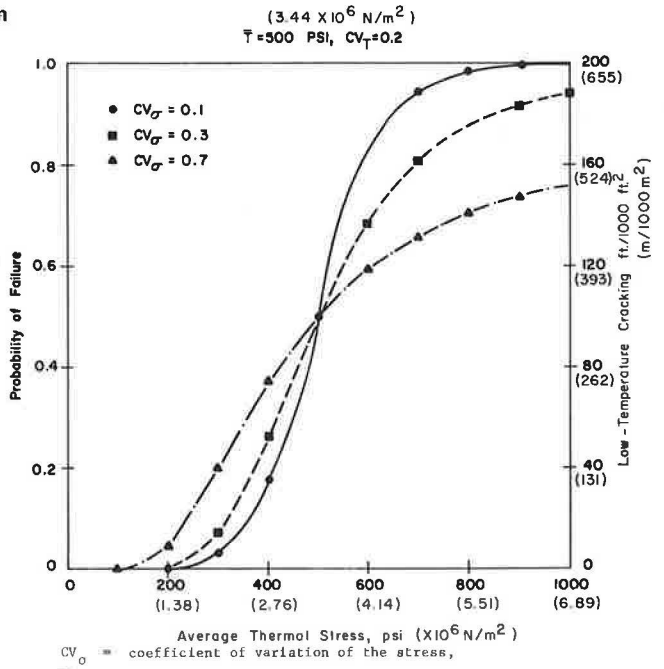

CV_σ = coefficient of variation of the stress,

$\bar{T}$ = mean value of the tensile strength,

CV_T = coefficient of variation of the strength.

Figure 5. Schematic diagram of assumed behavior of pavement strain, stiffness, and stress during normal day.

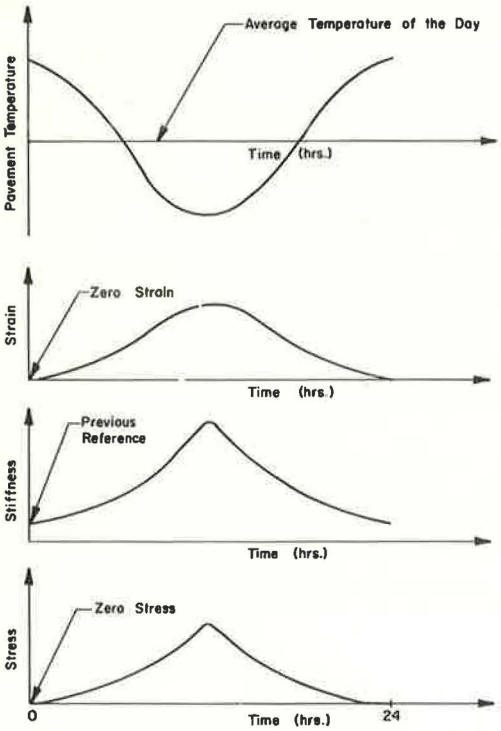

Figure 6. Conceptual diagram of relation between strain and number of cycle applications until failure under a constant strain fatigue mode.

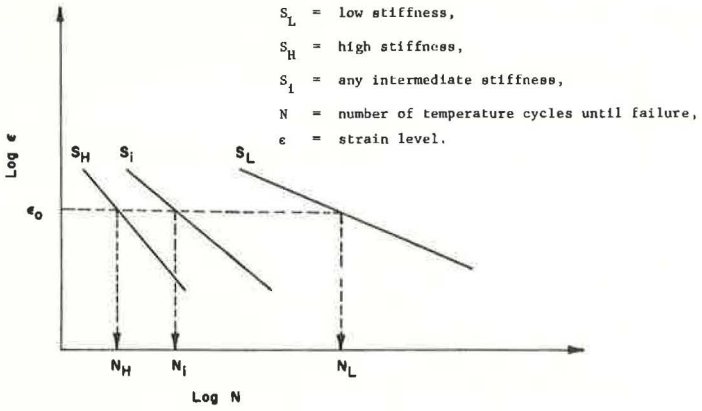

ϵ = strain, and
A_j, B_j = fatigue constants at a stiffness level j.

According to the preceding concept, the fatigue constants will vary with stiffness. An experiment was designed to determine these constants in the laboratory and to establish a criterion for estimating the cumulative damage. However, because of the high cost of such an experiment, it was suggested that the experiment be performed later, and, therefore, fatigue constants were estimated from available data. So that the cumulative damage due to temperature cycling could be estimated, the following formula was used:

$$D = \sum_{i=1}^{K} \sum_{j=1}^{M} \frac{n_{ij}}{N_{ij}} = \frac{n_{11}}{N_{11}} + \frac{n_{12}}{N_{12}} + \ldots + \frac{n_{1M}}{N_{1M}} + \frac{n_{21}}{N_{21}} + \frac{n_{22}}{N_{22}}$$

$$+ \ldots + \frac{n_{2M}}{N_{2M}} + \ldots + \frac{n_{K1}}{N_{K1}} + \frac{n_{K2}}{N_{K2}} + \ldots + \frac{n_{KM}}{N_{KM}} \qquad (9)$$

where

D = accumulated damage,
K = number of equal strain level groups,
M = number of equal stiffness level groups,
n = actual number of cycle applications, and
N = number of cycle applications until failure.

In this formula, it was assumed that the damage caused by each cycle was irrecoverable and hence the cumulative damage was a simple addition of all individual damages disregarding their sequence of occurrence.

The logarithm of the average number of cycles until failure $\overline{N}_{ij}$ has been shown to be normally distributed (5). For a particular significance level α, the number of cycle applications until failure $N_{\alpha_{ij}}$ can be expressed as

$$\log N_{\alpha_{ij}} = \log \overline{N}_{ij} - Z_\alpha SD_{\log N} \qquad (10)$$

where

Z_α = value from the normal tables that corresponds to a significance level α; and
$SD_{\log N}$ = standard deviation of the logarithm of N.

From Eqs. 9 and 10, the probability of failure P(F) can be expressed as

$$P(F) = \text{probability}\left(\sum_{i=1}^{K} \sum_{j=1}^{M} \frac{n_{ij}}{N_{\alpha_{ij}}} \geq 1.0 \right) \qquad (11)$$

The best way to explain the above concept is through a numerical example.

For a particular road section under particular environmental conditions, the accumulated damage $\left(\sum_{i=1}^{K} \sum_{j=1}^{M} \frac{n_{ij}}{N_{\alpha_{ij}}} \right)$ was estimated after each month from construction at different significance levels. The relationship between the accumulated damage and the significance levels after x months from construction is shown in Figure 7 which shows that P(F) = 8 percent. If one wants to transfer the probability of failure into cracking, the previously explained procedure must be used: Cracking in ft^2/1,000 ft^2 (m^2/1000 m^2) = 0.08 × 1,000 = 80.0, and cracking in lin ft/1,000 ft^2 (m/1000 m^2) = 80.0/5.0 = 16.0.

The estimated cracking from this model is referred to as thermal-fatigue cracking. The developed submodel for predicting thermal-fatigue cracking is unique in nature

Figure 7. Relation between accumulated damage and significance levels after x months.

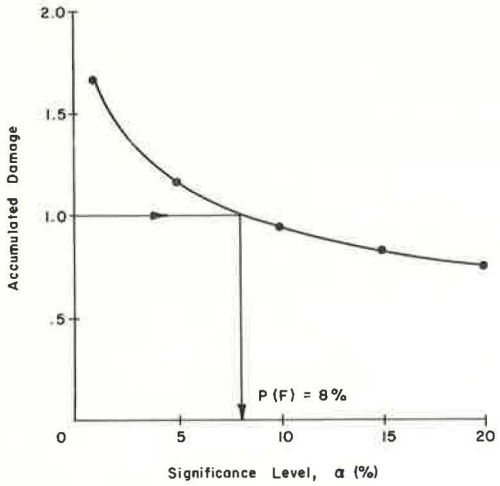

Figure 8. Summary flow chart of developed temperature cracking model.

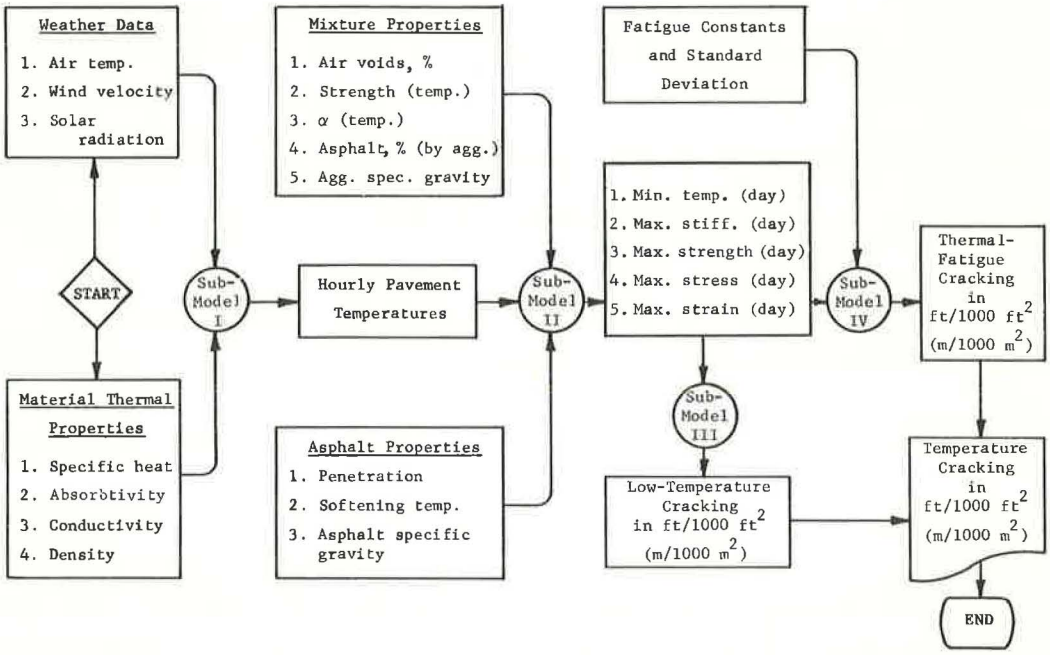

because this is the first time that both fatigue and stochastic concepts are being used to predict the distress resulting from temperature cycling. The usefulness and the behavior of the model are discussed in the next section.

WORKING MODEL

A summary flow chart of the developed computer program for the damage model is shown in Figure 8. The involved steps were

1. Calculate the daily mean air temperature and solar radiation;
2. Calculate hourly pavement temperature for each day;
3. Locate the maximum and minimum pavement temperatures for each day;
4. Estimate the stiffness at the middle of the temperature intervals and the increments of strain and stress by starting from the maximum temperature and moving down, on an hourly basis, to the minimum temperature;
5. Accumulate the increments of strain and stress to estimate the maximum strain and stress for that day;
6. Estimate the strength corresponding to the maximum stress;
7. Predict low-temperature cracking;
8. Predict thermal-fatigue cracking; and
9. Add the low-temperature and thermal-fatigue cracking to obtain the total temperature cracking.

Model Behavior

Figure 9 shows the relationship between temperature cracking and the number of years from construction as predicted by the model. In Figure 9, the values of temperature cracking correspond to assumed asphalt mixture properties and surrounding environmental conditions, and they are not necessarily typical values. However, the rate of increase in low-temperature and thermal-fatigue cracking is usually similar to what is shown; i.e., the rate of increase of low-temperature cracking is usually much less than that for thermal-fatigue cracking. Study cases performed with the system showed that the rate of increase of thermal-fatigue cracking is higher during the winter than the summer (Fig. 10). Furthermore, it is important to note that the major cause of temperature cracking is low temperature or thermal fatigue, depending on the asphalt mixture properties and the surrounding environmental conditions.

Model Verification

A search was carried out to locate some projects in which temperature cracking was measured and reported separately from traffic load cracking. Unfortunately, very few projects were found where such measurement was reported. Two of these projects were used to verify the system. A description of each project and the results of the analysis follow.

Ontario Test Roads—In this project, McLeod (1) made a survey of temperature cracking after 8, 9, 10, and 11 years of service of asphalt pavements on 3 southwestern Ontario test roads about 40 miles (64.4 km) apart that were constructed in 1960, all over clay subgrades. Each test road was 6 miles (9.66 km) long and contained three 2-mile (3.22 km) test pavements. The pavement in each 2-mile (3.22 km) test section contained a single 85/100 penetration asphalt cement. Three 85/100 penetration asphalt cements from three different asphalt suppliers were used in each of the three 6-mile (9.66 km) test roads. The properties of the asphalts from the different suppliers are given elsewhere (1). All the necessary information about the mixture properties was available except the tensile strength, which was assumed to have a maximum value of 500 psi (3.45 MPa). The environmental variables were estimated from the closest available weather station (6). The fatigue constants were kept the same throughout the verification. Figures 11, 12, and 13 show the comparison between the measured and predicted thermal cracking for the three asphalt suppliers. Because there is not any basis on which to differentiate between the three roads, they can be considered as replicates. However, because the fatigue constants were adjusted with only one section

Figure 9. Schematic diagram of relation between thermal cracking and the number of years from construction (not necessarily typical).

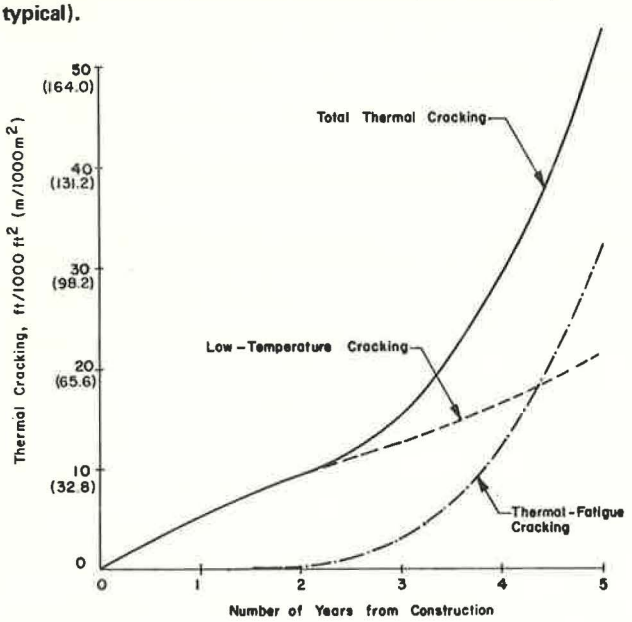

Figure 10. Detailed diagram of increase in thermal-fatigue cracking after each month from construction.

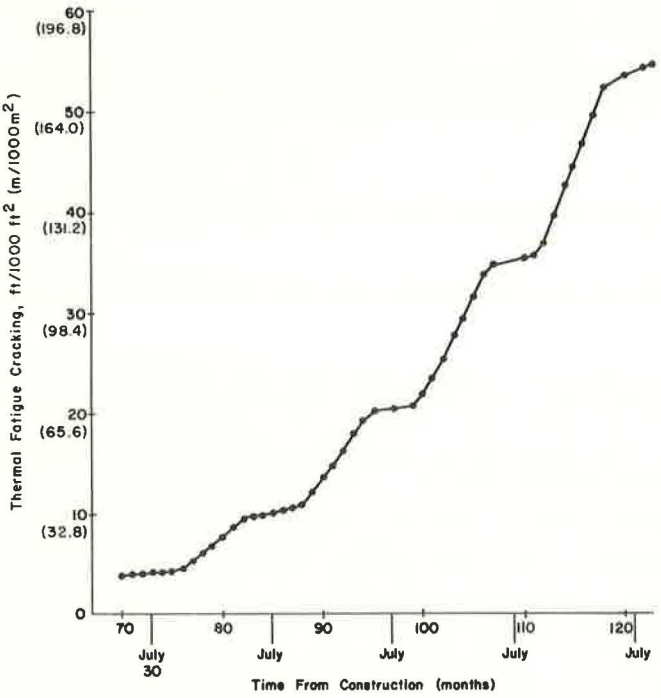

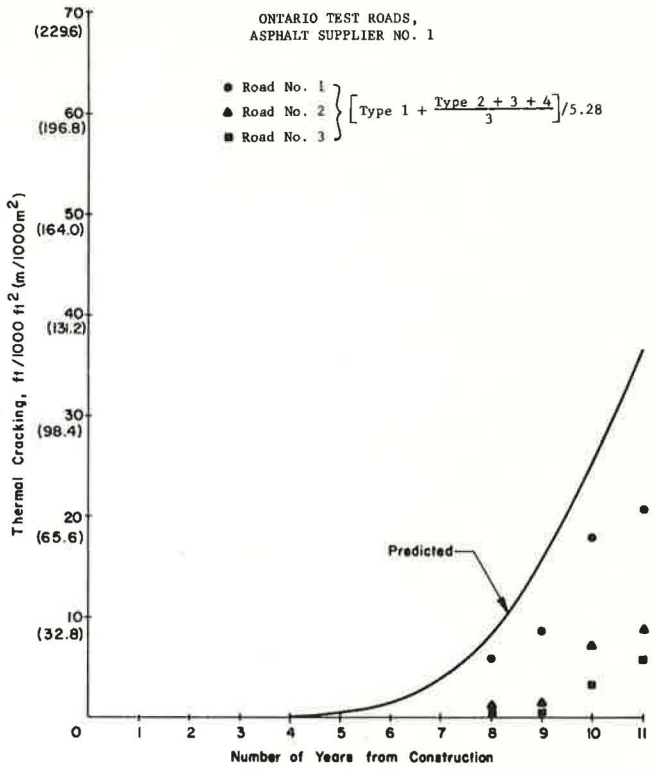

Figure 11. Comparison of predicted and measured thermal cracking (asphalt supplier 1).

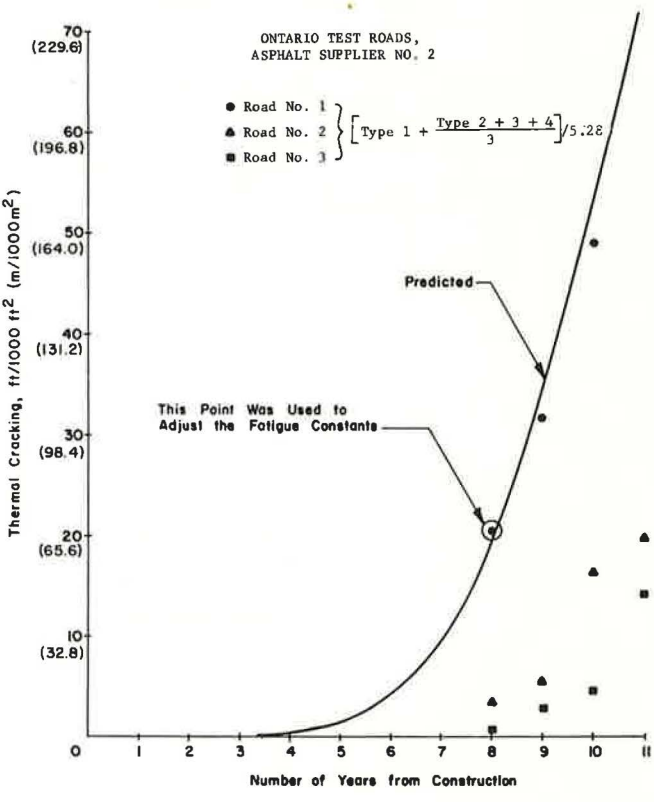

Figure 12. Comparison of predicted and measured thermal cracking (asphalt supplier 2).

Figure 13. Comparison of predicted and measured thermal cracking (asphalt supplier 3).

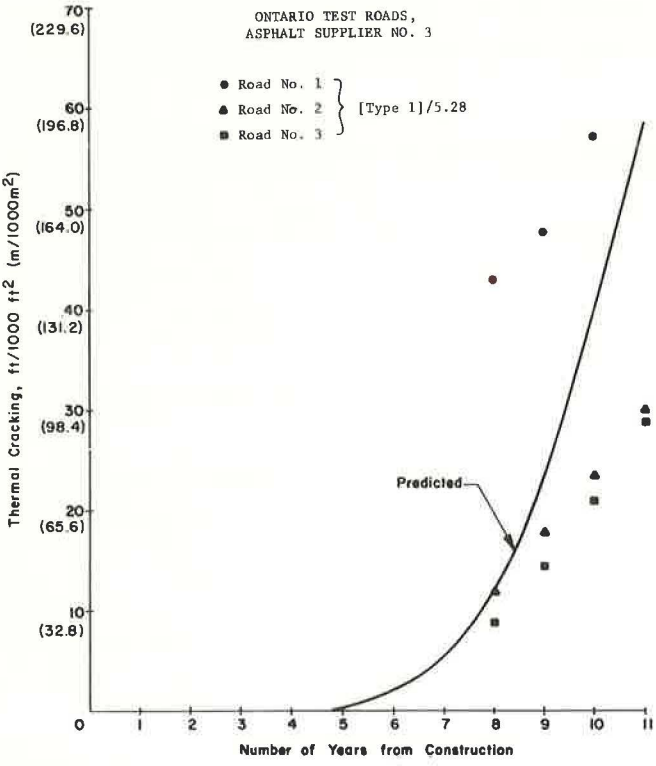

Table 1. Comparison of measured and predicted temperature cracking after 2 years from construction (Ste. Anne Test Road).

Asphalt Type	Section	Structure	Measured Crack (ft/1,000 ft²) (4)	Average (ft/1,000 ft²)	Predicted Crack (ft/1,000 ft²)
150/200 LVA	63	A	51.0	76.0	98.9
	67	B	154.0		
	64	C	22.9		
150/200 HVA	62	A	7.5	5.5	9.5
	66	B	5.6		
	65	C	3.3		
300/400 LVA	61	A	25.0	13.1	1.7
	68	B	1.25		

Note: 1 ft = 0.3048 m. 1 ft² = 0.0929 m².

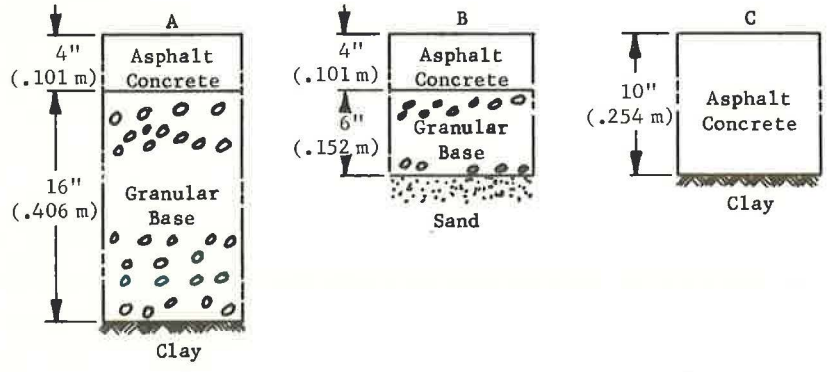

(road 4, asphalt supplier 2), it would be more appropriate to compare the predicted thermal cracking with that measured in road 1. In general, the agreement between the measured and predicted cracking seems to be encouraging.

Ste. Anne Test Road—The test road (2, 3, 4) was constructed in 1967 for the study of transverse cracking of asphalt pavements. It is located 25 miles (40.2 km) east of Winnipeg near Ste. Anne, Manitoba. The characteristics of the test road were described (4) as follows: "The road is composed of twenty-nine 400-ft (122 m) pavement sections, 24 ft (7.32 m) wide, constructed on clay and sand subgrades. The test section variables include two different types and three different grades of asphalt, two asphalt contents, two aggregate gradations, limestone and granite aggregates and three road structure designs." These variables were selected because it was thought that they were potentially important in the study of transverse pavement cracking. All the mixture properties are available (2, 3, 4) except the maximum tensile strength, which was determined for samples containing the optimum asphalt content by Christison et al. (7). The fatigue constants were kept the same as for the Ontario test roads. The comparison between the measured and predicted temperature cracking is given in Table 1, which indicates that the agreement is reasonable.

SUMMARY

A damage model for predicting temperature cracking is described. Analysis of the Ontario test roads and the Ste. Anne Test Road has shown that the model predictions are reasonable. The model has been computerized. The inputs to the program are the basic material properties and the conventional weather variables that are easy to obtain. The major output from the program is the temperature cracking in ft/1,000 ft^2 ($m/1000\ m^2$), which is measured each year from construction. Temperature cracking as predicted from the model is the appropriate addition of low-temperature and thermal-fatigue cracking. The model has been developed in a modular form so that any change that may develop through the advancement of asphalt concrete technology can be added without major revision of the basic framework.

ACKNOWLEDGMENTS

This investigation was conducted at the Center for Highway Research at the University of Texas at Austin. The authors wish to thank the sponsors, the Texas Highway Department, and the Federal Highway Administration, U.S. Department of Transportation.

The contents of this paper reflect the views of the authors, who are responsible for the facts and the accuracy of the data presented. The contents do not necessarily reflect the official views or policies of the Federal Highway Administration. This report does not constitute a standard, specification, or regulation.

REFERENCES

1. McLeod, N. W. A 4-Year Survey of Low Temperature Transverse Pavement Cracking on Three Ontario Test Roads. Proc., Association of Asphalt Paving Technologists, Vol. 41, Feb. 1972.
2. Burgess, R. A., Kopvillem, O., and Young, F. D. Ste. Anne Test Road—Relationships Between Predicted Fracture Temperatures and Low Temperature Field Performance. Proc., Association of Asphalt Paving Technologists, Vol. 40, Feb.1971, p. 148.
3. Deme, I. Ste. Anne Test Road—Transverse Cracking of the Pavements in the Mix Trial Area of the Test Road. Manitoba Highways, Internal Rept. 69-2, Aug. 1969, revised and amended as Rept. 71-2, March 1971.
4. Young, F. D., Deme, I., Burgess, R. A., and Kopvillem, K. O. Ste. Anne Test Road—Construction Summary and Performance After Two Years' Service. Proc., Canadian Technical Asphalt Association, Edmonton, Vol. 14, Nov. 1969.
5. McCullough, B. F. A Pavement Overlay Design System Considering Wheel Loads, Temperature Changes, and Performance. Univ. of California at Berkeley, PhD dissertation, July 1969.

6. Meteorological Observations in Canada. Monthly Records, Meteorological Branch, Dept. of Transport, Toronto, Jan. 1967 through Dec. 1970.
7. Christison, J. T., Murray, D. W., and Anderson, K. O. Stress Prediction and Low Temperature Fracture Susceptibility of Asphalt Concrete Pavements. Proc., Association of Asphalt Paving Technologists, Vol. 41, Feb. 1972.
8. Climatic Atlas of the United States. Environmental Data Service, Environmental Science Services Administration, U.S. Department of Commerce, June 1968.
9. Hudson, W. R., McCullough, B. F., Scrivner, F. H., and Brown, J. L. A Systems Approach Applied to Pavement Design and Research. Texas Highway Department; Texas Transportation Institute, Texas A&M Univ.; and Center for Highway Research, Univ. of Texas at Austin, Res. Rept. 123-1, March 1970.
10. Jain, S. P., McCullough, B. F., and Hudson, W. R. Flexible Pavement System—Second Generation, Incorporating Fatigue and Stochastic Concepts. Texas Highway Department; Texas Transportation Institute, Texas A&M Univ.; and Center for Highway Research, Univ. of Texas at Austin, Res. Rept. 123-10, Dec. 1971.
11. Carey, W. N., and Irick, P. E. The Pavement Serviceability-Performance Concept. HRB Bull. 250, Jan. 1960, pp. 40-58.
12. Shahin, M. Y., and McCullough, B. F. The Stiffness History of Asphalt Concrete Surfaces in Our Roads. Highway Research Record 466, 1973, pp. 96-112.

DISCUSSION

I. Deme, Shell Canada Limited

The paper by Shahin and McCullough represents a sound approach to the development of a model for predicting the extent of temperature cracking of flexible pavements. The problem is complex and congratulations are extended to the authors for a thorough and scholarly paper. However, several factors in the paper appear overly generalized, which leaves room for comment.

INITIATION AND PROGRESSION OF TRANSVERSE CRACKING

The initiation of transverse cracking in the Ste. Anne Test Road pavements was detected with continuously monitoring crack detection circuits and was recorded automatically with pavement temperatures measured at various depths (13). The pavements were inspected several times a week during the first two winters and at less frequent intervals in subsequent years.

Most of the transverse cracking occurred in the first winter after construction (1967/1968) during prolonged low-temperature cycles, when the asphalt concrete was cooled throughout its thickness (4). A study of 10 years of minimum daily temperature data was carried out to determine the most severe annual low-temperature cycle in southern Manitoba and to estimate its interval of recurrence (14). Figure 14 shows that the low-temperature cycle, during which many of the test pavements experienced their greatest cracking, has an estimated recurrence interval of 5 years in the lowest temperature range. If the potential for pavement stress buildup has not been eliminated altogether by transverse cracking, additional cracking with time could be expected as the pavements are exposed to low-temperature cycles that are more extreme or of greater duration than those experienced previously. Subsequent winters have not appeared to be much more severe than the 1967/1968 winter, and some of the pavements that cracked extensively have exhibited little or no additional transverse cracking. Some of the pavements that cracked to a lesser degree, or did not crack during the first winter, have cracked subsequently. For these pavements, laboratory studies have shown that age-hardening of the asphalt is significant in lowering pavement resistance to low-temperature-induced cracking (15), as stated by Shahin and McCullough.

In all cases, pavement transverse cracking occurred in winter (low-temperature periods), which pointed to thermal shrinkage (16) as the main mechanism of transverse

Figure 14. Interval of recurrence and duration of annual lowest temperature cycle.

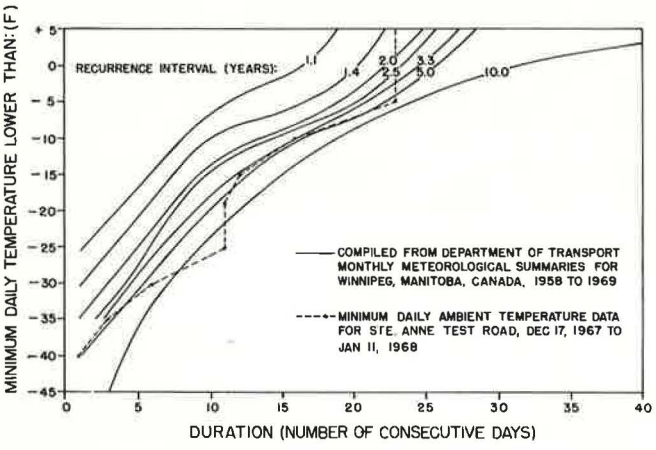

cracking in the pavements. Observations at the Ste. Anne Test Road have not yielded evidence to date of a long-term thermal-fatigue cracking mechanism as described by the authors. Increases in transverse cracking with pavement age have been attributed mainly to age-hardening of the asphalt binder coupled with the recurrence of low-temperature cycles.

INFLUENCE OF PAVEMENT STRUCTURE VARIABLES ON TRANSVERSE CRACKING FREQUENCY

The most significant factors influencing transverse cracking of the Ste. Anne Test Road pavements were asphalt type and grade (4). For the pavements that cracked, the frequency of transverse cracking was influenced by the subgrade type and the thickness of the asphalt concrete. For example, the 4-in. (100 mm) LV 150/200 penetration asphalt concrete pavement structure A (Table 1) with a heavy clay subgrade exhibited an average of 260 full-width cracks per mile (160 per km), and structure B (Table 1) with a sand subgrade had 660 cracks per mile (410 per km). However, the 10-in. (250 mm) full-depth asphalt concrete structure C on the clay subgrade had an average of 105 cracks per mile (65 per km), which is considerably less than the number of cracks in the 4-in. (100 mm) asphalt concrete structure A. These findings are significant in their effect on transverse cracking frequency and, as such, it would be more appropriate to compare them individually with the authors' predicted cracking frequency rather than collectively, as has been done (Table 1).

On the basis of a minimum observed spacing of 5 ft (1.5 m) between transverse cracks, Shahin and McCullough have assumed this to be the requirement of an unrestrained case for all pavements and have used this in predicting the probability of pavement failure. This is considered to be a generalization that could result in a large overestimate of distress for some pavements. For example, the LV 150/200 penetration asphalt pavements in structure A attained an average spacing between transverse cracks of 20 ft (6 m) the first winter after construction. This is considered approximately equal to the equilibrium crack spacing of a few hundred miles of old pavements constructed with a similar asphalt in clay subgrade areas. No further transverse cracking in these test road pavements has been observed since the first winter, and little additional transverse cracking is expected in the future.

The authors' damage model has the potential of serving as a useful aid in the selection of materials and designs to eliminate or minimize temperature-associated cracking of flexible pavements and to provide an estimate of related maintenance costs. However, as Shahin and McCullough have indicated, more inputs to the program are required.

REFERENCES

13. Deme, I., and Fisher, D. Ste. Anne Test Road—Instrumentation. Proc., Canadian Technical Asphalt Association, Ottawa, Vol. 13, Nov. 1968.
14. Deme, I. A Study of Transverse Cracking of Asphalt Pavements in Manitoba. Univ. of Manitoba, graduate thesis, July 1969.
15. Burgess, R. A., et al. Ste. Anne Test Road—Flexible Pavement Design to Resist Low Temperature Cracking. Proc., Third International Conference on the Structural Design of Asphalt Pavements, London, Sept. 1972.
16. Hills, J. F., and Brien, D. The Fracture of Bitumens and Asphalt Mixes by Temperature Induced Stresses. Proc., Association of Asphalt Paving Technologists, Vol. 35, Feb. 1966.

AUTHORS' CLOSURE

The authors appreciate Deme's interest in their work. Computer analysis of the Ste. Anne Test Road pavements indicated that the temperature cracking was due to low thermal shrinkage and thermal fatigue. What percentage of the temperature cracking was due to low temperature or thermal fatigue depended on the type of asphalt. Both of these mechanisms of temperature cracking are functions of the stiffness of the asphalt concrete, which is a function of the age-hardening of the asphalt. When the stiffness of the asphalt was estimated, age-hardening was accounted for through regression models. Our analysis indicated that pavement cracking occurred in winter; however, Deme's conclusion that the main mechanism is thermal shrinkage is not necessarily true, because cracking due to thermal fatigue also occurs in winter.

The calculation of thermal stresses for different pavement structures was not accounted for with the assumption that temperature cracking starts at the surface and that surface slab is fully restrained until the spacing of transverse cracks reaches 5 ft (1.5 m). The 5-ft (1.5 m) assumption was adopted from current literature; however, that does not mean that the spacing should reach 5 ft. More research is needed in the area of calculating thermal stresses for different pavement structures.

Finally, the authors agree with Deme that the most significant factors influencing transverse cracking are the asphalt type, grade, and age-hardening properties. Therefore, the results shown in Table 1 were reported for the different asphalt types.

PERFORMANCE OF FULL-DEPTH ASPHALT BASES ON SAN DIEGO COUNTY EXPERIMENTAL BASE PROJECT

J. F. Shook, The Asphalt Institute; and
J. R. Lambrechts*, Purdue University

The San Diego County experimental base project consists of 35 test sections designed to determine thickness requirements for five full-depth asphalt bases and two untreated granular bases. Testing was discontinued in 1973 after 7 years of traffic. This experiment was planned to determine specific thicknesses of various types of base courses required to give a desired level of performance, to relate certain measured properties of the pavement and pavement components to observed performance, and to study deflection and strain behavior of the test pavements to provide a better theoretical basis for translating future performance results to other environments. This paper is concerned with the first two objectives. Four full-depth asphalt bases were analyzed, and their relative thickness requirements were determined and related to pavement performance measured by a performance rating system and by the present serviceability index. Under test conditions and limitations of the analysis, it was possible to develop significant relationships between a panel rating of test section performance and the deflection and equivalent thickness for four full-depth asphalt base sections included in the experiment. The data did not yield significant relationships with either traffic or present serviceability index. Base weighting factors, relative to a high-quality asphalt concrete base, were developed from the analysis for asphalt cement, cutback asphalt, and emulsion-asphalt-treated bases by using a marginal-quality sandy gravel aggregate.

•THE San Diego County experimental base project was designed to determine thickness requirements for five full-depth asphalt bases and two untreated granular bases. There were 35 sections tested for 7 years; the project began in 1966 and was discontinued in 1973.

The experiment was located on a section of Sweetwater Road, San Diego County, California. Construction was completed July 1966. Average rainfall in San Diego was about 10 in. (254 mm) per year. Daytime temperatures ranged from 70 to 90 F (21 to 32 C) throughout the year. The project was constructed on an A-7-6 soil with poor drainage. Traffic volume in 1966 consisted of approximately 12,000 vehicles per day, of which about 600 were trucks.

This experiment was to accomplish the following objectives:

1. To determine specific thicknesses of various types of base courses required to give a desired level of performance,
2. To relate certain measured properties of the pavement and pavement components to observed performance, and
3. To study deflection and strain behavior of the test pavements to provide a better theoretical basis for translating future performance results to other environments.

Publication of this paper sponsored by Committee on Flexible Pavement Design.

*This paper is based on work performed while the author was at The Asphalt Institute and the University of Maryland.

This paper is concerned with the first two objectives. Four full-depth asphalt bases were analyzed and their relative thickness requirements were determined and related to pavement performance measured by a performance rating system and by the present serviceability index (PSI).

EXPERIMENT DESIGN

The basic experiment (design and analysis concepts, 1) was a 6 by 4 full-factorial design on type of base and base thickness. One additional base type was included at two thickness levels, and one standard design at a single thickness design level. Each base was constructed to four thickness levels, with a uniform 3-in. (76.2 mm) surface course and no subbase course. The experiment design is given in Table 1. The test section layout is shown in Figure 1.

Thickness design level in the experiment (Table 1) was defined as a thickness needed to give a projected design life. The purpose of this design was to permit analysis of the performance data at any point in time; however, there would be some thicknesses of each type of base that had closely the same level of performance.

The following materials were used in the experiment:

1. Asphalt concrete, conforming to California standard specifications, with Type B, ¾-in. (19 mm) maximum size, medium grading aggregate and a 60 to 70 penetration-grade asphalt. (This is similar to an ASTM D 1663-5A mix.) The asphalt concrete surface course mixture was similar, but ½ in. (12.7 mm) was the maximum size of the aggregate.
2. Untreated aggregate base, conforming to California standard specifications for class 2 base.
3. Cutback-asphalt-treated base with medium-quality special aggregate, plant-mixed with an MC-800 cutback asphalt. The special aggregate met these specifications.

Sieve Size	Percent Passing
¾ in.	100
No. 4	55 to 80
No. 30	25 to 55
No. 200	4 to 10

The sand equivalent was 25 min, the R-value 65 to 75, and the moisture vapor susceptibility 60 min.

4. Emulsified-asphalt-treated, medium-quality special aggregate, plant-mixed with an SM-K emulsion asphalt. The special aggregate was the same as in 3.
5. Asphalt-cement-treated, medium-quality special aggregate, plant-mixed with a 60 to 70 paving grade asphalt. The aggregate was the same as in 3.
6. Untreated county standard class 3 base. This is a granite-sand aggregate base material (R = 73 min) used by San Diego County.
7. Emulsified asphalt-treated county standard granite-sand base.
8. Standard section, combination of class 2 untreated base and the county granite-sand used as subbase.

Typical mix design and other characteristics for the asphalt base mixes are given in Table 2. Data also have been reported elsewhere (2, 3, 4).

MEASUREMENTS PROGRAM

The measurements program was conducted after construction of the San Diego project to document pavement performance and to measure pavement deflections and strains so that a better understanding of fundamental pavement behavior could be developed. Theoretical concepts based on multilayered elastic theory are being evaluated by using dynamic deflection and strain data collected on the project. It is the purpose of this study to look at the performance of the pavements as it relates to pavement thickness, base type, traffic, and similar factors.

Basic measures of performance and related factors made periodically are

Figure 1. Test section layout.

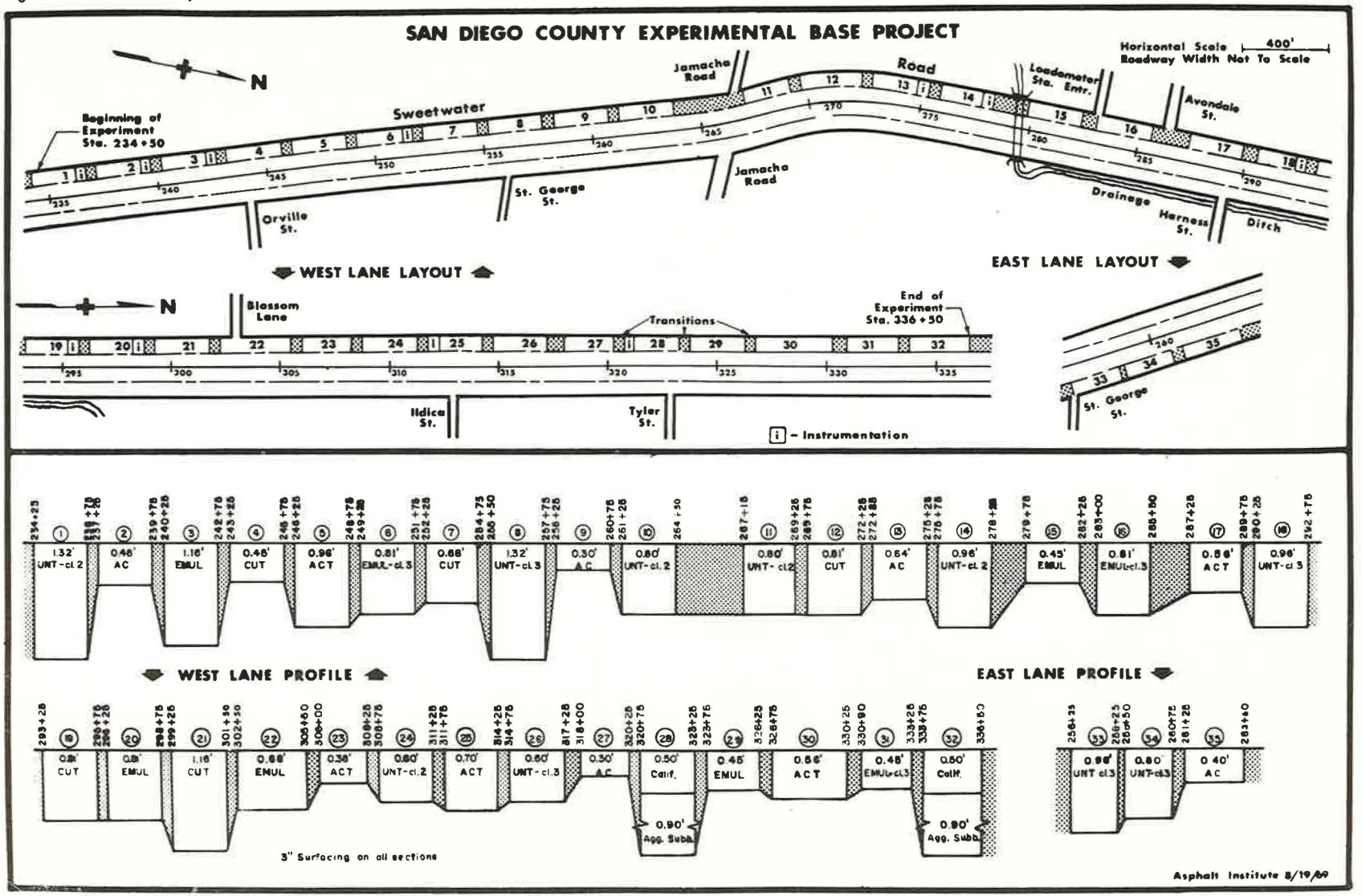

Table 1. Base type and thickness variables.

Base Type	Aggregate Quality	Base Thickness for Given Design Level[a]			
		A	B	C	D
Asphalt concrete	High	3.6	4.8	5.8	7.7
Untreated class 2 aggregate	High	7.2	9.6	11.5	15.8
Asphalt-cement-treated special aggregate	Medium	4.6	6.7	8.4	11.5
Cutback-asphalt-treated special aggregate	Medium	5.4	8.2	9.7	13.9
Emulsified-asphalt-treated special aggregate	Medium	5.4	8.2	9.7	13.9
Emulsified-asphalt-treated class 3 aggregate	Low	5.4		9.7	
Untreated class 3 aggregate	Low	7.2	9.6	11.5	15.8
Standard section				6.0[b]	

Note: 1 in. = 25.4 mm.

[a]Uniform 3-in. surface course. [b]Plus 10.8-in. subbase.

Table 2. Construction test data for asphalt base mixes.

Test	Asphalt Concrete	Asphalt-Cement-Treated	Emulsified-Asphalt-Treated	Cutback-Asphalt-Treated	Emulsified-Asphalt-Treated, Class 3
Stabilometer					
Compaction pressure, psi	500	500	500	500	500
S-value	42	59	35	35	33
R-value	83	82	82	83	84
Cohesiometer value	226	201	280	122	390
Asphalt content, percent	5.5	5.6	3.8	5.5	3.2
Density, pcf	138.7	133.9	133.9	130.9	142.8
Marshall					
Stability, lb	3,890	4,284	1,607	901	1,540
Flow, 0.01 in.	11	12	19	12	14
Density, pcf	139.3	129.1	122.9	132.3	132.5
Air voids, percent	4	11	15	9	7
VMA, percent	18	24	28	22	23
Test temperature, F	100	100	100	100	100
Extraction and grading					
Asphalt, percent	5.8	5.8	4.2	5.1	3.1
Moisture, percent	0.14	0.24	1.8	0.68	2.4
Grading, percent passing:					
1 in.					100
¾ in.	100	100	100	100	—
½ in.	92	93	96	96	100
⅜ in.	76	86	90	87	95
No. 4	53	73	75	74	95
No. 8	38	67	70	68	80
No. 16	30	64	64	63	59
No. 30	23	50	52	52	44
No. 50	14	24	25	24	31
No. 100	7	10	13	11	18
No. 200	4.6	6.0	8.7	6.6	10.6
Relative compaction, percent	95	97	95	96	96

Note: 1 psi = 6.894 kPa. 1 pcf = 16.01 kg/m^3. 1 lb$_f$ = 4.448 N. 1 F = 1.8 (1 C) + 32.

1. PSI, measured by the California Division of Highways with the CHLOE profilometer;
2. Performance rating, done by a panel of technologists and the project sponsors;
3. Cracking, surveyed regularly by San Diego County;
4. Rutting, by the rating panel; and
5. Traffic and axle weight studies, by San Diego County.

Measurements involving pavement deflection and strain can be divided into two categories: (a) those involving instrumentation placed in the road; and (b) those involving instrumentation brought to the road for purposes of measuring deflections under load at the pavement surface.

In the first category were LVDT deflection measurements, strain gauge measurements, and temperature measurements. Deflection and strain data were recorded under a moving truck that was driven over the in-place instruments at a known location and vehicle speed. These measurements have been used to test the validity of applying elastic theory to predictions of deflection and strain. Comparisons of calculated to measured values have been reported (5).

The Benkelman beam and the California deflectometer were used to measure deflections under load at the pavement surface. They have been used both to assist in theoretical studies and in studies to relate deflection to performance.

Both laboratory and field samples have been used for conventional testing and for obtaining material properties for theoretical studies. PSI was calculated by

$$PSI = 5.03 - 1.91 \log (1 + SV) - 0.01 \sqrt{C + P} - 1.38 \overline{RD}^2$$

where

SV = slope variance;
C + P = amount of class 2 and class 3 cracking plus patching, $ft^2/1{,}000\ ft^2$; and
$\overline{RD}$ = average rut depth.

All definitions are the same as those used on the AASHO Road Test (6).

Performance ratings were made periodically by an inspection team or panel of six technologists involved in the project. (Usually, only four or five members participated in any one rating session.) The panel inspected the sections, noted their condition on a scale graded from excellent to failed, and recommended further testing or possible maintenance needs. The ratings were completely subjective; no attempt was made to relate them to PSI or other measurements.

For analysis purposes, the panel ratings were given a numerical scale as follows: excellent, 5; good, 4; fair, 3; poor, 2; and failed, 1.

Additional evaluations were made by individuals, particularly of drainage conditions, and these have been useful in making subjective evaluations of the project findings.

Deflection values (Tables 3 through 6) were obtained with a Benkelman beam and an 18,000-lb (80 kN) axle load (EAL_{18}). About 10 measurements were made in each test section. The deflection values (Tables 3 through 6) are mean values plus two standard deviations ($\bar{X} + 2\sigma$) corrected to a standard temperature of 70 F (21 C). The procedures for taking deflection measurements, correcting for temperature, etc., are described elsewhere (7). Figure 2 shows typical plots of rating and PSI versus time.

PERFORMANCE DATA

This study is concerned with the performance of full-depth test sections in the experiment. Four of these, asphalt concrete, asphalt-cement-treated special aggregate, emulsified-asphalt-treated special aggregate, and cutback-asphalt-treated special aggregate, were analyzed. Performance of the other bases was not subjected to the analysis technique.

Data collected during 1970, 1971, and 1972 are given in Tables 3 through 6. Only these data were used in the analysis. The period from 1970 through 1972 was generally of declining performance and seemed to hold most promise for the analytical treatment used.

Table 3. Performance data for asphalt concrete base.

Section Number	Surface Thickness[a]	Base Thickness[a]	Year	EAL_{18}	PSI	Rating[b]	Deflection[a,c]	Rut Depth[a]	Cracking[d]
9	3.22	3.02	1966	0	3.2	5.0	33	0	0
	3.22	3.02	1970	83	2.9	2.0	106	—	0
	3.22	3.02	1971	118	3.0	1.5	148	0.75	73
	3.22	3.02	1972	152	—	1.0	141	0.38	75
27	3.24	3.88	1966	0	3.7	5.0	27	0	0
	3.24	3.88	1970	83	2.2	1.0	173	—	64
	3.24	3.88	1971	118	2.0	1.0	196	—	160
	3.24	3.88	1972	152	—	—[e]			160
35	3.22	4.86	1966	0	3.8	5.0	143	0	0
	3.22	4.86	1970	110	2.8	5.0	68	—	0
	3.22	4.86	1971	141	2.4	4.5	50	0.1	16
	3.22	4.86	1972	171	—	3.5	46	0	16
2	3.14	5.61	1966	0	3.4	5.0	26	0	0
	3.14	5.61	1970	83	2.7	3.5	78	—	0
	3.14	5.61	1971	118	2.8	4.0	103	<0.25	0
	3.14	5.61	1972	152	—	5.0	99	<0.25	0
13	3.28	7.78	1966	0	3.1	5.0	21	0	0
	3.28	7.78	1970	83	2.7	4.5	50	—	0
	3.28	7.78	1971	118	3.0	4.0	66	0.25	0
	3.28	7.78	1972	152	—	4.5	79	<0.25	0

Note: 1 in. = 25.4 mm. 1 lb_f = 4.448 N. 1 F = 1.8 (1 C) + 32. 1 ft^2 = 0.0929 m^2.

[a] In 10^{-3} in.
[b] 5 = excellent, 1 = failed.
[c] Deflection, $\bar{X} + 2\sigma$ corrected to 70 F.
[d] Class 2 and 3 (6), ft^2/1,000 ft^2.
[e] Section removed from test.

Table 4. Performance data for asphalt-treated base.

Section Number	Surface Thickness[a]	Base Thickness[a]	Year	EAL_{18}	PSI	Rating[b]	Deflection[a,c]	Rut Depth[a]	Cracking[d]
23	3.00	4.82	1966	0	3.8	5.0	26	0	0
	3.00	4.82	1970	83	3.2	5.0	23	—	0
	3.00	4.82	1971	118	3.2	5.0	33	0	0
	3.00	4.82	1972	152	—	5.0	32	0	0
30	3.44	6.80	1966	0	3.3	5.0	26	0	0
	3.44	6.80	1970	83	2.7	3.5	46	—	0
	3.44	6.80	1971	118	2.8	4.0	49	0	0
	3.44	6.80	1972	152	—	3.5	61	0	0
17	3.26	7.04	1966	0	3.5	5.0	27	0	0
	3.26	7.04	1970	83	2.8	5.0		—	0
	3.26	7.04	1971	118	3.0	5.0	66	0	0
	3.26	7.04	1972	152	—	3.5	55	0	0
25	3.16	8.56	1966	0	3.9	5.0	22	0	0
	3.16	8.56	1970	83	3.1	4.0	36	—	0
	3.16	8.56	1971	118	3.1	4.0	65	0	0
	3.16	8.56	1972	152	—	—[e]	58	—	0
5	3.38	11.2	1966	0	3.5	5.0	28	0	0
	3.38	11.2	1970	83	3.1	5.0	29	—	0
	3.38	11.2	1971	118	3.3	4.0	41	—	0
	3.38	11.2	1972	152	—	5.0	46	0.25	0

Note: 1 in. = 25.4 mm. 1 lb_f = 4.448 N. 1 F = 1.8 (1 C) + 32. 1 ft^2 = 0.0929 in^2.

[a] In 10^{-3} in.
[b] 5 = excellent, 1 = failed.
[c] Deflection, $\bar{X} + 2\sigma$ corrected to 70 F.
[d] Class 2 and 3 (6), ft^2/1,000 ft^2.
[e] Section removed from test.

Table 5. Performance data for emulsified-asphalt-treated base.

Section Number	Surface Thickness[a]	Base Thickness[a]	Year	EAL_{18}	PSI	Rating[b]	Deflection[a,c]	Rut Depth[a]	Cracking[d]
29	3.29	5.56	1966	—	3.7	5.0	27	0	0
	3.29	5.56	1970	83	2.9	2.5	71	—	5
	3.29	5.56	1971	118	2.9	2.0	101	—	40
	3.29	5.56	1972	152	—	1.5	96	0.25	116
15	3.26	6.04	1966	—	3.4	5.0	71	0	0
	3.26	6.04	1970	83	2.8	2.0	133	—	0
	3.26	6.04	1971	118	3.1	3.0	111	—	11
	3.26	6.04	1972	152	—	2.5	94	0	15
22	3.10	8.00	1966	—	3.3	—	37	—	0
	3.10	8.00	1970	83	2.7	—	—	—	18
	3.10	8.00	1971	118	2.1	—	—	—	—
	3.10	8.00	1972	152	—	—[e]	—	—	—
20	3.10	8.96	1966	—	3.5	5.0	23	0	0
	3.10	8.96	1970	83	3.2	3.0	37	—	15
	3.10	8.96	1971	118	4.0	3.0	46	—	0
	3.10	8.96	1972	152	—	3.0	49	0	0
3	3.12	12.42	1966	—	3.2	5.0	32	0	0
	3.12	12.42	1970	83	3.2	4.0	35	—	0
	3.12	12.42	1971	118	3.0	3.5	37	—	0
	3.12	12.42	1972	152	—	3.0	45	0	0

Note: 1 in. = 25.4 mm, 1 lb_f = 4.448 N, 1 F = 1.8 (1 C) + 32, 1 ft^2 = 0.0929 m^2.

[a]In 10^{-3} in.
[b]5 = excellent, 1 = failed.
[c]Deflection, $\bar{X} + 2\sigma$ corrected to 70 F.
[d]Class 2 and 3 (6), ft^2/1,000 ft^2.
[e]Section removed from test.

Table 6. Performance data for cutback-asphalt-treated base.

Section Number	Surface Thickness[a]	Base Thickness[a]	Year	EAL_{18}	PSI	Rating[b]	Deflection[a,c]	Rut Depth[a]	Cracking[d]
4	3.22	5.46	1966	—	3.2	5.0	34	0	0
	3.22	5.46	1970	83	2.6	5.0	48	—	0
	3.22	5.46	1971	118	2.7	4.0	49	—	0
	3.22	5.46	1972	152	—	5.0	73	0	11
7	3.12	7.80	1966	—	3.6	5.0	29	0	0
	3.12	7.80	1970	83	3.0	4.0	39	—	0
	3.12	7.80	1971	118	2.9	3.5	50	—	0
	3.12	7.80	1972	152	—	4.5	50	0.25	0
19	3.05	8.96	1966	—	3.7	5.0	109	0	0
	3.05	8.96	1970	83	2.8	4.0	58	—	3
	3.05	8.96	1971	118	2.8	2.5	78	—	43
	3.05	8.96	1972	152	—	1.5	71	0	83
12	3.26	10.02	1966	—	3.5	5.0	29	0	0
	3.26	10.02	1970	83	3.2	5.0	25	—	0
	3.26	10.02	1971	118	2.9	3.0	59	—	0
	3.26	10.02	1972	152	—	5.0	68	0	0
21	2.83	13.94	1966	—	3.4	5.0	34	0	0
	2.83	13.94	1970	83	3.0	5.0	—	—	0
	2.83	13.94	1971	118	2.6	5.0	32	—	0
	2.83	13.94	1972	152	—	5.0	33	0	0

Note: 1 in. = 25.4 mm, 1 lb_f = 4.448 N, 1 F = 1.8 (1 C) + 32, 1 ft^2 = 0.0929 m^2.

[a]In 10^{-3} in. [b]5 = excellent, 1 = failed. [c]Deflection, $\bar{X} + 2\sigma$ corrected to 70 F. [d]Cracking, class 2 and 3 (6), ft^2/1,000 ft^2.

Figure 2. Performance trends for asphalt concrete base (sections 9 and 13).

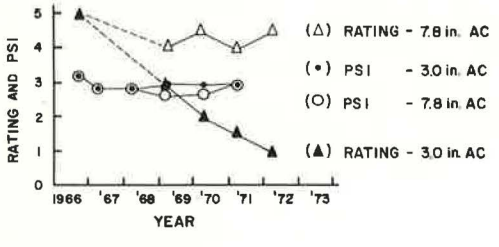

Figure 3. Hypothetical relations of years of service and base thickness for materials A, B, and C.

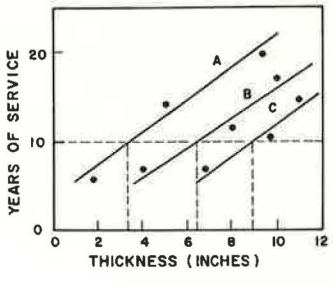

In 1972, after 6 years of traffic, 5 of the 35 test sections had been removed from traffic largely because of realignment to provide for left-turning traffic. Eleven test sections were rated poor or lower (rating numbers ≤2.0). All untreated class 3 aggregate base sections were rated poor or lower as were the standard sections. The thinnest section, level A, of the asphalt concrete base was rated failed. The thinnest and next to thinnest sections of the emulsified-asphalt-treated base mix were rated poor. The level C untreated class 2 aggregate base section was also rated poor. One of two level C cutback-treated base sections was also rated poor.

The latest available PSI data at the time of this analysis were for 1971. No sections were rated as low as 2.0, but six were rated 2.5 or less. Only one section had appreciable rutting in 1972, and only two had appreciable cracking in 1970, but cracking had increased appreciably by 1972. Most cracking observed by 1970 was believed to be load-associated. The cracking was longitudinal and began near the pavement edge and progressed inward. Tables 3 through 6 include only class 2 and 3 cracking, as defined at the AASHO Road Test (6).

PERFORMANCE ANALYSIS

One of the objectives of this experiment was to compare the behavior of various full-depth asphalt bases. In most design procedures now used, different bases require different thicknesses described by layer equivalencies or ratios of thickness that will give equal performance. Layer equivalencies now used by some agencies were determined from AASHO Road Test data (8, 9) or are based on engineering judgment. There are many indications, for the most part from theoretical considerations, that layer equivalencies are not constant but vary with subgrade, load, temperature (for asphalt-bound materials), moisture, and other factors. However, they are an integral part of many design procedures, have considerable economic implications, and will, no doubt, be used for some years to come. The performance analysis presented makes use of layer equivalencies as a weighting factor in the analysis.

As indicated, the experiment was based on statistical, factorial design principles in which base type and thickness were both variables. It was postulated that layer equivalencies could be determined by comparing thicknesses required to give equal performance. Performance could be described as years (and traffic) to some level of service (PSI, performance index, performance rating, etc.) or level of service after some time had passed. A hypothetical relationship of this principle (10) is shown in Figure 3.

Horner (10) pointed out the impracticality of using factorial designs in which each base type is built with the same thickness levels. Two designs of equal thickness but of radically different base types might take considerably different lengths of time to reach a given level of performance. For this reason, the San Diego experiment was designed by using a scheme in which each base type has its own set of thickness levels:

Base Type	Base Thickness, in., for Expected Years of Service		
	A Years	B Years	C Years
A	a	d	g
B	b	e	h
C	c	f	i

Partial replication (one replicate thickness per base type) was provided for. Also, because the objective of the experiments was to test bases, no subbases were included, and a uniform surface course thickness was used throughout.

Analysis of the data would be reasonably simple, and multiple regression techniques would be used if the performance lines proved to be parallel and the regression coefficients significant. In this report, analyses are assumed to be linear when log performance is plotted against log thickness. Considering the data scatter, the characteristics of AASHO Road Test performance data (6, 11, 12), and the ease of analysis, this seems a reasonable assumption at this time.

The model for determining performance under this assumption would be

$$\log P = a_1 + b \log T_1$$

where

P = measure of performance (rating, PSI, etc.), and
T_1 = thickness of base type i = A, B, C, etc.

The slopes are equal, and layer equivalencies between materials A and B are determined by the relationship

$$T_B/T_A = 10^{(a_A - a_B)/B}$$

The first analysis was made by using rating (by the inspection team) as the measure of performance. However, original attempts to follow the plan outlined above were not successful because of the wide scatter in the data. For this reason attempts were made to modify the model or to pool data to provide a stronger data base.

It was observed that drainage conditions were poor and variable and that Benkelman beam deflections also were variable. Because Benkelman beam measurements are considered to reflect subgrade conditions to a high degree, deflection measurements were used in an attempt to improve the relationship. Data for 1970, 1971, and 1972 were used because they produced a reasonably balanced set of data for analysis. Because 3 years were involved, traffic, in terms of EAL_{18}, was also added to the original model.

The first pass through the analysis procedure used the multiple correlation program CORREL for multivariate analysis of data (13):

$$Y = a_0 + a_1X_1 + a_0X_2 + a_3X_3$$

where

Y = f (rating);
X_1 = f (traffic, EAL_{18});
X_2 = f (deflection);
X_3 = f (equivalent thickness of the asphalt concrete base, pD_2);
D_2 = actual thickness of the base; and
1/p = weighting factor or ratio of the thickness of a given base to the thickness of asphalt concrete base required to give equal performance.

The two significant differences between this model and the more simple model tried originally were the inclusion of deflection and traffic and the use of an equivalent thickness of asphalt concrete base rather than actual base thickness as the variable.

For the first pass through the analysis, values of 1/p were assumed from analyses of the data made by Finn (5) and by the project steering committee with earlier data. Values of 1/p used were as follows: 1.0 for asphalt concrete base, 1.2 for asphalt-treated, 1.7 for emulsion-treated, and 1.5 for cutback-treated.

Four different relationships were used: one arithmetic relationship between variables and three with log transformations of the variables. In all four relationships, the degree of correlation between rating and the other variables remained fairly constant regardless of the transformation used. The correlation between rating and both deflection and equivalent pavement thickness was significantly different from zero at the 99 percent level. The common assumption that rating should vary directly with pavement thickness and inversely with deflection was verified in the analysis. A significant inverse relationship between equivalent pavement thickness and deflection was also shown to exist.

The only predictor that did not show a good degree of correlation with the rating was the traffic variable, EAL_{18}. At the 80 percent level, this correlation was not significantly different from zero. Although this was not a desirable outcome, it did permit pooling of the data for 1970, 1971, and 1972 for the next step in the analysis. It is not

easy to explain the lack of significant correlation between EAL_{18} and the rating factor. When plotted, these variables show no real trend; however, if the individual pavement sections are observed separately, a very good trend or relationship may be seen (Fig. 2). This seems to indicate that the poor correlation for the entire sample is due to a lack of range in the traffic variable. As is evident from the data, the number of equivalent axle loads is not truly a random variable.

From the above considerations, the following model was adopted in an attempt to determine analytically the values of 1/p:

$$\log R = a_0 + a_1 d + a_2 \log pD_2$$

where

R = rating,
d = deflection in 10^{-3}-in. units,
p = base weighting factor set equal to 1.0 for asphalt concrete, and
D_2 = actual base thickness.

CORREL (13) was run on pairs of base types, each pair consisting of data for the 3 years for the asphalt concrete base and one of the remaining three base types. A range of p-values was chosen for each run from 1/p = 0.8 to 2.1. By plotting 1/p versus correlation coefficients between log rating and log pD_2, it was possible to determine the best fit 1/p value for each base type: for asphalt concrete, 1.0 (assumed); asphalt-treated, 0.85; emulsion-treated, 1.7; and cutback-treated, 1.2.

By using these values of 1/p to determine new equivalent thicknesses, a new performance relationship was determined. The final performance equation computed with the MULTR multiple regression computer program (13) in which rating as the dependent variable is

$$\log R = 0.604583 - 0.0034831\ d + 0.195726 \log pD_2$$

where

R = panel rating;
d = deflection in 10^{-3}-in. units;
p = base weighting factor, as given previously;
D_2 = base course thickness;
R^2 = squared multiple correlation coefficient = 0.64; and
S.E. = standard error of estimate = 0.117491.

R^2 and S.E. indicate that the regression equation does a fair job of explaining variations in the rating.

Three additional performance models were also attempted in which the same technique and variables (with the addition of D_1 = surface thickness, $D = D_1 + pD_2$) and $R^2 = 0.649$ were used:

$$\log PSI = a_0 - a_1 d + \log a_2\ pD_2$$

$$\log R = a_0 - a_1 d + \log a_2\ (D)$$

$$\log PSI = a_0 - a_1 d + \log a_2\ (D)$$

Thus, for example, $\log R = 0.4929623 - 0.0035115\ d + 0.2789277 \log D$ for S.E. = 0.116091.

The reason for using PSI as the dependent variable is obvious because PSI is a standard measure that has been developed and used since the AASHO Road Test. The use of $D = D_1 + pD_2$ was made to approximate the structural number concept adopted on the AASHO Road Test and used elsewhere (8).

The analyses using the PSI and D variables indicated that values of 1/p remained essentially unchanged; therefore, they were used as originally determined. However,

neither of the equations using PSI resulted in a significant correlation. None of the R^2 values was greater than 0.3, and the coefficients on the thickness variable were negative. These results were judged not acceptable, and the model was rejected.

The two successful performance equations [$\log R = a_0 + a_1 d + a_2 \log pD_2$ and $\log R = a_0 - a_1 d + \log a_2(D)$] appear to be equal in their ability to represent the data, although, in the equation using $D = D_1 + pD_2$, thickness effects have more weight in predicting rating.

In addition to the multiple regression discussed earlier, several simple correlations were tried between rating and PSI. None resulted in a significant correlation. It was necessary to conclude, therefore, that PSI could not be used to indicate test section performance.

FACTORS FOR ANALYZING PERFORMANCE

One of the major conclusions of a workshop on structural design of asphalt concrete pavements (14) was the need to relate pavement distress to performance. Performance data from the San Diego experimental base project should be of some help in meeting this need.

A workshop group on relating distress to pavement performance (14) indicated that there are basically two methods in use for serviceability evaluation of pavements: a road-user-related index or rating system and a mechanistic evaluation primarily based on deflection measurements. The group stated that a present serviceability rating or PSI pavement evaluation system is the most satisfactory method available for evaluating pavement performance. For this evaluation, the group emphasized the need for (a) a better relationship between serviceability, performance, time, and traffic; (b) a study of the effects of maintenance on serviceability trends; (c) a data feedback system; and (d) quantitative distress information.

The San Diego project measurements program included five measures that possibly could be used to evaluate pavement performance: (a) PSI, (b) a panel rating, (c) cracking, (d) rut depth, and (e) deflection. In this study, deflection has been used only to remove subgrade variability influences. Cracking was used only as it influenced PSI measurements. No direct use was made of rut depth, which in most cases was small.

The panel ratings are in many respects indicators of maintenance needs, and they reflect subjective evaluations of the pavement condition by using only visual data. PSI was based on a mechanical evaluation of the pavement surface condition, except for the limited influence of cracking. A relationship between the two would indicate to some extent how well PSI might reflect a visual maintenance need-related rating.

Comparisons between PSI and ratings (Tables 3 through 6 and Fig. 2) indicate that the two measures do not reflect pavement performance in the same way. The correlation between the two was extremely poor, as explained earlier.

If deflection and equivalent thickness (pD_1 or $D = D_1 + pD_2$) are considered structural variables, it is concluded, on the basis of the analyses presented here, that rating was a reasonably good indicator of pavement performance but PSI was not. The relationship between rating, deflection, and $D = D_1 + pD_2$ is shown in Figure 4.

The base type weighting factors ($1/p$) determined in the performance analysis also are significant because they are related to layer coefficients or layer equivalency values used in many pavement design methods (8, 9).

The base weighting factors and the original values assumed in designing the experiment are given in Table 7. Even though a discussion of equivalency factors is beyond the scope of this paper, it is encouraging that the three treated bases performed as well as or better than expected relative to the high type of asphalt concrete base. These three mixes were designed and constructed with a marginal-quality sandy gravel similar to many available in a larger quantity elsewhere, and the results could have wide applicability provided proper account is given to different environmental conditions.

CONCLUSIONS

From test conditions and limitations of the analysis, the following conclusions may be drawn from performance data from the San Diego experimental base project. The

Figure 4. Rating versus D.

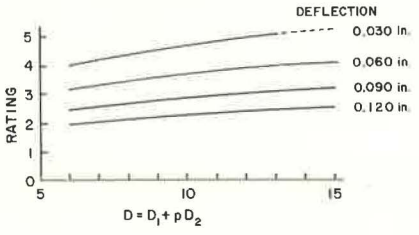

Table 7. Summary of base weighting factors.

Base Type	Design	Analysis
Asphalt concrete	1.0	1.0 (assumed)
Asphalt-treated	1.4	0.85
Emulsified-asphalt-treated	1.7	1.7
Cutback-asphalt-treated	1.7	1.2

conclusions apply only to the four full-depth base sections incorporated in the experiment at all thickness levels.

It was possible to develop significant relationships between a panel rating of test section performance and the structural variables, deflection and equivalent thickness. The data did not yield significant relationships with either traffic or PSI.

Base type weighting factors were developed from the analysis. The analysis indicated that the relative performance of the full-depth, asphalt-treated bases with a marginal-quality sandy gravel aggregate compared to the high-quality asphalt concrete base was as good as or better than assumed in the original design of the experiment. Their relevance to other conditions and environments is still to be determined.

ACKNOWLEDGMENT

We would like to thank San Diego County, which was the primary sponsor of this project and which was responsible for road design and plans, contract administration, and construction control, and The Asphalt Institute, which consponsored the project and designed the basic experiment. We would also like to thank all the cooperating organizations that participated in the testing and research activities: the California Division of Highways, Los Angeles County, Orange County, the Chevron Asphalt Company, the Shell Oil Company, and the Union Oil Company.

REFERENCES

1. Guidelines for Satellite Studies of Pavement Performance. NCHRP Rept. 2A, 1964.
2. Riley, J. C., and Shook, J. F. San Diego County Experimental Base Project: Design and Construction. The Asphalt Institute, College Park, Maryland, Research Rept. 67-4, June 1967.
3. Kingham, R. I. Full-Scale Experimental Base Construction in San Diego County. Presented at ASCE National Meeting on Transportation Engineering, San Diego, Calif., Feb. 19-23, 1968.
4. Shook, J. F. San Diego County Experimental Base Project. Presented at 22nd Annual California Street and Highway Conference, Monterey, Jan. 30, 1970.
5. Hicks, R. G., and Finn, F. N. Analysis of Results From the Dynamic Measurements Program on the San Diego Test Road. Proc., AAPT, Vol. 39, 1970.
6. The AASHO Road Test, Report 5, Pavement Research. HRB Special Report 61E, 1962.
7. Asphalt Overlays and Pavement Rehabilitation. The Asphalt Institute, College Park, Maryland, Manual Series 17(MS-17), 1st ed., Nov. 1969.
8. AASHO Interim Guide for Design of Flexible Pavement Structures. American Association of State Highway Officials, 1972.
9. Thickness Design—Full-Depth Asphalt Pavement Structures for Highways and Streets. The Asphalt Institute, College Park, Maryland, Manual Series 1 (MS-1), 8th ed., Dec. 1969.
10. Horner, T. Y. Experimental Design and Analysis of Experiments for Comparison of Paving Materials. The Asphalt Institute, Aug. 1965.

11. Shook, J. F., and Finn, F. N. Thickness Design Relationships for Asphalt Pavements. Proc., International Conference on the Structural Design of Asphalt Pavements, Univ. of Michigan, Ann Arbor, Aug. 1962.
12. Painter, L. J. Analysis of AASHO Road Test Data by The Asphalt Institute. Proc., International Conference on the Structural Design of Asphalt Pavements, Univ. of Michigan, Ann Arbor, Aug. 1962.
13. Cooley, W. W., and Lohnes, P. R. Multivariate Data Analysis. John Wiley and Sons, New York, 1971.
14. Structural Design of Asphalt Concrete Pavement Systems. HRB Special Report 126, 1971.

DEVELOPING STRUCTURAL DESIGN MODELS FOR ONTARIO PAVEMENTS

Nabil Kamel, Ministry of Transportation and Communications, Ontario

This paper describes the applications of layered system analysis in designing Ontario pavements. The Brampton Test Road experiment provided this investigation with various data on material properties, climatic conditions, traffic, and performance. Test sections were analyzed by using Bistro and Chevron computer programs, which predict the structural response of stresses, strains, and deflections in pavement sections. The moduli values required for the analysis were derived from laboratory test data provided by The Asphalt Institute. The calculated structural responses were then correlated to observed field behavior and performance of test sections. Pavement responses, as predicted by the layered system analysis, could be closely related to observed behavior and performance. The analysis shows relationships existing between observed surface rut depth and vertical compressive strain on the subgrade surface. The measured Benkelman beam rebounds and calculated subgrade surface deflections are also correlated. Charts to predict pavement performance for various peak Benkelman beam rebounds are developed, and equivalencies of various types of Brampton base materials are derived based on a criterion of equal loss of serviceability. The paper presents a structural design system for flexible pavements and discusses, through an example problem, how this system is incorporated into the overall pavement management system in Ontario.

•DURING the past 5 years, considerable attention has been devoted in Canada and the United States to developing rational pavement design and management systems (1, 2, 3, 4, 5, 6, 7, 8). A pavement management system includes a number of subsystems, i.e., planning, structural design, construction, maintenance, performance evaluation, a data bank, and research. These subsystems are structured together and aimed at producing the best pavement design and management process.

A major component of any pavement management system is the structural design subsystem. The primary outputs of this subsystem are to predict performance (i.e., serviceability history) and associated cost and benefits of various design strategies. Many researchers have attempted to use structural analysis to estimate stresses, strains, and deflections in pavement structures. The structural analysis alone, however, has no significance if it is not related to pavement serviceability history, which is the designer's primary concern. The development of transformation functions that relate structural responses and performance is a comprehensive task and as yet has not been extensively developed in pavement design technology. Kamel (9, 10) and Kamel et al. (11) attempted to develop such functions for conditions in southern Ontario by examining data from the Brampton Test Road and developing charts to predict serviceability losses with traffic (or pavement age) for various vertical stress levels on a subgrade surface.

For this investigation, the Brampton Test Road experiment provided extensive data on material properties, traffic, climate, and performance. The basic purpose of this

Publication of this paper sponsored by Committee on Theory of Pavement Design.

investigation was to determine whether structural analysis could be used to predict serviceability and age (or traffic) histories of various pavement designs used at Brampton. The analysis was then extended to develop a second generation set of pavement structural design models for Ontario's pavement design and management system (1).

This paper reports the structural analysis of the Brampton Test Road sections by using computerized nonlinear, elastic-layered techniques. It presents several relationships obtained between the calculated structural responses, observed behavior, and measured performance of the in-service test sections. It discusses base layer equivalencies for various Brampton materials and the application of the results to pavement design and management systems in Ontario.

STRUCTURAL ANALYSIS OF THE BRAMPTON TEST ROAD

In August and September of 1965, a full-scale experiment known as Brampton Test Road was constructed on Highway 10 north of Brampton, Ontario. Details of the project, construction, objectives, and findings are discussed by Schonfeld (12) and Phang (13, 14). Figure 1 shows a layout of the experimental pavement sections, which consist of 36 test sections and incorporate 5 types of base materials. The test sections of cement-treated base suffered from shrinkage fracture early in the experiment and were not considered in this investigation.

The structural analysis was performed by means of calculating stresses, strains, and deflections throughout each of the test sections. The details of the structural models used for calculations, material characterization, and structural analysis procedures are given by Kamel, Phang, Morris, and Haas (11). Chevron and Bistro multilayered, elastic computer programs were used to calculate the structural responses, and iterative procedures were used to account for the nonlinear characteristics of the materials. The moduli values required for the analysis were derived from results of repeated load triaxial compression tests, which were conducted on Brampton materials (15, 16).

The stiffness moduli of the asphalt concrete, s, were calculated by using McLeod's modified method (17). The stiffness-temperature relationships were then constructed by using a loading time of 0.03 sec, which corresponds to traffic moving at 60 mph (100 km/h) (18).

The temperature at the middepth of each asphalt concrete layer was estimated by using Southgate's models (19). The corresponding stiffness modulus for each layer was then obtained, and the structural layered analysis was performed for each pavement section. The results are given in Table 1.

STRUCTURAL ANALYSIS AND PAVEMENT PERFORMANCE RELATIONSHIPS

Pavement Serviceability and Performance

At the AASHO Road Test, Carey and Irick (20) developed the best known procedure for defining and obtaining serviceability. Their concept of the present serviceability rating (PSR) explicitly recognized the road user by means of a panel rating procedure. PSR was then correlated to a set of physical measurements called the present serviceability index (PSI). The integration of PSI over time or load applications was termed the performance.

The present performance rating (PPR) was developed concurrently in Canada by the Roads and Transportation Association of Canada (RTAC) along similar lines except that it used a 10-point rather than a 5-point scale (21, 22). In 1968, the pavement management committee of RTAC changed the term PPR to riding comfort index (RCI) (3). The new term recognized that serviceability is only an evaluation of riding comfort quality and does not include structural condition or safety characteristics. RCI is employed throughout this paper.

At Brampton, RCI was estimated from correlations between RCI and a roughness index profilometer patterned after the British Road Research Laboratory design (23, 24).

Figure 1. Layout of experimental pavement sections.

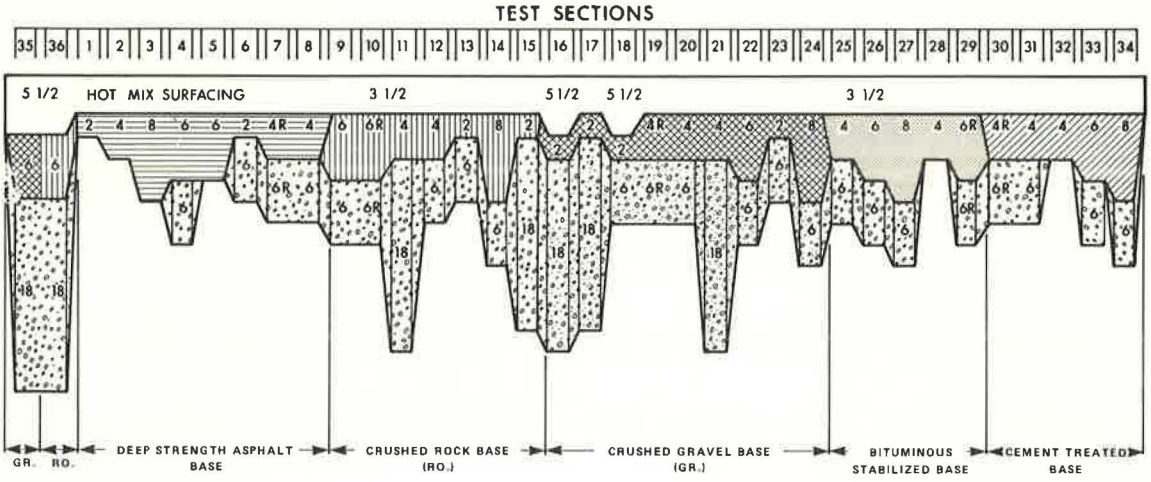

LEGEND

R. = REPLICATED (I.E. DUPLICATED DESIGN)

GR. = CRUSHED GRAVEL BASE

RO. = CRUSHED ROCK BASE

Table 1. Results of layer analysis.

Base Type	Section Number	Surface Deflection (in.)	Subgrade Deflection (in.)	Vertical Stresses on Subgrade Surface σ_v (psi)	Vertical Strain on Subgrade Surface ϵ_v (in./in. $\times 10^{-3}$)
Asphalt concrete, no subbase	1	0.0183	0.0172	30.3	0.917
	2	0.0134	0.0120	20.7	0.609
	3	0.0096	0.0074	12.0	0.292
	5	0.0104	0.0088	14.6	0.398
Asphalt concrete, 6.0-in. subbase	4	0.0103	0.0064	9.32	0.229
	6	0.0172	0.0110	18.00	0.573
	7, 8	0.0128	0.0083	12.90	0.352
Crushed rock, 6.0-in. subbase	9, 10	0.0241	0.0095	14.90	0.505
	12	0.0226	0.0108	17.20	0.601
	13	0.0240	0.0133	20.60	0.792
	14	0.0236	0.0083	12.60	0.405
Crushed rock, 18-in. subbase	11	0.0249	0.0053	7.04	0.205
	15	0.0232	0.0056	8.07	0.227
	36	0.0211	0.0046	5.28	0.148
Crushed gravel, 18-in. subbase	16	0.0208	0.0053	6.71	0.187
	17	0.0227	0.0056	8.04	0.225
	21	0.0278	0.0056	7.30	0.214
	35	0.0216	0.0047	5.36	0.150
Crushed gravel, 6-in. subbase	18	0.0181	0.0099	15.40	0.499
	19, 20	0.0240	0.0109	17.50	0.629
	22	0.0247	0.0090	14.70	0.580
	24	0.0223	0.0080	12.50	0.384
Bituminous-stabilized, 6-in. subbase	25	0.0210	0.0102	16.70	0.561
	26, 29	0.0211	0.0086	13.40	0.429
	27	0.0200	0.0076	11.70	0.342
Bituminous-stabilized, no base	28	0.0241	0.0189	28.60	1.230

Note: 1 in. = 25.4 mm, 1 psi = 6.8948 kPa.

Relationship of Pavement Rutting and Vertical Strain on Subgrade Surface

Measurements of the pavement surface rut depth were taken at Brampton on each test section at 20 wheel-path locations by using a 4-ft (1.2 m) transverse span gauge. The observed surface rutting is related to the vertical compressive strain (ϵ_v) and the vertical compressive stress (σ_v) on the subgrade surface.

The calculated ϵ_v gave better relationships with surface rut depth (RD). Some sample results are shown in Figure 2. Although the data are scattered, it appears that there is a correlation between RD and ϵ_v. In addition, it appears that the full-depth asphalt concrete sections do not follow the same pattern as the conventional sections in that higher strains can be tolerated by the former without excessive rutting.

Trenching was not done at Brampton; consequently it is not conclusively known to what relative extent rutting has occurred in various layers. However, by comparing the RD of the full-depth and the deep-strength asphalt sections, a significant amount of rutting was observed in the subbase. At the AASHO Road Test, an average of 45 percent of the rutting for loops three to six occurred in the subbase (25).

A detailed description of this phase of the analysis is given by Haas, Kamel, and Morris (26). It was emphasized that present technology is only able to recommend criteria for precluding excessive rutting (27, 28); it is not sufficiently developed to be able to confidently predict the actual amount of rutting that might occur for any given design situation. The current state of the art is extensively discussed by Morris and Haas (29).

Relationship of Riding Comfort Index, Traffic, and Vertical Stress on Subgrade

The observed performance, in terms of RCI values, is related to the calculated σ on subgrade surface, and a linear relationship was found at various pavement ages (1965-1970).

The relationships of serviceability loss with traffic at various σ_v levels were subsequently constructed by using the preceding relationships based on the traffic history at Brampton. A typical chart is shown in Figure 3. It can be seen that RCI decreases more rapidly as the vertical stress on the subgrade surface increases. This phase of the analysis is discussed by Kamel (9). These charts can be used to predict pavement serviceability history if traffic history and computed vertical stress on subgrade surface are known. The application of these results to a pavement design system is demonstrated by Kamel, Phang, Morris, and Haas (11).

Relationship of Riding Comfort Index, Traffic, and Benkelman Beam Rebounds

Benkelman beam rebound measurements have been made periodically at Brampton. The computer values of subgrade surface deflections gave a good relationship with the initial, mean-peak rebound values observed in spring 1966. Figure 4 shows these relationships for (a) full-depth asphalt concrete sections and (b) all other Brampton sections considered. A good linear relationship is obtained for the latter with r^2 equal to 0.936 and a standard error of estimate equal to 0.007 in. (0.18 mm). The relationship for all except the full-depth sections is

$$x = 7\,\delta_s$$

where

x = mean-peak initial Benkelman beam rebound, and
δ_s = computed subgrade surface deflection.

This relationship depends on the moduli values that were used for the layer analysis. For the asphalt concrete layers, these moduli were based on a loading time of 0.03 sec, which corresponds to a speed of about 60 mph (100 km/h). If lower speeds (i.e., longer

Figure 2. Surface RD versus δ_s for some Brampton Test Road sections.

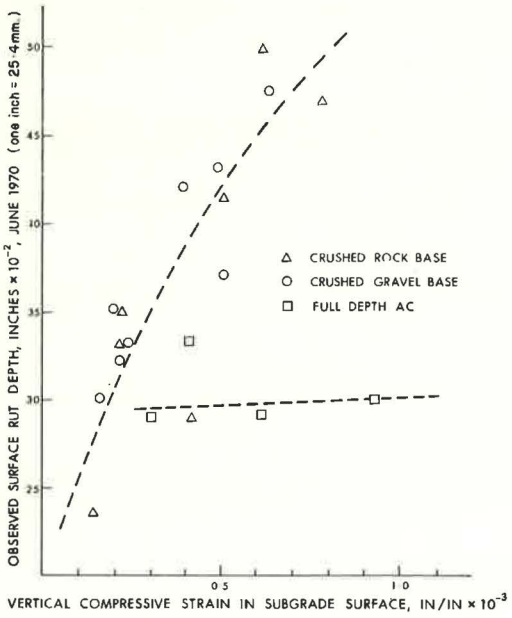

Figure 3. Loss of riding comfort with traffic (or pavement age) for various subgrade stress levels (data from Brampton Test Road).

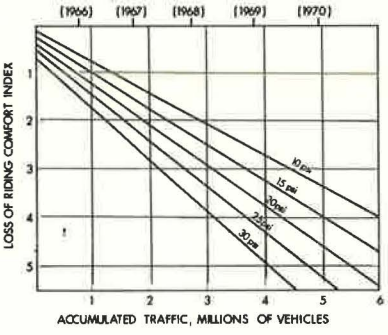

Figure 4. Calculated δ_s versus measured initial mean-peak Benkelman beam rebounds.

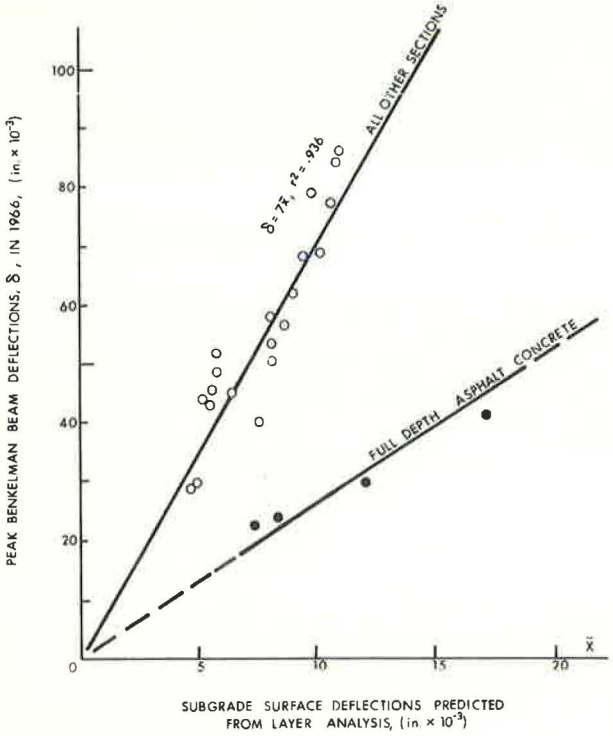

loading times) were used, the estimated moduli values would be less and higher subgrade surface deflections should be predicted. In turn, those computed deflections would then more closely correspond in actual magnitude to the rebound measurements of Benkelman beam, which are taken at creep speed.

The computed subgrade surface deflections were also related to the performance of the corresponding in-service experimental pavement sections. Figure 5 shows the good relationships obtained for the full-depth asphalt concrete sections and for all other pavement sections.

Figure 6, a summary of Figure 5 relationships, shows the effect of the magnitude of the subgrade surface deflections δ_s and pavement age A on pavement performance. Pavement age in such relationships reflects the effects of a variety of variables, i.e., climate, aging, subgrade movements, etc. The relationships clearly indicate that RCI decreases as δ_s increases and as A increases. The relative influence of δ_s and A varies more in the case of full-depth asphalt concrete than in all other sections. The influence is less in the former case.

Figure 6 also shows that the loss of RCI between any 2 consecutive years, for any particular level of δ_s, seems to be fairly constant for each of the two behavior patterns. The annual loss is comparatively smaller for the full-depth sections. This suggests that pavements with equal δ_s may be subject to relatively equal annual loss of RCI, where such annual losses increase as δ_s increases.

The foregoing relationships of Figure 4 were used to determine the subgrade surface deflections corresponding to Benkelman beam rebounds of 0.02, 0.04, 0.06, 0.08, and 0.10 in. (0.5, 1.0, 1.5, 2.0, 2.5 mm). These deflection values were then used to determine the corresponding RCI values at various pavement ages from Figure 6. These derived RCI values were found to give the best correlations with Brampton's traffic if plotted on a log scale (Fig. 7) against traffic on arithmetic scales.

Figure 7 clearly shows the serviceability history of the different pavement sections and the behavior under traffic for various pavement strengths. Although these relationships primarily apply to the Brampton Test Road conditions, they should give a general picture of the basic performance characteristics of flexible pavements in similar climatic regions.

DEVELOPMENT OF BASE LAYER EQUIVALENCIES

The equivalencies of various materials have generally been based on equal structural response. In this study, equivalencies are developed on the basis of equal terminal serviceability or equal loss of serviceability. This criterion seems to be more realistic because pavement performance must be the end concern. Equivalencies based on this criterion enable the designer to generate thickness combinations without having to consider the problem of strength differences.

The step-by-step development of the base layer equivalencies is discussed by Haas, Kamel, and Morris (26). Brampton base layer equivalency values (in inches of the granular base) for 1 in. (25.4 mm) of each material type are as follows:

1. Granular base (crushed gravel or crushed rock), 1.0;
2. Sand subbase, 0.6;
3. Bituminous-stabilized base, 1.1;
4. Asphalt concrete base (with subbase), 2.0; and
5. Full-depth asphalt concrete base, 3.4.

That is, 1 in. (25.4 mm) of granular base $\approx$ 1 in. (25.4 mm) of bituminous-stabilized base $\approx$ 2 in. (50.8 mm) of sand subbase $\approx$ ½ in. (12.7 mm) of asphalt concrete base $\approx$ ⅓ in. (8.4 mm) of full-depth asphalt concrete. The values obtained are very close to those presently employed by the Ministry of Transportation and Communications of Ontario.

APPLICATION OF ANALYSES TO PAVEMENT DESIGN IN ONTARIO

Haas and Hudson (30) proposed that two levels of terminal serviceability be applied to pavements: a desirable terminal level and a minimum acceptable level at which the

Figure 5. Relationship between RCI and calculated δ_s.

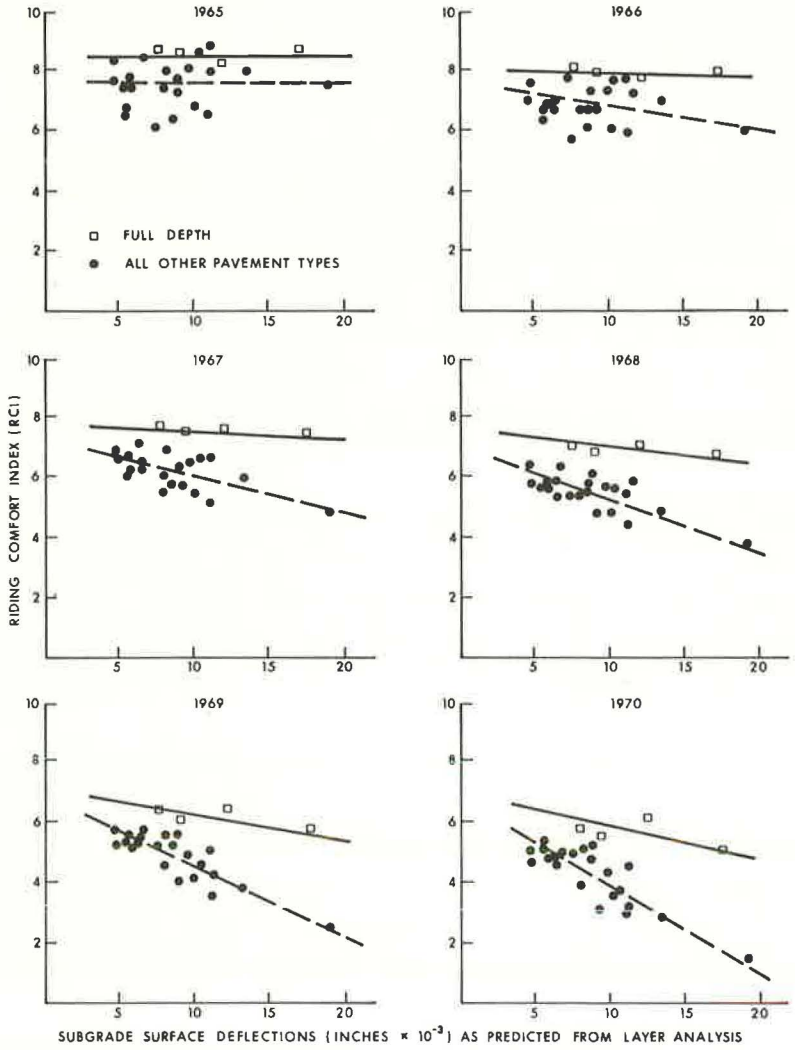

Figure 6. Summary of relationship between RCI and calculated δ_s.

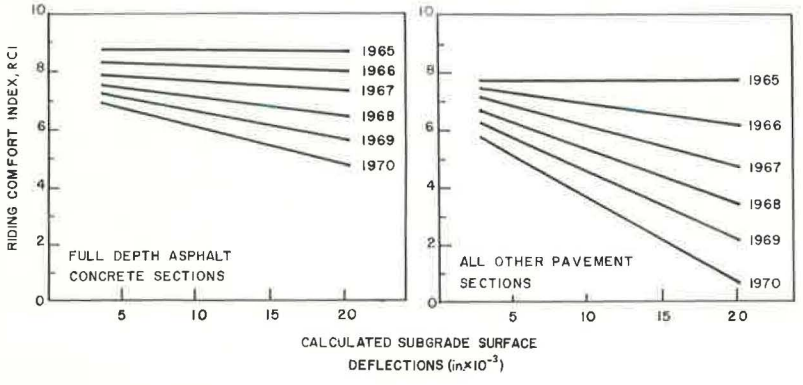

riding quality is so bad that it may affect the normal operation of a passenger car. In this study, an RCI of 4.5 is used by the pavement design and evaluation committee of the Canadian Good Roads Association (3, 21, 22).

Development of Deflection-Based Design Curves

The minimum acceptable RCI of 4.5 on the RCI, traffic, and Benkelman beam curves is shown in Figure 7. The diagram for all pavement sections but the full depth shows that pavements having 0.05-in. (1.3 mm) maximum rebound reach a terminal RCI of 4.5 after about 6 million vehicle passes. This agrees well with the extensive data examined in the Canadian Good Roads Association studies (21).

The relationships of Figure 7 were used to develop the deflection-based design curves of Figure 8. The accumulated traffic value corresponding to the intersection of each performance line of peak rebound with the terminal RCI line was determined. The determined traffic value was then transformed into average daily traffic (ADT) numbers for various pavement ages and was plotted against the corresponding peak Benkelman beam rebound. The deflection-based design curves of Figure 8 are for all pavement sections except the full depth. Similar design curves for full-depth asphalt concrete can be developed by using the upper part of Figure 7.

Pavement Design Approach

Table 2 gives the Ontario flexible pavement design thickness guidelines used by the Ministry of Transportation and Communications for different traffic and highway classes.

Jung and Phang (31) assigned moduli values, E, to various Ontario subgrade soils and developed a thickness design chart that basically reflects the thicknesses given in

Figure 7. Performance relationships for various peak Benkelman beam rebounds.

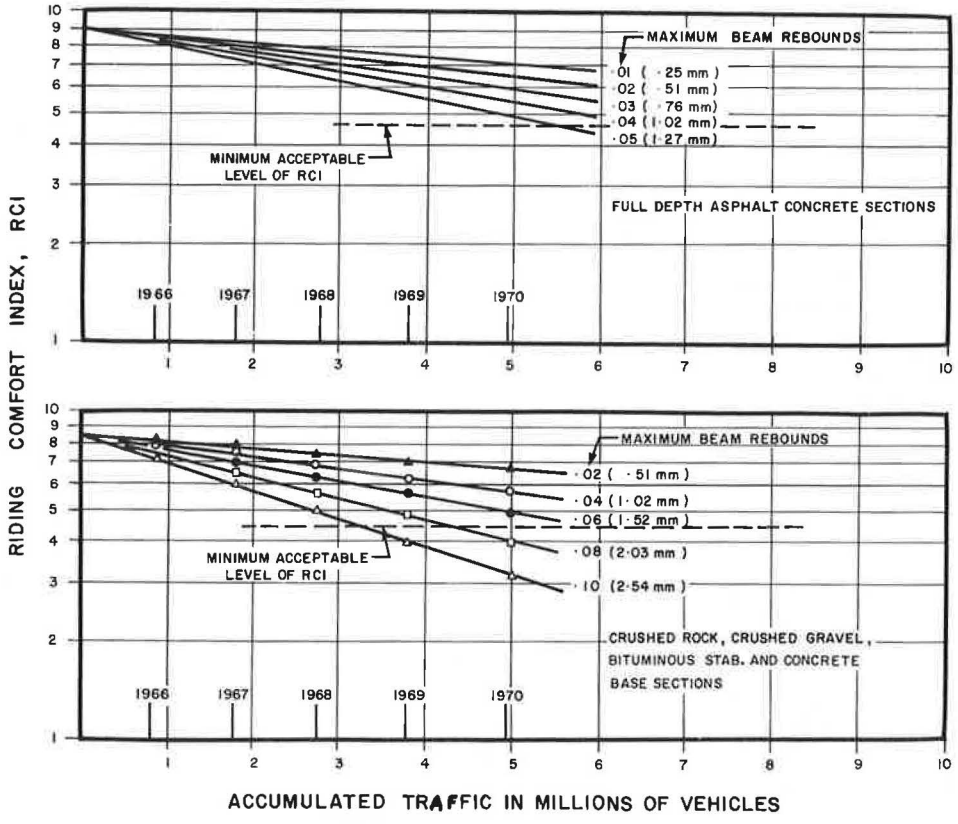

Figure 8. Deflection-based design curves.

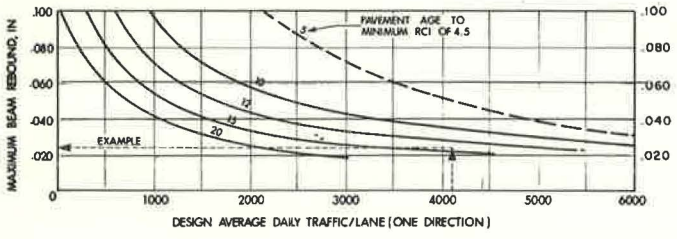

Table 2. Flexible pavement design thickness guidelines.

Road Class	Standard Surface Thickness of Hot Mix (in.)	Total Pavement Thickness of Subgrade[a]: Granular Type of Material Suitable as Granular Borrow	Sandy Silt and Clay Loam Till: Silt <40, Very Fine Sand and Silt <45	Sandy Silt and Clay Loam Till: Silt 40-50, Very Fine Sand and Silt 45-60	Sandy Silt and Clay Loam Till: Silt >50, Very Fine Sand and Silt >60	Lacustrine Clays	Varved and Leda Clays	Design ADT (both directions)[b]	Maximum Beam Rebound[c] ($\bar{x} + 2\sigma_1$)
Multilane									
>8,000 AADT	5½	17-20	25-29	29-33	33-37	29-33	29-45	12,500	0.022
Two lanes									
6,000 to 8,000 AADT	5½	17-20	25-29	29-33	33-37	29-33	29-45	9,000	0.025
4,000 to 6,000 AADT	5	16-19	24-28	28-32	32-36	28-32	28-44	6,500	0.030
2,000 to 4,000 AADT	4	14-17	22-26	26-30	30-34	26-30	26-38	4,300	0.038
1,000 to 2,000 AADT	2½	11-14	19-23	23-27	23-31	19-27	23-31	2,100	0.055

Note: 1 in. = 25.4 mm.

[a]In inches of granular base A (i.e., 1 in. of granular base A = ½ in. of hot mix = 1½ in. of granular subbase C).

[b]Design ADT = AADT $\left(1 + \text{percentage of traffic growth per year} \times \frac{\text{initial life}}{2}\right)$, assumed traffic growth = 4.5 percent per year, lane factor = 80 percent, and initial pavement life = 13 years.

[c]Calculated from maximum rebound of CGRA study.

Figure 9. Relationship of pavement thickness and maximum Benkelman beam rebound relationship for various Ontario subgrade soils.

SUBGRADE MODULI VALUES (Em),psi

GRAN. TYPE MATERIALS	SANDY SILT AND CLAY LOAM TILL: SILT < 40 V.F. SA. AND SILT < 45	SANDY SILT AND CLAY LOAM TILL: SILT 40-50 V.F. SA. AND SILT 45-60	SANDY SILT AND CLAY LOAM TILL: SILT > 50 V.F. SA. AND SILT > 60	LACUSTRINE CLAYS	VARVED AND LEDA CLAYS
9000 - 12000	4500 - 6500	3500 - 5500	3000 - 4500	4000 - 6000	2500 - 4000

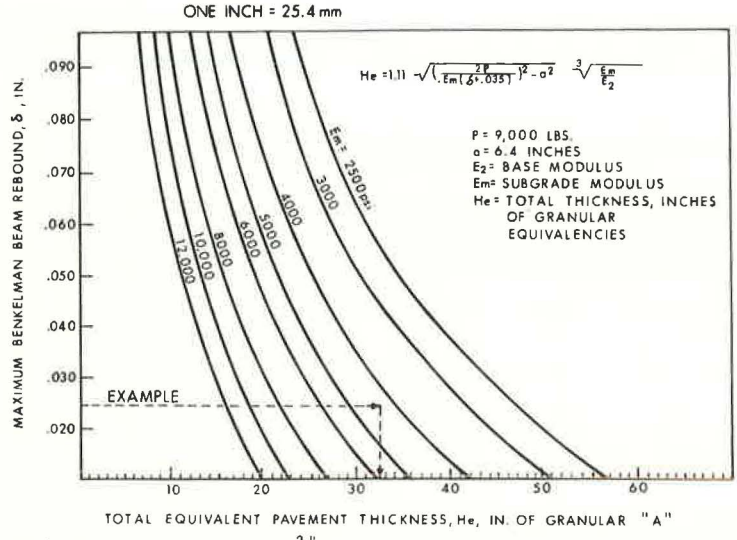

Table 2. In this investigation, the thickness design chart was related to maximum Benkelman beam rebounds (Table 2) for different traffic and highway classes. The chart is shown in Figure 9.

The application of the foregoing results to a pavement design system is shown in Figure 10, which is a simplified flow chart of the major steps required in the design process.

Example Problem

A four-lane divided highway is designed to carry a present AADT of 8,000 vehicles. An average simple growth rate of traffic is assumed to be 4 percent. The two pavement widths are 24 ft (7.3 m) each with 10-ft and 6-ft (3.0 and 1.8 m) outside and inside shoulders respectively. More than 90 percent of the project is constructed on fill materials (clay). The project is in a new location and extended for about 5 miles (8 km).

The designer follows these steps (Fig. 10):

1. Assume that the analysis period = 20 years and E-subgrade clay = 4,500 psi (310 MPa).
2. Calculate the design ADT per lane. Design ADT is defined as the average daily traffic per lane at the middle of the initial life span. Assume the initial life is 14 years and the lane factor is 80 percent. This would result in a design ADT of about 4,100 vehicles per day per lane.
3. Consider the available materials. Assume that this is restricted to an asphalt concrete (HL1-8) and granular type A materials.
4. Generate alternative pavement initial lives and calculate the corresponding maximum rebound for each by using Figure 8. Consider one initial life alternative at 14 years. The deflection-based design curves of Figure 8 show that a pavement section carrying a design ADT per lane of 4,100 and initial life of 14 years should be designed for a maximum rebound of 0.025 in. (0.6 mm). This is only one alternative; the designer could generate other designs of various strengths and initial life spans.
5. Derive the required pavement thickness from Figure 9. About 33 in. (840 mm) of equivalent to granular A material is required for the subgrade clay soil. This total pavement thickness of granular base A could be converted to different alternative combinations of material thickness by using the base layer equivalencies developed previously (i.e., 1 in. of asphalt concrete = 2 in. of granular base A = 3 in. of subbase). The following combination may be used. The designer may choose 1½ in. (38 mm) of asphalt concrete surface HL 1, which is equivalent to 3 in. (76 mm) of granular base A; 10½ in. (267 mm) of asphalt concrete binder HL 2-8, which is equivalent to 21 in. (229 mm) of granular base A; and 9 in. (535 mm) of granular base A—a total equivalency of 33 in. (840 mm). This, of course, is one possible thickness combination. Many other alternative combinations can be considered in the analysis.

Figure 11 shows a cross section of the deep-strength design under consideration as well as the expected serviceability age history of the pavement strategy. Because this design problem deals with design of a major highway, it is recommended that the serviceability level should not drop below RCI = 6. Consequently resurfacing may be required at 10 years (Fig. 11).

The design problem is not complete until a final design strategy has been recommended. This paper concentrated on the parts of the design phase of Ontario pavement management that deal primarily with the structural models and their inputs. As indicated in Figure 10, overlay design must be completed to the end of the analysis period. This may be done in the same manner as described by Phang and Slocum (1). Economical evaluation must also be conducted after estimation of expected materials, construction, and maintenance costs for each strategy. The designer can then, along with other considerations, recommend a final strategy for construction.

This example is an actual work project in the 1973-77 construction program of the Ministry of Transportation and Communications, Ontario. The construction is for Highway 406, St. Catharine's area, Hamilton district. The pavement selection committee of the Ministry, in its recommendation for the most economical design for the

Figure 10. Flow chart of pavement design system.

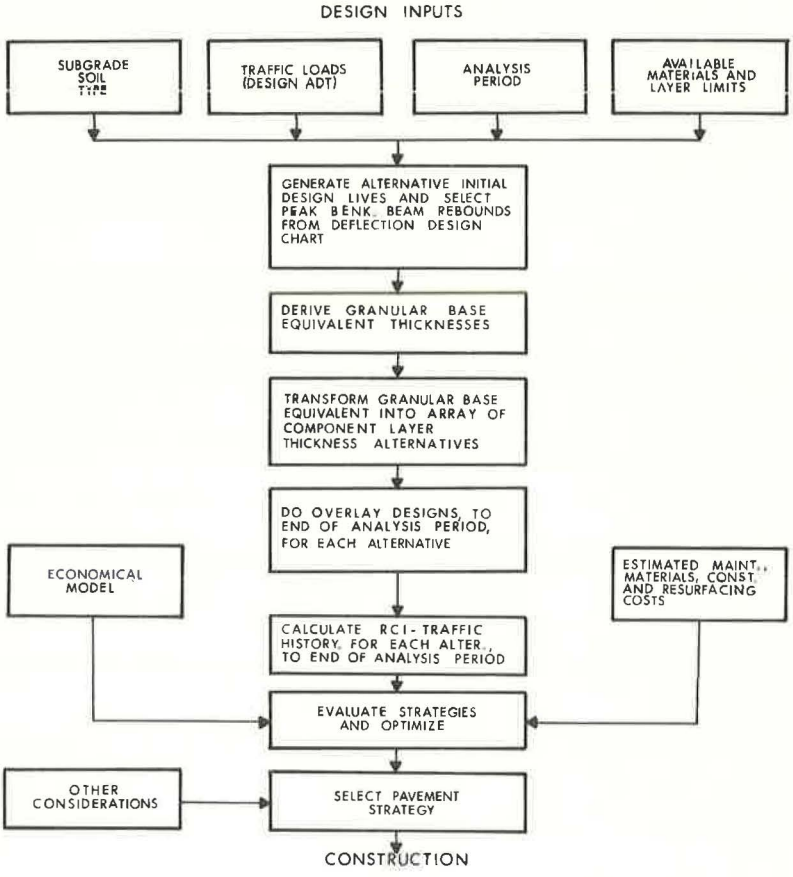

Figure 11. Recommended deep-strength design strategy.

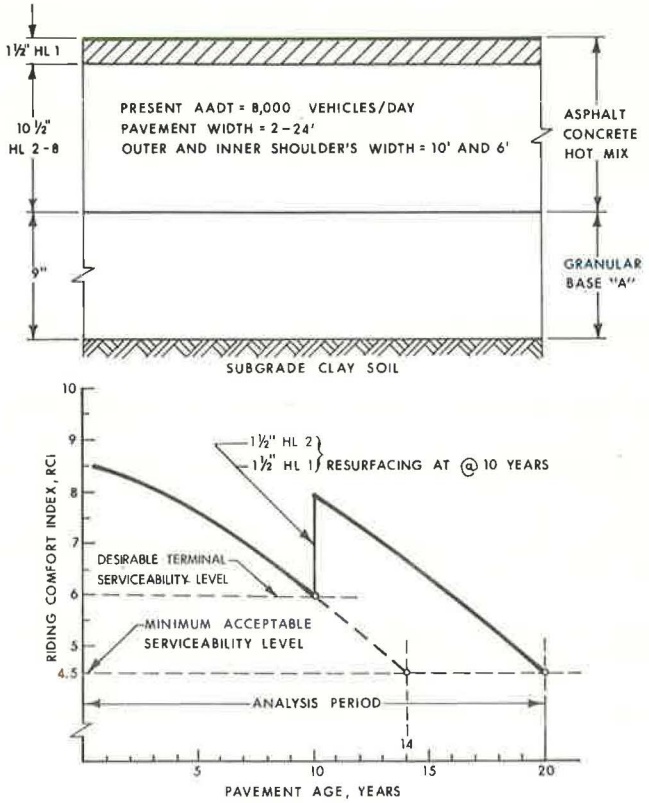

project, has referred to a deep-strength asphalt concrete pavement section having the same total granular equivalency of 33 in. (840 mm) with 1½ in. (38 mm) sand asphalt, and 1½ in. (38 mm) HL 1 resurfacing after 10 years. Figure 11 shows the recommended pavement strategy by the pavement selection committee.

CONCLUSIONS

The general purpose of this investigation was to determine whether layered system analyses could be applied to designing Ontario pavements. This goal was fulfilled through analyses of the Brampton Test Road in the following steps:

1. The basic properties of the five pavement materials under consideration for input to the layered system analyses were established from laboratory testing of the original materials in simulated field conditions.
2. The structural response of the various pavement sections in terms of stresses, strains, and deflections under simulated traffic loading were calculated by iterative, linear elastic, and computerized, layered system models: Chevron and Bistro.
3. The calculated structural responses were related to the measured performance (in terms of the serviceability age or traffic histories) and to the measured behavior (in terms of surface rutting and Benkelman beam rebounds).
4. The calculated responses and analyses were explicitly placed within the context of the Ontario pavement management system described by Phang and Slocum (1). It was demonstrated that a second generation set of design curves for this management system could be developed. The layer equivalency values for the materials of the Brampton Test Road could be developed by using layered system analysis results and a criterion of equal loss of serviceability. These layer equivalencies correspond quite well with those currently used in Ontario.

REFERENCES

1. Phang, W. A., and Slocum, R. Pavement Investment Decision Making and Management System. Ministry of Transportation and Communications, Ontario, Rept. RR 174, 1971.
2. Haas, R. C. G., and Hutchinson, B. G. A Management System for Highway Pavements. Proc. Australian Road Research Board, 1970.
3. Wilkins, E. B. Outline of a Proposed Management System for the C. G. R. A. Ontario Dept. of Highways, Rept. IR 29, 1969.
4. Hutchinson, B. G. A Design Framework for Highway Pavements. Ontario Joint Highway Research Program, Ontario Dept. of Highways, Rept. RR 127, 1968.
5. Hudson, W. R., et al. A Systems Approach Applied to Pavement Design and Research. Texas Highway Dept., Texas A&M Univ., and Univ. of Texas at Austin, Rept. 123-1, March 1970.
6. Peterson, D., et al. Utah's System for Planning Roadway Improvements. Materials and Tests Division, Utah State Department of Highways, 1971.
7. Output Measurements for Pavement Management Studies in Canada. Presented at Third Internat. Conf. on Structural Design of Asphalt Pavements, London, Sept. 1972.
8. Hudson, W. R., and McCullough, B. F. Flexible Pavement Design and Management, Systems Formulation. NCHRP Rept. 139, 1973.
9. Kamel, N. Performance Analysis of the Brampton Test Road Using Elastic Layered Theory. Univ. of Waterloo, MA science project, Dec. 1971.
10. Kamel, N. Applying Structural Analysis of the Brampton Test Road to Pavement Investment Decision Making and Management System. Ontario Joint Transportation and Communications Research Program, internal rept., 1972.
11. Kamel, N., Phang, W., Morris, J., and Haas, R. C. G. Layer Analysis of the Brampton Test Road and Application to Pavement Design. Highway Research Record 466, 1973, pp. 113-126.
12. Schonfeld, R. Construction of a Full-Scale Experiment as Part of Unit-Price Contract. Ontario Dept. of Highways, Rept. RR 119, 1969.

13. Phang, W. A. Four Years' Experience at the Brampton Test Road. Ontario Dept. of Highways, Rept. RR 153, Oct. 1969.
14. Phang, W. A. The Effect of Seasonal Variation on the Performance of Selected Base Materials. Ontario Dept. of Highways, Rept. IR 39, April 1970.
15. Kallas, B. F. The Brampton, Ontario Experimental Base Project. Interim rept. Feb. 1967, unpublished.
16. Kallas, B. F. The Brampton, Ontario Experimental Base Project. Interim rept., Sept. 1967, unpublished.
17. McLeod, N. W. Prepared Discussion of Ste. Anne Test Road. Canadian Technical Asphalt Assn., 1969.
18. Barksdale, R. D. Compressive Stress Pulse Times in Flexible Pavements for Use in Dynamic Testing. Highway Research Record 345, 1971, pp. 32-44.
19. Southgate, H. F. An Evaluation of Temperature Distribution and Its Relationship to Pavement Deflection. Kentucky Dept. of Highways, 1968.
20. Carey, W. N., and Irick, P. E. The Pavement Serviceability Performance Concept. HRB Bull. 250, 1960.
21. A Guide to the Structural Design of Flexible and Rigid Pavements in Canada. Road and Transportation Assn. of Canada, 1965.
22. Manual on Pavement Investigations. Canadian Good Roads Assn., Technical Publ. 11, 1959.
23. Chong, G. Measurement of Road Rideability in Ontario. Ontario Dept. of Highways, Rept. IR 29, 1969.
24. Scott, W. J. Roads and Their Riding Qualities. Jour., Institute of Civil Engineers, Road Engineering Design, Road Rept. 25, 1947.
25. The AASHO Road Test, Report 5, Pavement Research. HRB Spec. Rept. 61-E, 1962.
26. Haas, R. C. G., Kamel, N., and Morris, J. Brampton Test Road: Application of Layer Analysis to Pavement Design. Ontario Joint Transportation and Communications Research Program, Ministry of Transportation and Communications, Ontario, Res. Rept. RR 182, May 1973.
27. Dormon, G. M. The Extension to Practice of Fundamental Procedure for the Design of Asphalt Pavements. Univ. of Michigan, 1962.
28. Klomp, A. G. J., and Dormon, G. M. Stress Distribution and Dynamic Testing in Relation to Road Designing. Proc., Australian Road Research Board, 1964.
29. Morris, J., and Haas, R. C. G. Designing for Rutting in Asphalt Concrete Pavements. Presented to Annual Conference, Canadian Technical Asphalt Assn., Vancouver, Nov. 1972.
30. Haas, R. C. G., and Hudson, W. R. The Importance of Rational and Compatible Pavement Performance Evaluation. HRB Spec. Rept. 116, 1971.
31. Jung, F. W., and Phang, W. A. Elastic Layer Analysis Related to Performance of Flexible Pavements. Printed in this Record.

DIGITAL FILTERING METHODS FOR CHARACTERIZING PAVEMENT PROFILES

Roger S. Walker*, Department of Computer Science,
University of Texas at Arlington; and
W. Ronald Hudson, Department of Civil Engineering,
University of Texas at Austin

Obtaining suitable descriptor variables for pavement characterization is a major problem for today's pavement design engineer. Ideally, a set of such variables would provide a way to measure pavement performance and to relate it to pavement distress. With the surface dynamics (SD) profilometer, it is possible to accurately and rapidly obtain road profile information. Pavement serviceability, or performance, and distress are interrelated with pavement profile and, thus, the SD profilometer provides useful data from which various statistics can be obtained for possible use as pavement descriptor variables. One set of such variables is road profile quantities such as amplitude measurements for specific wavelength bands. If it is possible to obtain an adequate model that relates performance to various road profile characteristics as measured by specific descriptors and if various distress manifestations can be related to the same set of descriptors, then pavement performance and distress can be related by means of distress-performance models. This paper discusses possible uses of digital filtering techniques on road profile data in an effort to find a set of ideal pavement descriptors. Included are discussions of current descriptors; digital filtering techniques, including basic definitions; and ways such techniques can be used to obtain better pavement descriptors. The discussions are intended primarily to prompt further investigations into these methods and their trial use in road profile analysis.

•ONE of the major problems in developing improved pavement design methods today is obtaining suitable descriptor variables for characterizing pavement riding quality. An ideal set of such variables should provide a means for obtaining some measure of pavement performance and for relating performance to pavement distress. The surface dynamics (SD) profilometer provides an accurate and rapid means of obtaining road profile information. Pavement profile is interrelated with pavement serviceability or performance and distress and, thus, this device provides data from which various statistics can be obtained for use as pavement descriptors. Road profile quantities such as amplitude measurements for specific wavelength bands are one set of such variables. If a model that relates performance to various road profile characteristics as measured by specific descriptors can be obtained, and, in turn, if various distress manifestations can be related to the same set of descriptors, then pavement performance and distress can be related via distress-performance models.

This paper discusses the possible use of digital filtering techniques on road profile data as a tool in an effort to find such a set of pavement descriptors. The discussion includes comments on initial and current descriptors, i.e., slope variance and power spectral estimates. Digital filtering techniques, including basic definitions, and an

Publication of this paper sponsored by Committee on Pavement Condition Evaluation.
*This paper is based on work while the author was with the Center for Highway Research, The University of Texas at Austin.

example application are introduced. How such filtering techniques can aid in obtaining better pavement descriptors is presented. The discussions, which are limited to digital filtering concepts, are primarily intended for prompting further investigations into these methods and their trial use in road profile analysis. The ideas presented are the results of several years of experience in using and analyzing profile data from the SD profilometer.

CURRENT PAVEMENT CHARACTERIZATION METHODS

The SD profilometer provides separate analog profile records for both right- and left-wheel paths for a given pavement section. This record can be converted to equally spaced discrete measurements according to a sampling signal synchronized with the distance traveled. For this paper the digitized profile data are approximately 2 in. (50.8 mm) apart [6 data points/ft (1.8/m)]. For discussion purposes the set of digitized profile data for either the right- or left-wheel paths are $X = x_1, x_2, \ldots, x_n$ where x_i represents the discrete profile values, and n is the section length in half inches.

Roughness index and slope variance statistics were used as the primary pavement characterization descriptors during initial research investigations at the Center for Highway Research and the Texas Highway Department. These two statistics were selected because of their relationship with features that induce forces on the rider and because of their previous acceptance in the highway field. The roughness index is the normalized sum of the vertical deviations of the profile throughout a pavement section, and slope variance is the variance of surface profile slopes calculated for the length of the section. Present serviceability index (PSI) models (3) were developed by correlating these variables along with condition survey statistics.

Several disadvantages of using slope variance as a pavement surface characterization statistic or estimator of pavement serviceability have been noted. First, slope variance as computed at the AASHO Road Test [9-in. (228.6 mm) base] is quite dependent on wheel bounce (5, 7). Consequently, considerable variation in replication measurements for various combinations of pavement roughness and profilometer operating speeds is common. Second, the complexity of a section of pavement cannot be adequately characterized by a single statistic such as slope variance. In fact, the effect of certain wavelengths is completely ignored by this statistic (7). Third, slope variance is somewhat difficult to relate or picture physically and, largely because of the mentioned disadvantages, probably it provides at best a correlation coefficient of about 0.82, and this for profilometer operating speeds of 20 mph (8.94 m/s). (At greater operating speeds, this correlation dropped significantly.) That is, only about 67 percent of the mean rating of the panel's opinion (3) could be explained by slope variance. Roughness index was similarly disadvantaged by these problems, and it exhibited less correlation with the mean subjective ride quality ratings. Adequate serviceability index (SI) prediction models were obtained only after including both condition survey information and slope variance.

Because of the complexities of a road profile, the characterization of a pavement section by its individual wavelength components appears to be much more viable than the use of a single statistic such as slope variance or roughness index. In addition, with wavelength information, various problems such as wheel bounce can be isolated or accounted for to provide more accurate pavement characterizations.

With these shortcomings, the use of power spectral estimates was investigated next as providing more comprehensive descriptor variables. Power spectral estimates like slope variance are statistical quantities, but the power spectrum affords a set of profile descriptors instead of a single measure.

Figure 1 shows the relationship between mean subjective ride quality ratings or PSR and the road profile (64-band) spectral estimates for a large sampling of typical pavements in Texas (3, 7). The power spectral estimates for several frequencies or wavelength bands are shown for various road roughness classes, characterized by PSR. The average spectral amplitudes of 86 pavement sections with various roughnesses (grouped by PSR intervals) were obtained. Generally, the rougher the road was, the greater the spectral amplitudes were (Fig. 1). However, for the higher frequencies

Figure 1. Wavelength versus power spectral estimates (7).

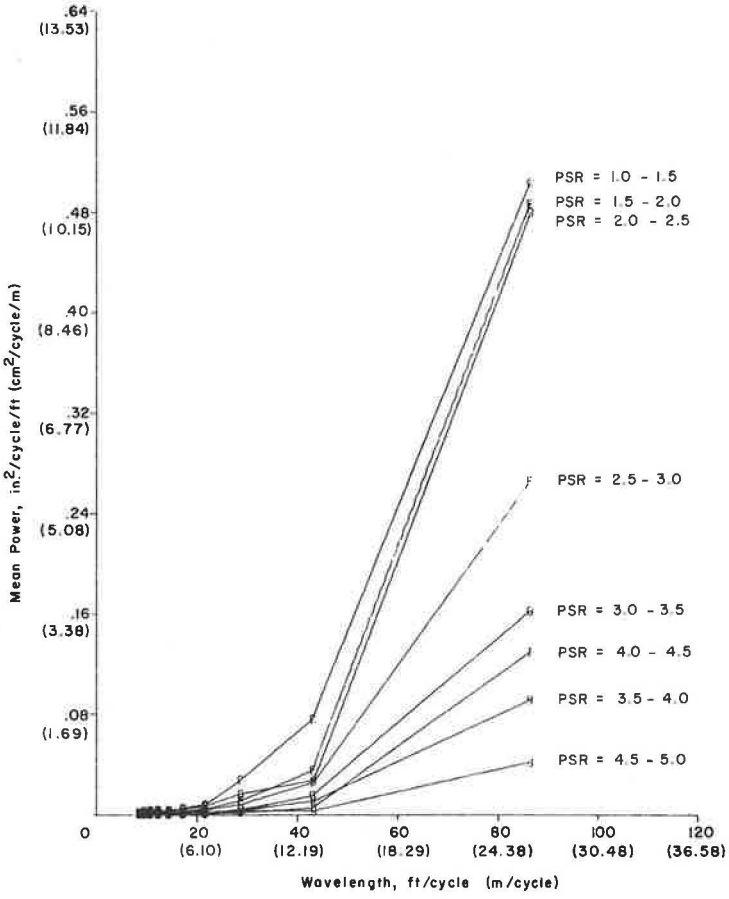

Figure 2. SI histogram for measurements on US-71.

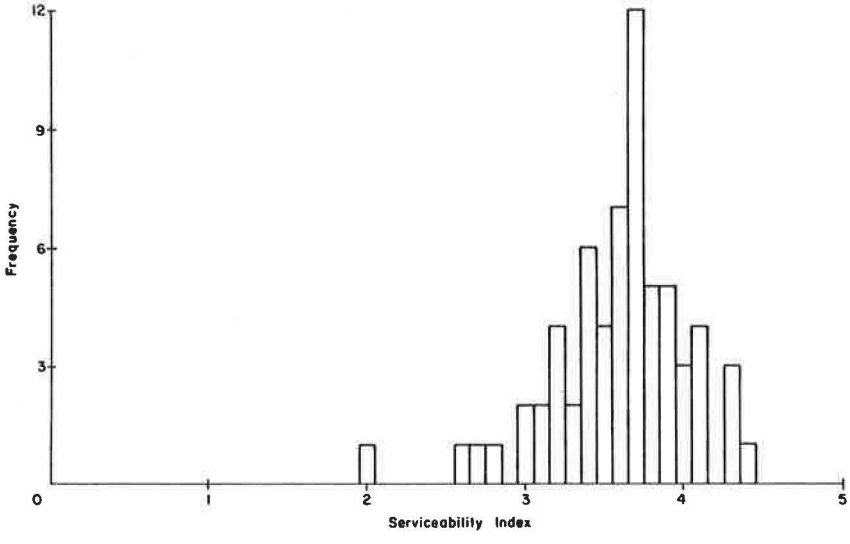

or smaller wavelengths, these groupings are less discriminating as roughness indicators.

Sometimes it is helpful to focus on the amplitude spectrum of a section of road profile rather than its power or covariance spectrum. Such estimates are usually more easily realized physically by the highway engineer than are the power spectral estimates (i.e., the root-mean-square amplitude of the profile irregularities in inches is more easily understood than power in $in.^2$/cycle/ft. Such amplitudes may be obtained from the power spectral estimates from $x_i = \sqrt{2Q_i \Delta f}$ where Q_i is the two-sided power or covariance spectral component for the i th frequency band and Δf is the width of the band containing this variance.

Specific amplitude estimates were highly correlated with pavement riding quality, and a PSI model was developed that was superior to the original slope variance and roughness index models and that has since been extensively used for SI measurement in Texas. In addition, it is also currently being used as the SI measurement standard for calibration with Mays Road Meters (6).

The SI model based on road profile spectral estimates also has a very significant operational advantage over the slope variance or roughness index models in that condition survey information is not required. That is, the SI value is derived only as a function of the spectral estimates, thus permitting more rapid and continuous SI measurements. Figures 2 and 3 show the usefulness of this procedure for obtaining large-scale SI measurements. Figure 2 is useful for computing a SI histogram for several miles of pavements on US-71 south of Austin, Texas, and Figure 3 is useful for providing continuous SI samples for several miles of I-10 east of San Antonio.

There are, however, several problems in using power spectral analysis methods in characterizing road profile data. The primary problem is that the spectral estimate is a mean power estimate for each particular band; thus, the degree of roughness variation within a section is not measured (7).

Assuming that the profile data meet the usual statistical assumptions (Gaussian, stationary, etc.) and enough data are present, this mean provides a good estimate of the real profile amplitude from which a good indication of the characteristics of the individual time or distance ensembles can be obtained. On the other hand, if these assumptions are not met, which is usually the case, then the amplitude estimate can become distorted. In addition, so that reliable spectral estimates can be obtained, pavement sections must be several hundred feet long [1,200-ft (365.76 m) minimum lengths were used]. These constraints thus make it difficult, if not impossible, to get accurate information on localized effects, which must be examined carefully in studies relating distress to performance.

Filtering techniques offer another analysis tool in which the amplitudes of selected wavelength bands can be observed as a function of distance. This permits more localized examinations of the true average amplitude variations. Digital filtering techniques are attractive for analyzing the digitized road profile data because they easily can be developed and applied.

Digital Filtering Definitions

Digital filtering is the process of spectrum shaping by using a digital computer as the basic building block (1). Hence, the goals of digital filtering are similar to those of continuous or analog filtering. Whereas continuous filter theory is based on linear differential equations, digital filter theory is based on linear difference equations.

Digital filters can be applied to the discrete road profile data by convolving these data with the weighing function (impulse response) of a specific filter. The convolution is

$$y_n = \sum_{i=0}^{N} w_i \, x_{n-i} \qquad (1)$$

Figure 3. Continuous SI measurements on I-10.

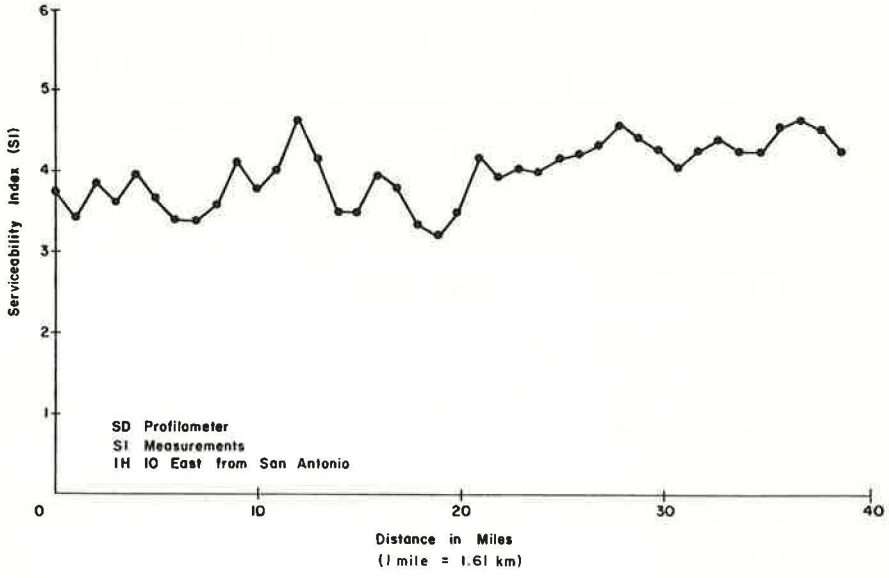

Figure 4. Recursive digital filter (4).

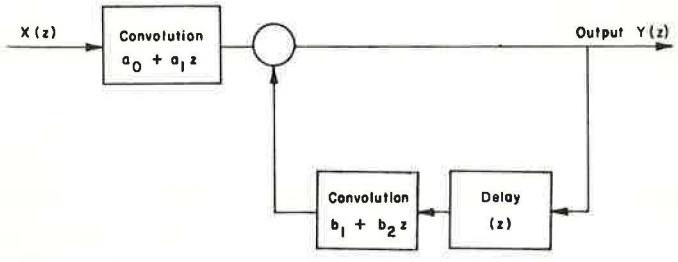

Figure 5. Filter frequency response.

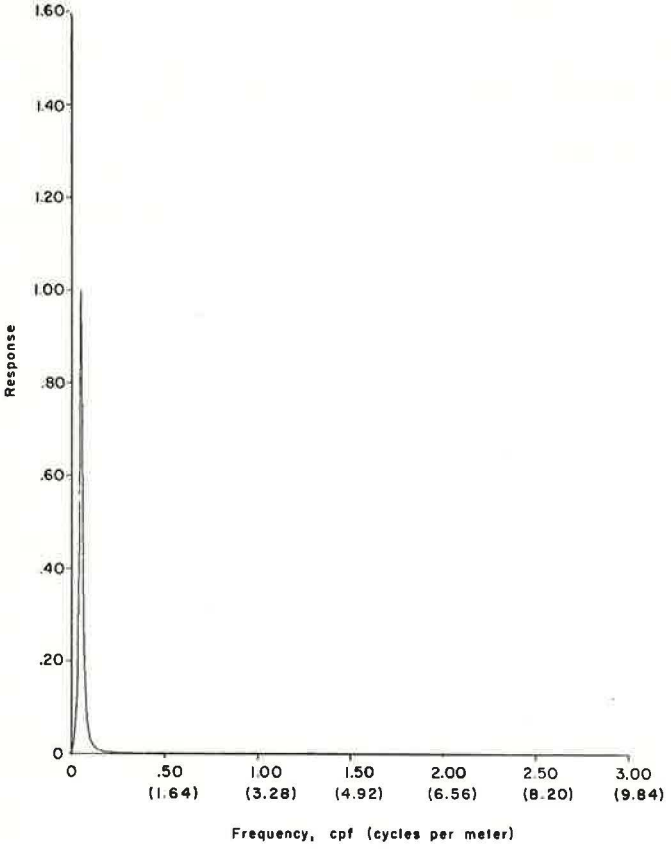

where

$X = \{x_0, x_1, \ldots, x_M\}$ represents M + 1 values of the input series or road profile,
$W = \{w_0, w_1, \ldots, w_N\}$ represents N + 1 values of the filter weighing function, and
$Y = \{y_0, y_1, \ldots, y_{N+M}\}$ represents the N + M + 1 values of the filtered output series.

Equation 1 can also be expressed in terms of its z-transform as

$$Y(z) = W(z)\, X(z) \tag{2}$$

where

$X(z) = x_0 + x_1 z + x_2 z^2 + \ldots x_M z^M$,
$W(z) = w_0 + w_1 z + w_2 z^2 + \ldots w_N z^N$, and
$Y(z) = y_0 + y_1 z + y_2 z^2 + \ldots y_{M+N} z^{M+N}$.

Variable z, which represents the operation of delaying a data sample one sample interval (z^N by N sample intervals), is related to the Laplace variable S by

$$z = e^{-TS} \tag{3}$$

where T is the Δt sample interval.

Some digital filters can also be expressed as a ratio of two polynomials in z or

$$W(z) = \frac{A(z)}{B(z)} = \frac{a_0 + a_1 z + \ldots a_N z^N}{b_0 + b_1 z + \ldots b_M z^M} \tag{4}$$

By using long division (4), w(z) can be expanded into a simple polynomial:

$$\frac{A(z)}{B(z)} = w_0 + w_1 z + w_2 z^2 + \ldots \tag{5}$$

If the filter is stable, the coefficients will converge to zero and, hence, w(z) may be closely approximated by a finite number of terms (i.e., K) or

$$W(z) = \frac{A(z)}{B(z)} \approx w_0 + w_1 z + \ldots w_K z^K \tag{6}$$

This approximation can then be used as a filter by standard digital convolution. If the rational filter

$$W(z) = \frac{a_0 + a_1 z}{1 + b_1 z + b_2 z^2} \tag{7}$$

is used to filter a set of profile data then the standard output Y(z) can be expressed as

$$Y(z) = \frac{a_0 + a_1 z}{1 + b_1 z + b_2 z^2}\, X(z)$$

or

$$Y(z) + zY(z)\,[b_1 + b_2 z] = [a_0 + a_1 z]\, X(z)$$

and thus

$$Y(z) = [a_0 + a_1 z]\, X(z) - zY(z)\,[b_1 + b_2 z] \tag{8}$$

That is, Y(z) is equal to the input convolved with the series (a_0, a_1) minus the output delayed one sample interval and convolved with the series (b_1, b_2).

Figure 4 shows this feedback system, which is realized by the recursive algorithm of Eq. 8. The general recursive equation for rational filters can be expressed as

$$y_n = \sum_{i=0}^{M} a_i x_{n-i} - \sum_{j=1}^{M} b_j y_{n-j} \tag{9}$$

Such filters (1, 2, 4) may be synthesized in the z plane, or standard S plane filters can be converted to such recursive relationships.

Recursive filters may also be used for obtaining zero phase filters by the uses of both forward and reverse recursive algorithms (4).

A Specific Application

As noted before, one advantage in using digital filtering techniques for analyzing road profile data is that a plot of the filtered profile amplitude versus distance can be obtained. Statistical methods that first group similar variances and then obtain more realistic average and extreme amplitude estimates for road sections can then be applied.

Figure 5 shows the frequency response of a simple band pass filter that was applied to about 2 miles (3.2 km) of Texas pavements where nearby swelling clay mounds occurred in 20-ft (6.10 m) wavelengths. The coefficients used in obtaining this filter are given in Eq. 10:

$$y_n = (-5.375 \times 10^{-6})x_{n-1} + (5.375 \times 10^{-6})x_{n-5} + 3.954\, y_{n-1} - 5.870\, y_{n-2} + 3.876\, y_{n-3} - 0.9610\, y_{n-4} \tag{10}$$

for a Nyquist frequency of 2.96 cycles/ft (9.71 cycles/m).

Figures 6, 7, and 8 show the plots of this data before and after filtering where zero phase filtering was performed. Zero phase filtering, which causes no phase shift in the irregularities in the profile corresponding to any frequency, was obtained (4). After the forward recursive algorithm of Eq. 10 was used, the time reverse algorithm of Eq. 11 was applied:

$$y_n = (-5.375 \times 10^{-6})x_{n+1} + (5.375 \times 10^{-6})x_{n+5} + 3.954\, y_{n+1} - 5.870\, y_{n+2} + 3.876\, y_{n+3} + 0.9610\, y_{n+4} \tag{11}$$

The plots in Figures 6, 7, and 8 are useful for showing the results of the filtered data superimposed on the original profile data. The filtered data should be examined, for example, first to segment the pavement section on the basis of amplitude characteristics and then to compute average amplitude statistics.

Digital Filtering for Pavement Surface Characterization

Probably the most important use of digital filtering will be to investigate more localized pavement characteristics. For example, if a large set of amplitude plots for several key wavelengths can be obtained for a specific type of pavement cracking condition at various failure stages, then multivariate analysis techniques, considering the average amplitude variation and the maximum amplitude value of the filtered profile data, might yield a statistical correlation.

Pavement performance has already been somewhat related to specific wavelength amplitudes (7); thus, these same bands might provide initial frequency bands for consideration. Additional rating sessions might also be conducted, and more precise amplitude estimates might be obtained for correlation with the subjective ratings.

Another useful method of applying these filtering methods would be to establish a set of typical upper amplitude levels for construction specifications and control rather than a single number as $\frac{1}{8}$ in. (3.2 mm) for 10-ft (3.05 m) wavelengths. So that this

Figure 6. Profile before and after filtering, 0 to 67 ft (0 to 20 m).

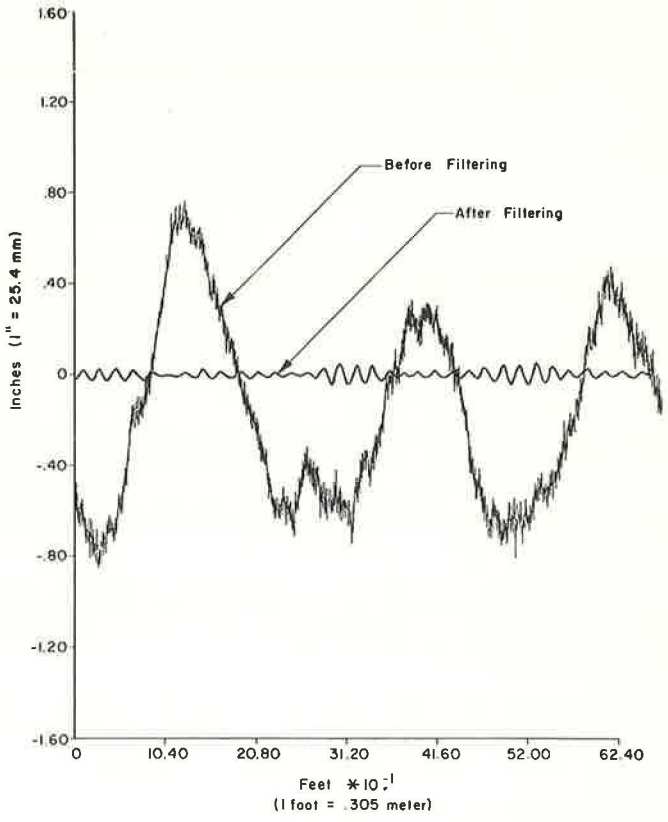

Figure 7. Profile before and after filtering, 67 to 135 ft (20 to 41 m).

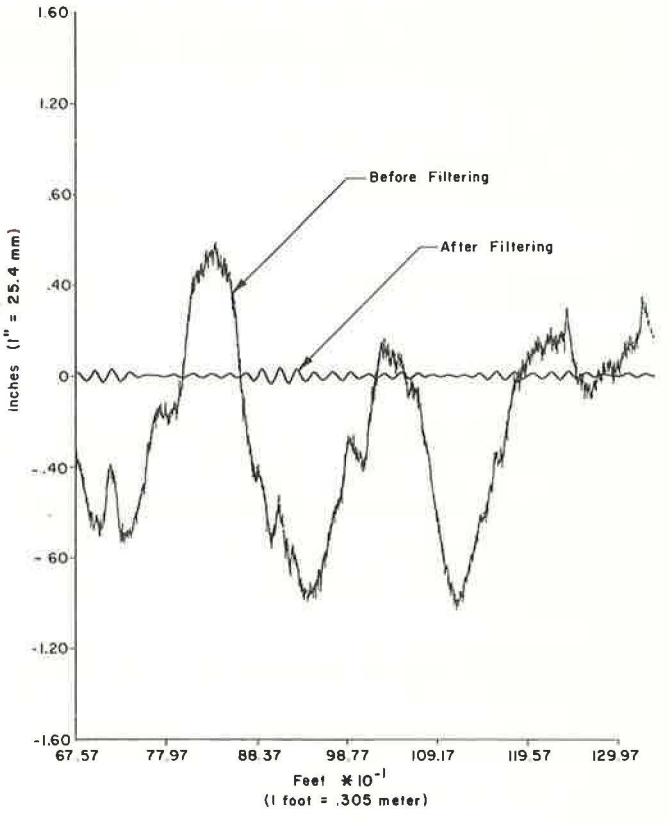

Figure 8. Profile before and after filtering, 135-200 ft (41 to 61 m).

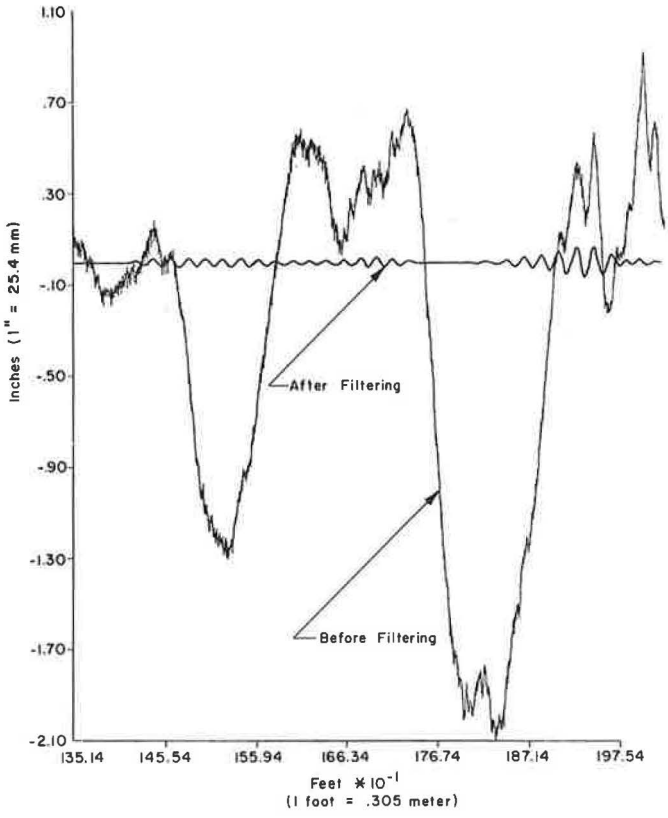

Figure 9. Example of not-to-exceed amplitude levels for construction specifications.

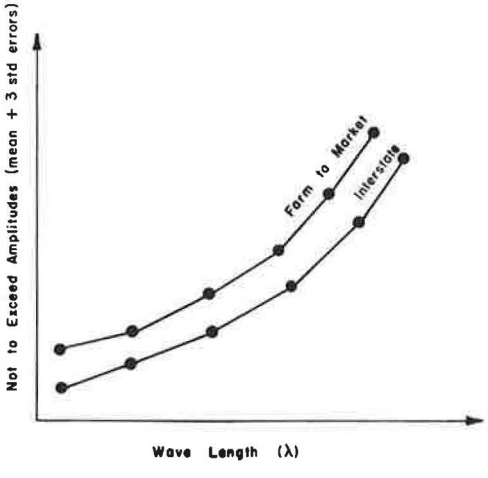

could be done, a representative sampling of profiles from pavements of highly acceptable riding quality could be measured. Band pass filters could then be designed and used on these data to obtain several sets of filtered profile data. Mean and upper amplitude ranges (e.g., three standard errors) could then be established for appropriate roughness regions for each band of these data to establish a set or spectrum of not-to-exceed amplitude regions (Fig. 9). If the mean of the absolute values of the profile elevation deviations at any wavelength exceeds the established threshold value, then the pavement is not satisfactory. Root-mean-square amplitudes could be also used. Initially, filters centered at the bands used in the SI model might be used. Once such ranges are established, the SD profilometer could then be used for evaluation of new or recently overlayed pavements so that areas violating these critical regions could be found rapidly. The use of a small digital controller within the SD profilometer could easily detect such violations immediately during profile measurements.

Of course, the use of digital filters is not without complications. First, which frequency or wavelength bands should be considered for a given application? Second, which statistical or set of statistical methods should be used for summarizing the filtered data? Third, digital filters like analog filters have certain inherent characteristics (e.g., response time, etc.), which must be considered, although the zero phase filter does provide an advantage over analog filtering method.

The numerous combinations of frequency bands can likely be minimized by the power spectral analysis methods discussed, and the numerous data summarizing methods might be limited to those that lend themselves to physical interpretation. This tool, however, should add new dimensions to road profile analysis techniques and perhaps aid in initial solutions relating distress and performance.

ACKNOWLEDGMENT

This investigation was conducted at the Center for Highway Research, University of Texas at Austin. The authors wish to thank the sponsors: the Texas Highway Department and the Federal Highway Administration, U.S. Department of Transportation.

The contents of this report reflect the views of the authors, who are responsible for the facts and the accuracy of the data. The contents do not necessarily reflect the official views or policies of the Federal Highway Administration. This report does not constitute a standard, specification, or regulation.

REFERENCES

1. Gold, B., and Rader, C. Digital Processing of Signals. McGraw-Hill, 1969.
2. Rader, C. M., and Gold, B. Digital Filter Design Techniques. Lincoln Laboratory, Massachusetts Institute of Technology, Lexington, Tech. Note 1965-63, Dec. 1965.
3. Roberts, F. L., and Hudson, W. R. Pavement Serviceability Equations Using the Surface Dynamics Profilometer. Center for Highway Research, Univ. of Texas at Austin, Res. Rept. 73-3, April 1970.
4. Shanks, J. L. Recursion Filters for Digital Processing. Geophysics, Vol. 32, No. 1, Feb. 1967.
5. Walker, R. S., Hudson, W. R., and Roberts, F. L. Development of a System for High-Speed Measurement of Pavement Roughness, Final Report. Center for Highway Research, Univ. of Texas at Austin, Res. Rept. 73-5F, May 1971.
6. Walker, R. S., and Hudson, W. R. A Correlation Study of the Mays Road Meter With the Surface Dynamics Profilometer. Center for Highway Research, Univ. of Texas at Austin, Res. Rept. 156-1, Feb. 1973.
7. Walker, R. S., and Hudson, W. R. The Uses of Spectral Estimates for Pavement Characterization. Center for Highway Research, Univ. of Texas at Austin, Res. Rept. 156-2, Aug. 1973.

SPONSORSHIP OF THIS RECORD

GROUP 2—DESIGN AND CONSTRUCTION OF TRANSPORTATION FACILITIES
W. B. Drake, Kentucky Department of Transportation, chairman

PAVEMENT DESIGN SECTION
Carl L. Monismith, University of California, Berkeley, chairman

Committee on Flexible Pavement Design
Roger V. LeClerc, Washington Department of Highways, chairman
Robert A. Crawford, W. B. Drake, Frank B. Hennion, John W. Hewett, R. G. Hicks, William S. Housel, Michael P. Jones, R. E. Livingston, J. W. Lyon, Jr., Richard A. McComb, Chester McDowell, Carl L. Monismith, William M. Moore, Frank P. Nichols, Jr., Dale E. Peterson, William A. Phang, Donald R. Schwartz, James F. Shook, Eugene L. Skok, Jr., Robert E. Smith, Richard Lonnie Stewart, B. A. Vallerga, Paul G. Veltz, Stuart Williams

Committee on Pavement Condition Evaluation
Karl H. Dunn, Wisconsin Department of Transportation, chairman
Frederick Roger Allen, Frederick E. Behn, Max P. Brokaw, Ralph C. G. Haas, R. G. Hicks, William H. Highter, W. Ronald Hudson, David J. Lambiotte, J. W. Lyon, Jr., Alfred W. Maner, K. H. McGhee, William A. Phang, Bayard E. Quinn, Freddy L. Roberts, G. Y. Sebastyan, Lawrence L. Smith, Elson B. Spangler, Eldon J. Yoder

Committee on Theory of Pavement Design
W. Ronald Hudson, University of Texas at Austin, chairman
Richard G. Ahlvin, Ernest J. Barenberg, Richard D. Barksdale, James L. Brown, Santiago Corro Caballero, Ralph C. G. Haas, Eugene Y. Huang, William J. Kenis, Fred Moavenzadeh, Carl L. Monismith, R. G. Packard, Dale E. Peterson, Robert L. Schiffman, G. Y. Sebastyan, James F. Shook, Roberto Sosa Garrido, William T. Stapler, Ronald L. Terrel, Aleksandar S. Vesic, E. B. Wilkins, Loren M. Womack

Lawrence F. Spaine, Transportation Research Board staff

Sponsorship is indicated by a footnote on the first page of each report. The organizational units and the chairmen and members are as of December 31, 1973.